2026年甘肃省国家级教学成果奖培育成果

成果应用及效果证明材料

科研成果

项目名称	五实赋能·一点辐射·育训并举：应用型高校电子技术实践教学体系创新与实践
项目类别	教学改革
项目负责人	边玉国
承担学校	兰州工业学院

1. 科研项目（大功率非车载直流充电机的研究与应用）

六、项目验收管理部门意见

验收主管部门意见
负责人签字：　　（盖章） 年　月　日
市科技局相关计划项目管理处意见
负责人签章： 2021 年 7 月 9 日
市科技局综合计划管理处意见
负责人签字：　　（验收专用章） 2021 年 7 月 9 日

注：本证书用于市级科技计划项目的验收审批。一式四份，市科技局专项计划项目管理处、综合计划管理处、项目主管部门和项目承担单位各一份。

7

兰州市科技计划项目
验收证书

兰科验字[2021]第 79 号

项目名称：	大功率非车载直流充电机的研究与应用
项目编号：	2018-4-36
完成单位：	兰州工业学院
参加单位：	
验收组织部门：	兰州市科技局
验收主持部门：	高新处
验收日期：	2021 年 3 月 23 日

兰州市科学技术局　制

四、项目主要参加人员名单

姓名	性别	出生年月	技术职称	学历	工作单位/部门	承担的主要研究任务	本人签名
吴记胖	女	1966.10	教授	研究生	兰州工业学院	总体方案设计	吴记胖
郭志成	男	1978.12	讲师	研究生	兰州工业学院	硬件电路设计	郭志成
周德东	男	1968.1	副教授	本科	兰州工业学院	硬件调试	周德东
李晓青	女	1986.9	讲师	研究生	兰州工业学院	软件仿真	李晓青
朱东山	男	1984.4	工程师	本科	兰州工业学院	系统联调	朱东山
郭宁	女	1985.6	讲师	研究生	兰州工业学院	资料整理	郭宁
高迪	女	1984.1	讲师	研究生	兰州工业学院	软件设计	高迪
林娟	女	1984.3	副教授	研究生	兰州工业学院	系统联调	林娟

5

4. 项目实际到位经费情况：　　单位：万元

项目总经费	国家拨款	省科技拨款	市科技拨款	区县、部门拨款	自筹（含贷款）	其它
10.00275	00.00	00.00	10.00	00.00	00.00275	00.00

5. 项目经费支出情况：　　单位：万元

合　计	10.00275	8.外协费	0.00
1.人员费	0.00	9.差旅费	0.94215
2.设备购置费	0.00	10.图书、资料费	0.20
3.设备试制费	0.00	11.知识产权事务费	0.8376
4.现有仪器设备使用费	0.00	12.国际合作交流费	0.00
5.实验用材料费	6.1230	13.咨询、论证、会议费	0.80
6.燃料及动力费	0.00	14.调研费	0.00
7.测试及试验费	0.30	15.其他费用	0.80

6. 项目累计经济效益

新增产值（万元）	0.00	新增销售额（万元）	0.00
新增利税（万元）	0.00	出口创汇（万美元）	0.00

2

二、目标任务完成情况

1. 主要技术与经济指标完成情况

（1）主要技术与经济指标

① 申请实用新型专利1项；

② 发表与本课题相关学术论文2~3篇；

③ 研制大功率非车载直流充电机样机1台。

（2）主要技术与经济指标完成情况

① 授权实用新型专利2件、软著3件；

② 发表与本课题相关学术论文3篇；

③ 研制出大功率非车载直流充电机样机1台。

2. 项目实施的绩效

通过项目实施，培养青年骨干4名，2人晋升高级职称，获得市厅级学术奖励4项。

三、验收组意见

2021年3月23日，兰州市科技局组织有关专家成立验收组，对兰州工业学院承担的市级科技计划项目“大功率非车载直流充电机的研究与应用”（项目编号：2018-4-36）进行验收。验收组听取了项目汇报，查阅了相关资料，并就有关问题进行了质询答辩。经充分讨论，形成如下意见：

1.项目承担单位提供的资料齐全，符合项目验收要求。

2.项目基于高效率DC/DC变换及控制、智能化动力电池充电、有源谐波治理等技术研制了大功率非车载直流充电机，完成了合同书要求的各项任务，具有功率模块结构化、高效化、智能化的功能，各项技术指标符合要求。

3.项目获得授权实用新型专利2件、软件著作权3件，发表与课题相关学术论文3篇，研制出大功率非车载直流充电机样机1台。

4.项目专项经费使用合理，符合科研经费管理的相关规定。

验收组一致同意该项目通过验收

验收组组长（签字）：

2021年3月23日

2.科研项目（基于云平台的大型多级泵站智能化监控系统设计）

兰州市科学技术局文件

兰科字〔2025〕88号

关于下达2025年度兰州市科技发展指导性计划项目的通知

各有关单位:

为鼓励和引导全市各类创新主体自主开展科技研发活动，结合科技发展和人才服务需求，经组织申报、审核和研究，现下达2025年度兰州市科技发展指导性计划。

兰州市科技发展指导性计划项目执行期原则上不超过2年，无特殊原因2年内未结题验收的，项目自行终止，并降低项目单位和项目负责人科研诚信评级，评级结果将在后期省级科技项目推荐及市级科技项目申报时予以应用。执行期内的项目课题组成员不得申报其他市级科技、人才项目，项目内容及人员不得变更。项目完成后，由市科技局组织结题验收工作。

请各项目单位接此通知后，与市科技局分管业务科室签订《兰州市科技计划项目任务合同书》，并结合各自实际，配套落实项目自筹经费，确保项目顺利实施。

附件：2025年度兰州市科技发展指导性计划项目明细表

2025年12月31日

附件

2025年度兰州市科技发展指导性计划项目明细表

序号	项目名称	承担单位	支持资金（万元）	主管科室
2025-5-056	基于云服务平台的大型多级泵站智能化监控系统设计	兰州工业学院	0	高新技术科

3. 科研获奖

甘肃省电子学会科学技术进步奖

奖励证书

为表彰甘肃省电子学会科技进步奖获奖者，特颁发此证书。

项目名称：水族箱智能监控系统的研制

奖励等级：一等

获 奖 者：周德东、孙志强、刘大为、尚威武、赵丹阳、张寰、范静、董煜

证书编号：2019-DZKJ1-014

甘肃省电子学会

2019年10月30日

甘肃省电子学会科学技术进步奖

奖励证书

为表彰甘肃省电子学会科技进步奖获奖者，特颁发此证书。

项目名称：Intel80C31辐射效应测试系统

奖励等级：一等

获 奖 者：郭志成、周德东、刘梅、吴记群、任晓芳、赵又新、李晓青、朱东山、郭宁、林娟、刘大为、马慧霞

证书编号：2019-DZKJ1-008

甘肃省电子学会

2019年10月30日

甘肃省电子学会科学技术奖

证　书

周德东同志，您参与完成的电流互感器状态评估方法及极性智能检测技术研究项目，获得2018年度甘肃省电子学会科学技术二等奖，特颁发此证书。

甘肃省电子学会

证书号：2018-GSDZXH-K2-16-R01

二〇一八年十一月二十九日

甘肃省电子学会科学技术进步奖

奖励证书

为表彰甘肃省电子学会科技进步奖获奖者，特颁发此证书。

项目名称：车联网环境下基于驾驶行为的交通建模方法研究

奖励等级：一等

获 奖 者：刘大为、吴记群、周德东、朱东山、王筱芳、郭志成、郭宁、林娟

证书编号：2019-DZKJ1-001

甘肃省电子学会

2019年10月30日

甘肃省电子学会科学技术奖

证　书

周德东 同志，您参与完成的 基于物联网建立新型智能交通系统的策略研究 项目，获得 2018 年度甘肃省电子学会科学技术 三 等 奖 ，特颁发此证书。

甘肃省电子学会

证书号：2018-GSDZXH-K3-2-R02

二〇一八年十一月二十九日

兰州工业学院青年科技创新项目
结项证书

项目名称：无人机自主无线充电平台的研究与实现

项目编号：2019K-007

评审等级：合格

负 责 人：朱东山

承担单位：电气工程学院

参 与 人：付 蓉 范 静 李晓青 党 媛 石栋栋

本项目经审核准予结项，特发此证。

证书编号：2021JX-016

兰州工业学院

2022年4月

甘肃省高等学校科学研究项目
结项证书

项目类型：创新基金项目

项目名称：城市垃圾发电运输一体化智能管理系统应用研究

项目编号：2021A-157

评审等级：合格

负 责 人：朱东山

承担单位：兰州工业学院

参 与 人：党媛、吴记群、李晓青、刘大为、傅龙飞

本项目经审核准予结项，特发此证。

证书编号：2023JT-0579

甘肃省教育厅

2023年9月22日

甘肃省机械工程学会
科学技术奖
证　书

为表彰甘肃省机械工程学会科学技术奖获得者，特颁发此证书。

项目名称：液力耦合调速型风电机组控制技术研究与实现

奖励等级：**一等奖**

获 奖 者：李晓青

2024年7月31日

证书号：2024-1-4-R1

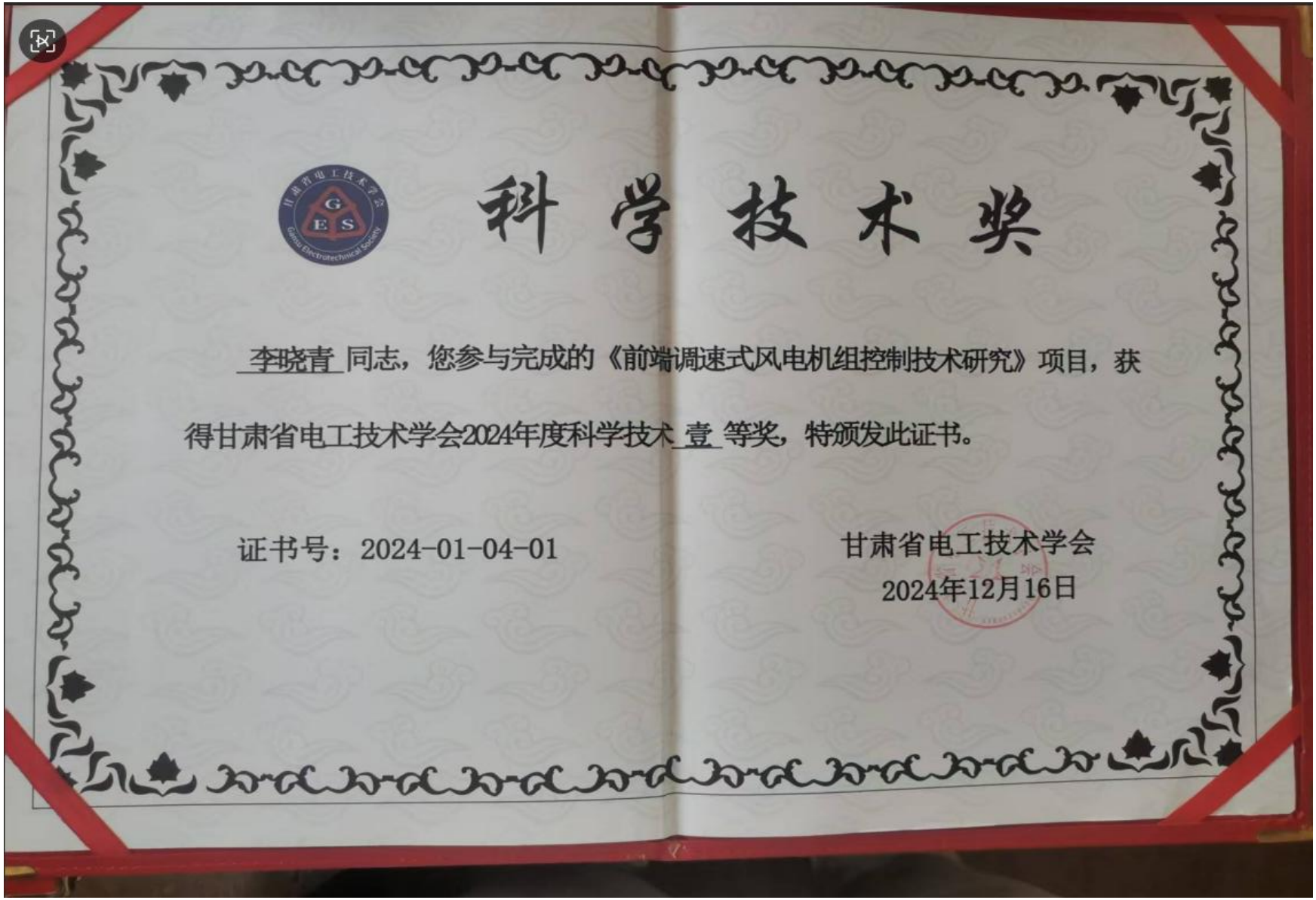

科学技术奖

李晓青同志，您参与完成的《前端调速式风电机组控制技术研究》项目，获得甘肃省电工技术学会2024年度科学技术壹等奖，特颁发此证书。

证书号：2024-01-04-01

甘肃省电工技术学会

2024年12月16日

甘肃省电子学会科学技术奖

证　书

郭志成 同志，您参与完成的 电力提灌工程大型泵站综合自动化监控系统的研究 项目，获得2018年度甘肃省电子学会科学技术 一 等 奖，特颁发此证书。

甘肃省电子学会

证书号：2018-GSDZXH-K1-8-R02

二〇一八年十一月二十九日

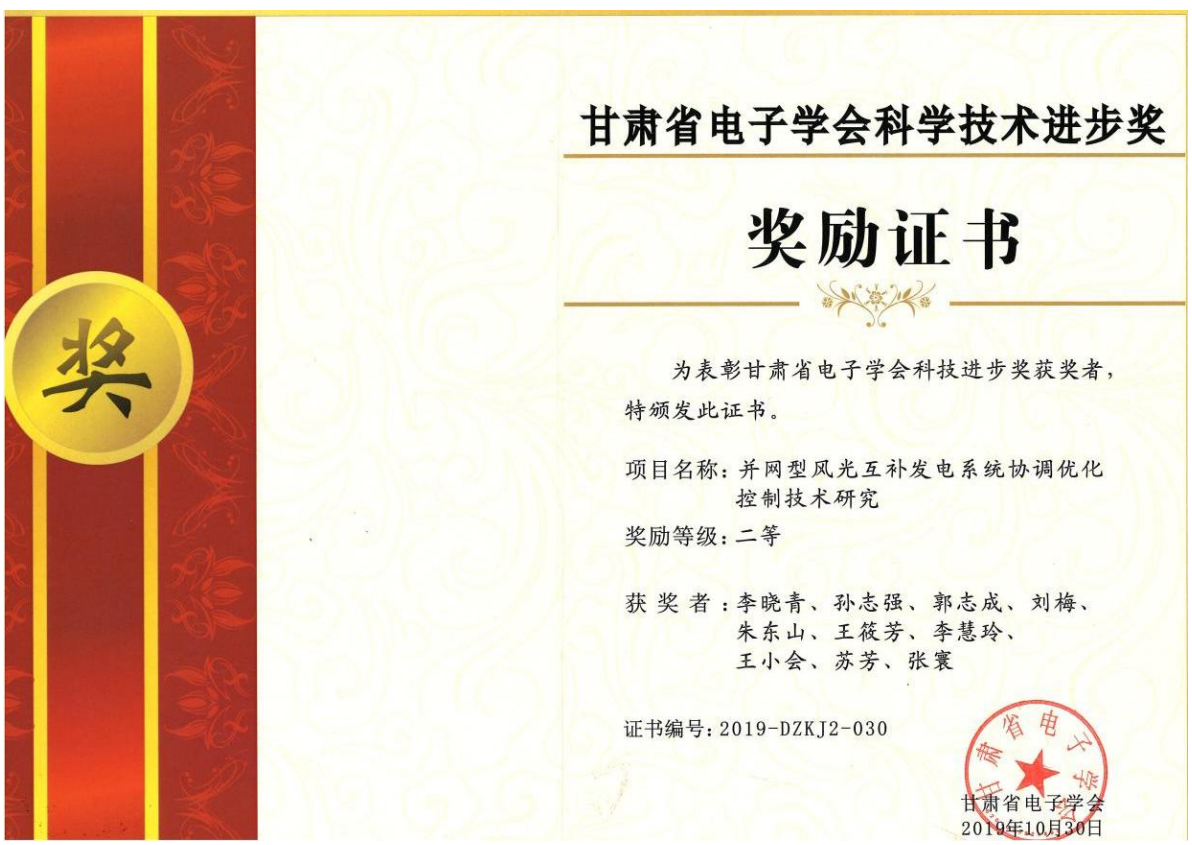

甘肃省电子学会科学技术进步奖

奖励证书

为表彰甘肃省电子学会科技进步奖获奖者，特颁发此证书。

项目名称：并网型风光互补发电系统协调优化控制技术研究

奖励等级：二等

获 奖 者：李晓青、孙志强、郭志成、刘梅、朱东山、王筱芳、李慧玲、王小会、苏芳、张寰

证书编号：2019-DZKJ2-030

甘肃省电子学会

2019年10月30日

4. 国家发明专利

证书号第6473710号

发明专利证书

发明名称：智能水族箱综合控制系统

发　明　人：周德东;郭志成;张寰;李双科;吴记群;李晓青;朱东山
范静

专　利　号：ZL 2018 1 0716262.6

专利申请日：2018年07月03日

专利权人：兰州工业学院

地　　址：730050 甘肃省兰州市七里河区龚家坪东路1号

授权公告日：2023年11月10日　　授权公告号：CN 108646636 B

国家知识产权局依照中华人民共和国专利法进行审查，决定授予专利权，颁发发明专利证书并在专利登记簿上予以登记。专利权自授权公告之日起生效。专利权期限为二十年，自申请日起算。

专利证书记载专利权登记时的法律状况。专利权的转移、质押、无效、终止、恢复和专利权人的姓名或名称、国籍、地址变更等事项记载在专利登记簿上。

局长
申长雨

国家知识产权局
2023年11月10日

第1页(共2页)

其他事项参见续页

证书号第6473710号

专利权人应当依照专利法及其实施细则规定缴纳年费。本专利的年费应当在每年07月03日前缴纳。未按照规定缴纳年费的，专利权自应当缴纳年费期满之日起终止。

申请日时本专利记载的申请人、发明人信息如下：

申请人：

兰州工业学院

发明人：

周德东;郭志成;张寰;李双科;吴记群;李晓青;朱东山;范静

1. Research on the Shortest Variable-Slip Mode DC-Side Voltage Control of APF Command Current

2020 IEEE 3rd International Conference on Electronics Technology (ICET)

IEEE Catalog Number: CFP20P18-USB
ISBN: 978-1-7281-6282-9

Additional copies of this publication are available from

Curran Associates, Inc.
57 Morehouse Lane
Red Hook, NY 12571 USA
+1 845 758 0400
+1 845 758 2633 (FAX)
email: curran@proceedings.com

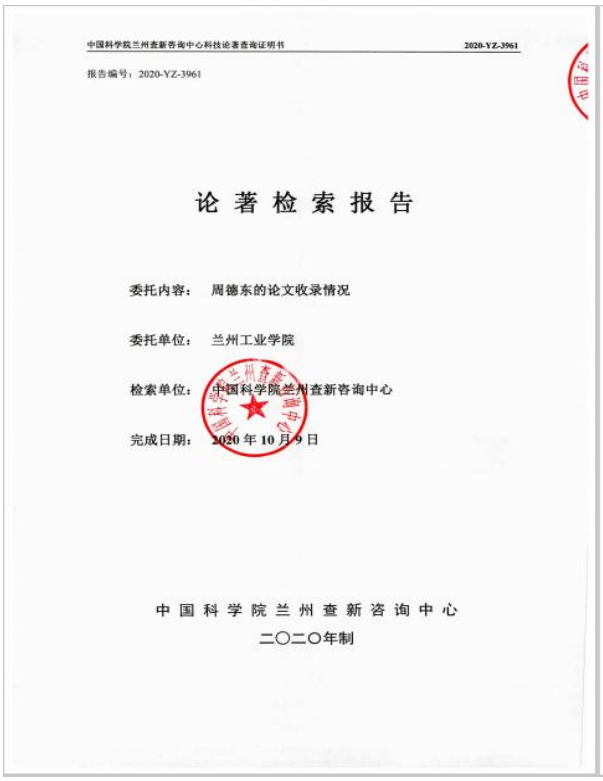

中国科学院兰州查新咨询中心科技论著查询证明书 2020-YZ-3961

报告编号：2020-YZ-3961

论 著 检 索 报 告

委托内容： 周德东的论文收录情况

委托单位： 兰州工业学院

检索单位： 中国科学院兰州查新咨询中心

完成日期： 2020 年 10 月 9 日

中 国 科 学 院 兰 州 查 新 咨 询 中 心

二〇二〇年制

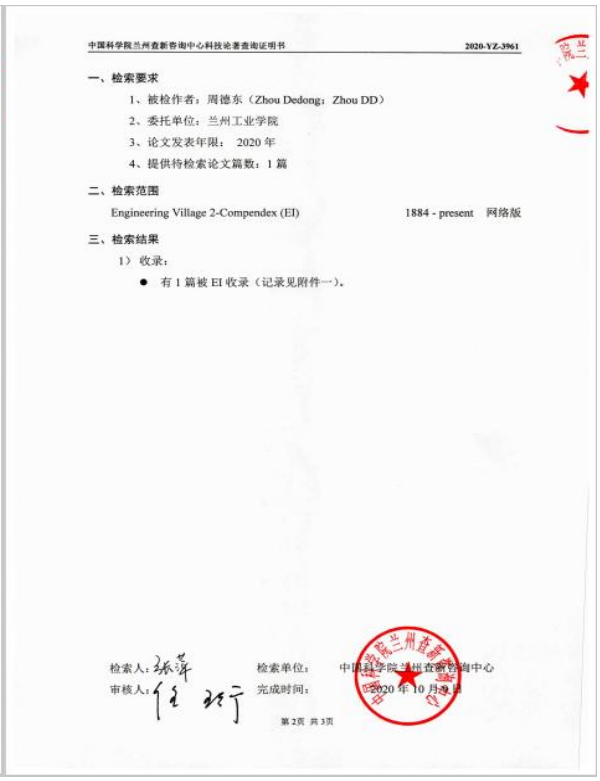

中国科学院兰州查新咨询中心科技论著查询证明书 2020-YZ-3961

一、检索要求

1、被检作者：周德东（Zhou Dedong；Zhou DD）

2、委托单位：兰州工业学院

3、论文发表年限： 2020 年

4、提供待检索论文篇数：1 篇

二、检索范围

Engineering Village 2-Compendex (EI) 1884 - present 网络版

三、检索结果

1） 收录：

- 有 1 篇被 EI 收录（记录见附件一）。

检索人： 检索单位： 中国科学院兰州查新咨询中心

审核人： 完成时间： 2020 年 10 月 9 日

第 2 页 共 3 页

中国科学院兰州查新咨询中心科技论著查询证明书 2020-YZ-3961

附件：

一、EI 收录情况

<RECORD 1>
Accession number:20202808913839
Title:Research on the Shortest Variable-Slip Mode DC-Side Voltage Control of APF Command Current
Authors:Zhou, Dedong (1); Zhao, Danyang (1)
Author affiliation:(1) Lanzhou Polytechnical College, School of Electrical Engineering, Lanzhou, China
Source title:2020 IEEE 3rd International Conference on Electronics Technology, ICET 2020
Abbreviated source title:IEEE Int. Conf. Electron. Technol., ICET
Part number:1 of 1
Issue title:2020 IEEE 3rd International Conference on Electronics Technology, ICET 2020
Issue date:May 2020
Publication year:2020
Pages:508-512
Article number:9119662
Language:English
ISBN-13:9781728162836
Document type:Conference article (CA)
Conference name:3rd IEEE International Conference on Electronics Technology, ICET 2020
Conference date:May 8, 2020 - May 12, 2020
Conference location:Chengdu, China
Conference code:161271
Publisher:Institute of Electrical and Electronics Engineers Inc.
Abstract:During the startup process, the APF is converted from uncontrolled rectifying to controlled rectifying, and a step-function signal is input to the DC side to cause the increase of capacitor voltage and generate an inrush current. The existing method for suppressing the APF grid-connected voltage is a long charging time, complicated hardware circuit, and complicated parameter setting. Aiming at the above problems, this paper proposes the shortest variable-slip mode control of APF DC-side voltage command current link, establishes the shortest command current generating circuit under dq coordinates, generates DC-side voltage command current through sliding mode variable structure controller, and enhances the system. Robustness, reduced DC side charging time, improved APF compensation performance. The simulation results prove the correctness and feasibility of the control method.
 © 2020 IEEE.
Number of references:10
Main heading:Charging time
Controlled terms:Electronics engineering - Electronics industry
Uncontrolled terms:Capacitor voltages - Command currents - Compensation performance - Dc side voltage controls - Hardware circuits - Parameter setting - Sliding mode variable structure - Start-up process
DOI:10.1109/ICET49382.2020.9119662
Database:Compendex
Compilation and indexing terms, Copyright 2020 Elsevier Inc.

（End）

文本复制检测报告单(简洁)

No:BC20210927134840224931T899　　检测时间:2021-09-27 13:48:40

检测文献: Research on the Shortest Variable-Slip Mode DC-Side Voltage Control of APF Command Current
作者: Dedong Zhou, Danyang Zhao

检测范围:
- 中国学术期刊网络出版总库
- 中国重要会议论文全文数据库
- 中国重要报纸全文数据库
- 中国专利全文数据库
- 英文数据库(涵盖期刊、博硕、会议的英文数据以及德国Springer、英国Taylor&Francis 期刊数据库等)
- 港澳台学术文献库
- 优先出版文献库
- 图书资源

时间范围: 1915-01-01至2020-05-07

检测结果

去除本人文献复制比: 2.6%
去除引用文献复制比: 2.6%　　总文字复制比: 2.6%
单篇最大文字复制比: 0.7% (On fractional control method for four-wheel-steering vehicle)

重复字数:	[263]	总段落数:	[1]
总字数:	[10014]	疑似段落数:	[1]
单篇最大重复字数:	[66]	前部重合字数:	[61]
疑似段落最大重合字数:	[263]	后部重合字数:	[202]
疑似段落最小重合字数:	[263]		

指　标:　疑似剽窃观点　疑似剽窃文字表述　一稿多投　疑似整体剽窃　过度引用　重复发表

表格: 0　公式: 检测中　疑似文字的图片: 0　脚注与尾注: 0

1. Research on the Shortest Variable-Slip Mode DC-Side Voltage Control of APF Command Current 总字数: 10014

相似文献列表

去除本人文献复制比: 2.6%(263)　文字复制比: 2.6%(263)　疑似剽窃观点: (0)

1	On fractional control method for four-wheel-steering vehicle - 《Science in China(Series E:Technological Sciences)》 - 2009-03-15	0.7% (66) 是否引证: 否
2	Rapid acquisition method of sea vessel radiating transient noise effective time based on the power-law Tonghui Yu;Cangen Xiong;Xiubo Wang;Xuefeng Dai;Tongjie Qin; - 《Proceedings of the 2nd International Conference on Mechatronics Engineering and Information Technology(ICMEIT 2017)》 - 2017-05-13	0.7% (66) 是否引证: 否
3	Torque-ripple Minimization in Switched Reluctance Motors Using Sliding Mode Variable Structure Control - 《第二十九届中国控制会议论文集》 - 2010-07-29	0.6% (62) 是否引证: 否
4	The Construction of Miniaturization Direct-current Servo System - 《Proceedings of Asia Simulation conference 2008/the 7th International Conference on System Simulation and Scientific Computing (ICSC '2008)》 - 2008-10-01	0.6% (60) 是否引证: 否
5	Sliding Mode Variable Structure Control for Radial Suspension Forces of Bearingless Permanent Magnet Synchronous Motor Based on Inverse System Method - 《2009 IEEE 6^(th) International Power Electronics and Motion Control Conference-ECCE Asia Conference Digests》 - 2009-05-17	0.6% (57) 是否引证: 否

说明:
1. 总文字复制比: 被检测论文总重合字数在总字数中所占的比例
2. 去除引用文献复制比: 去除系统识别为引用的文献后，计算出来的重合字数在总字数中所占的比例

3. 去除本人文献复制比: 去除作者本人文献后，计算出来的重合字数在总字数中所占的比例
4. 单篇最大文字复制比: 被检测文献与所有相似文献比对后，重合字数占总字数的比例最大的那一篇文献的文字复制比
5. 指标是由系统根据《学术论文不端行为的界定标准》自动生成的
6. 红色文字表示文字复制部分;绿色文字表示引用部分;棕灰色文字表示作者本人文献部分
7. 本报告单仅对您所选择比对资源范围内检测结果负责

cnki@cnki.net
http://check.cnki.net/
http://e.weibo.com/u/3194559873/

Research on the Shortest Variable-Slip Mode DC-Side Voltage Control of APF Command Current

Dedong Zhou
School of Electrical Engineering
Lanzhou Polytechnical College
Lanzhou, China
e-mail: zhaodd0106@163.com

Danyang Zhao
School of Electrical Engineering
Lanzhou Polytechnical College
line 3: Lanzhou, China
e-mail: 815285941@qq.com

***Abstract*—During the startup process, the APF is converted from uncontrolled rectifying to controlled rectifying, and a step-function signal is input to the DC side to cause the increase of capacitor voltage and generate an inrush current. The existing method for suppressing the APF grid-connected voltage is a long charging time, complicated hardware circuit, and complicated parameter setting. Aiming at the above problems, this paper proposes the shortest variable-slip mode control of APF DC-side voltage command current link, establishes the shortest command current generating circuit under *dq* coordinates, generates DC-side voltage command current through sliding mode variable structure controller, and enhances the system. Robustness, reduced DC side charging time, improved APF compensation performance. The simulation results prove the correctness and feasibility of the control method.**

Keywords-APF DC side voltage; sliding mode variable structure; new command current generating circuit; dq rotating coordinates

I. INTRODUCTION

Active power filter (APF), as a dynamic compensation device, can dynamically compensate the constantly changing harmonics and reactive power in the power grid. At present, research on APF is mainly focused on the main circuit topology and the control strategy during steady-state operation. However, there is no satisfactory method for the impact of DC-side capacitor charging during grid connection. However, during the APF startup process, due to the large voltage difference on the DC side, an inrush current will be generated on the power grid, which may cause the protection device to malfunction and damage the power equipment in serious cases. The influence is of great significance to improve its compensation effect [1-6].

At present, in the research of APF startup, the reference [7] proposes the subsection startup control method. When APF is connected to the grid, the voltage control loop is disconnected first, and the inner voltage of the current loop is used to suppress the impulse voltage. problem. The reference literature [8] proposed Bang-Bang control, which effectively suppressed the inrush current and reduced the switching time, but there were problems of complicated hardware structure and tedious parameter setting. The method of slow-setting given in the reference literature [9], given the power grid voltage division to reduce the impulse voltage, also has the problems of long switching time and so on. Literature [10] proposed a DC-side voltage control strategy for equalizing the phases of the regulated current.

This paper proposes a sliding mode variable structure control for the shortest APF DC-side voltage command current link in *dq* coordinates. A mathematical model of APF in *dq* coordinates is established. The traditional i_p-i_q method requires multiple coordinate transformations in *dq* coordinates. Capacitor charging time, a new type of command current generating circuit suitable for *dq* coordinates is designed to make the link shortest and has strong robustness. The DC-side voltage is controlled by a sliding mode variable structure, which makes the DC-side voltage rise with the sliding mode surface and suppress the impulse voltage. The correctness and feasibility of the control method are verified by simulation.

II. APF MATHEMATICAL MODEL IN DQ COORDINATE

The structure diagram of parallel APF is shown in Figure 1, and the mathematical model in *dq* coordinate is established.

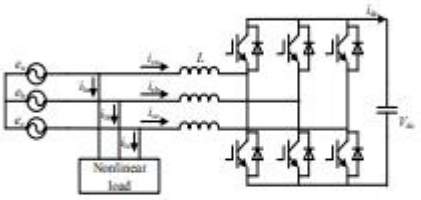

Figure 1. The Schematic diagram of Shunt active power filter.

Suppose that the initial phase angle of the a-phase voltage on the AC side of the main circuit is φ, the amplitude is E_m, the initial phase angle of i_{sa} is ψ. and the amplitude is I_m. The AC voltage and current are converted into rotating *dq* coordinates. Let the initial phase angle of the *d*-axis be θ and the acceleration be ω. The mathematical model of the voltage and current in the *dq* coordinate can be expressed as follows:

$$\begin{bmatrix} e_d \\ e_q \end{bmatrix} = C_{3s2s} \begin{bmatrix} e_a \\ e_b \\ e_c \end{bmatrix} = E_m \begin{bmatrix} \cos(\varphi - \theta) \\ \sin(\varphi - \theta) \end{bmatrix} \tag{1}$$

$$\begin{bmatrix} i_{sd} \\ i_{sq} \end{bmatrix} = C_{3s2s} \begin{bmatrix} i_{sa} \\ i_{sb} \\ i_{sc} \end{bmatrix} = I_m \begin{bmatrix} \cos(\psi - \theta) \\ \sin(\psi - \theta) \end{bmatrix} \tag{2}$$

The switch function of APF main circuit can be expressed as follow:

$$S_K = D_K + \sum_{n=1}^{\infty} (-1)^n \frac{2\pi}{n} \sin(nD_K\pi)\cos(n\omega_c t) \tag{3}$$

where, S_K is the on-off of the bridge wall, D_K is the fundamental component of each phase, K is the three phases a, b and c, and the expression of DC current I_{dc} can be obtained:

$$i_{dc} = i_a D_a + i_b D_b + i_c D_c \tag{4}$$

The expressions of voltage and current at AC side and DC side of converter are obtained by converting D_K to dq coordinate:

$$\begin{cases} u_d = D_d V_{dc} \\ u_q = D_q V_{dc} \end{cases} \tag{5}$$

$$i_{dc} = \frac{3}{2}(i_{sd} D_d + i_{sq} D_q) \tag{6}$$

The mathematical model of the APF main circuit in dq coordinates can be obtained:

$$\begin{cases} e_d = L\dfrac{\mathrm{d}i_{sd}}{\mathrm{d}t} - \omega L i_{sq} + u_d \\ e_q = L\dfrac{\mathrm{d}i_{sq}}{\mathrm{d}t} + \omega L i_{sd} + u_q \\ \dfrac{3}{2}(u_d i_{sd} + u_q i_{sq}) = V_{dc} i_{dc} \end{cases} \tag{7}$$

III. A New Type of Command Current Generating Circuit

Set the load current as I_{La}, I_{Lb}, I_{Lc}, and the three-phase power supply voltage as V_a, V_b, V_c, and convert formula (1) (2) to $\alpha\beta$ coordinate and dq coordinate.

$$\begin{bmatrix} V_\alpha \\ V_\beta \end{bmatrix} = \sqrt{\frac{2}{3}} \begin{bmatrix} 1 & -\frac{1}{2} & -\frac{1}{2} \\ 0 & \frac{\sqrt{3}}{2} & -\frac{\sqrt{3}}{2} \end{bmatrix} \begin{bmatrix} V_a \\ V_b \\ V_c \end{bmatrix} \tag{8}$$

$$\begin{bmatrix} i_{L\alpha} \\ i_{L\beta} \end{bmatrix} = \sqrt{\frac{2}{3}} \begin{bmatrix} 1 & -\frac{1}{2} & -\frac{1}{2} \\ 0 & \frac{\sqrt{3}}{2} & -\frac{\sqrt{3}}{2} \end{bmatrix} \begin{bmatrix} i_{La} \\ i_{Lb} \\ i_{Lc} \end{bmatrix} \tag{9}$$

$$\begin{bmatrix} i_{Ld} \\ i_{Lq} \end{bmatrix} = \begin{bmatrix} \cos\theta & \sin\theta \\ -\sin\theta & \cos\theta \end{bmatrix} \begin{bmatrix} i_{L\alpha} \\ i_{L\beta} \end{bmatrix} \tag{10}$$

In the formula, θ can be calculated from the tangent values of the voltage components on the α and β axes.

The DC component on the $\alpha\beta$ axis can be expressed as

$$V_d = \left|\vec{V}_{dq}\right| = \left|\vec{V}_{\alpha\beta}\right| = \sqrt{V_\alpha^2 + V_\beta^2} \tag{11}$$

The voltage is always zero on the q-axis component. Then the load current in the dq coordinate can be expressed as:

$$\begin{bmatrix} i_{Ld} \\ i_{Lq} \end{bmatrix} = \frac{1}{\sqrt{V_\alpha^2 + V_\beta^2}} \begin{bmatrix} V_\alpha & V_\beta \\ -V_\beta & V_\alpha \end{bmatrix} \begin{bmatrix} i_{L\alpha} \\ i_{L\beta} \end{bmatrix} \tag{12}$$

The load current on the dq coordinate can be decomposed into a steady state component and an oscillation equivalent component:

$$\begin{cases} i_{Ld} = \bar{i}_{Ld} + \tilde{i}_{Ld} \\ i_{Lq} = \bar{i}_{Lq} + \tilde{i}_{Lq} \end{cases} \tag{13}$$

In the formula, the power frequency positive sequence load current is generated by the power supply, and its steady-state components are represented by i^+_{Ld1h} and i^+_{Lq1h}, and the remaining sub-steady-state harmonic components are represented by i_{Ldnh} and i_{Lqnh}, which are filtered by the high-pass filter and APF , And the high-pass filter can be filtered by two low-pass filters, it can be expressed as:

$$\begin{cases} i_{Ldnh} = i_{Ld} - i^+_{Ld1h} \\ i_{Lqnh} = i_{Lq} - i^+_{Lq1h} \end{cases} \tag{14}$$

Another reference compensation current component on the d-axis is the output $i_{dc\text{-}ref}$ of the sliding mode controller, and another reference component on the q-axis is 0. The modified APF instruction current generation circuit diagram in dq coordinates is shown in the figure below.

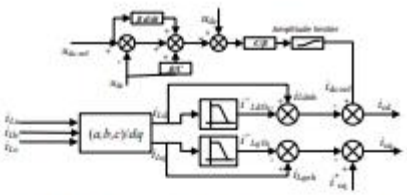

Figure 2. The diagram of command current generation circuit in dq coordinate.

IV. Design of Voltage Variable Sliding Mode Controller for APF DC Side

According to the APF mathematical model, the controllable state space model is derived as:

$$\frac{\mathrm{d}}{\mathrm{d}t}\begin{bmatrix} i_{cd} \\ i_{cq} \\ u_d \end{bmatrix} = \begin{bmatrix} -\frac{i_{cd}}{L} + \omega i_{cq} - \frac{S_d}{L} + \frac{e_d}{L} \\ -\omega i_{cd} + \frac{i_{cq}}{L} - \frac{S_q}{L} + \frac{e_q}{L} \\ \frac{e_d}{Cu_d} i_{cd} + \frac{e_q}{Cu_d} i_{cq} - \frac{u_d}{C} \end{bmatrix} \tag{15}$$

where, S_d and S_q are the mathematical models of switch function S_k in dq coordinate. It can be concluded that the relative order of the above formula is 3. Rewrite the above formula to obtain:

$$\frac{\mathrm{d}}{\mathrm{d}t}\begin{bmatrix} i_{cq} \\ u_d \\ \dot{u}_d \end{bmatrix} = \begin{bmatrix} f(i_{cq}) + C_1 \\ f_1(u_d) - f_2(u_d) \\ f'(i_{cq}) \cdot f_1(u_d) - \frac{1}{u_d}(f_1^2(u_d)) \\ -f_2^2(u_d)) + C_2 \end{bmatrix} \tag{16}$$

where, $f(i_{cq})=-i_{cq}/L$, $f_1(u_d)=(i_{cd}e_d+i_{cq}e_q)/Cu_d$, $f_2(u_d)=u_d/C$, $C_1=(e_q\cdot sat_M-\omega Li_{cd})/L$, $C_2=(s_d e_d+s_q e_q)/LC$

Let the expression of the error vector e be as follows:

$$\vec{e} = \begin{bmatrix} e_1 \\ e_2 \\ e_3 \end{bmatrix} = \begin{bmatrix} i_{cq} - i_{cq\text{-}ref} \\ u_d - u_{d\text{-}ref} \\ \dot{u}_d - \dot{u}_{d\text{-}ref} \end{bmatrix} \tag{17}$$

Let the feedback coefficients be k_1, k_2, and k_3, where $\beta = k_3 / k_2$. The expressions of the sliding mold surface S_1 and S_2 are:

$$\begin{cases} S_1 = k_1 e_1 = 0 \\ S_2 = k_2 e_2 + k_3 e_3 = e_2 + \beta e_3 = 0 \end{cases} \tag{18}$$

Substituting state space model formula (15) into formula (18), we get:

$$S_2 = \left[(u_d - u_{d\text{-}ref}) - \frac{\beta u_d}{C} - \beta \frac{\mathrm{d}u_{d\text{-}ref}}{\mathrm{d}t} + \frac{\beta}{Cu_d} e_q i_{cq} \right] \frac{Cu_d}{\beta e_d} + i_{cd} \tag{19}$$

Let be

$$i_{d\text{-}ref} = -\left[(u_d - u_{d\text{-}ref}) - \frac{\beta u_d}{C} - \beta \frac{\mathrm{d}u_{d\text{-}ref}}{\mathrm{d}t} + \frac{\beta}{Cu_d} e_q i_{cq} \right] \frac{Cu_d}{\beta e_d} \tag{20}$$

Rewrite the slip surface:

$$\begin{cases} S_1 = (i_{cq} - i_{cq\text{-}ref}) = 0 \\ S_2 = (i_{cd} - i_{cd\text{-}ref}) = 0 \end{cases} \tag{21}$$

Then $i_{cd\text{-}ref}$ can be expressed as:

$$i_{cd\text{-}ref} = -\left[(u_d - u_{d\text{-}ref}) + \beta \frac{\mathrm{d}u_{d\text{-}ref}}{\mathrm{d}t} - \frac{\beta u_d}{C} \right] \frac{Cu_d}{\beta} \tag{22}$$

According to equation (22), draw the block diagram of DC side voltage controller as follows:

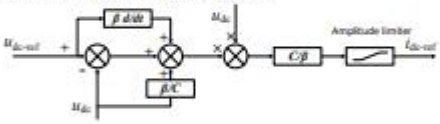

Figure 3. The diagram of Sliding mode variable structure controller.

V. Simulation Verification

In order to verify the feasibility of the proposed control strategy, the APF overall simulation circuit model was drawn with MATLAB software. The APF control structure in dq coordinates is shown in Figure 4, and the hardware simulation parameters in the circuit are shown in Table 1.

TABLE I. Simulation Parameters

Parameter	*Value*
Effective value of grid line voltage (U/V)	380
DC voltage (V_{dc}/V)	600
AC inductor(L/H)	3e-3
DC side capacitance(C/F)	2.2e-3
load(H)	10/2e-3

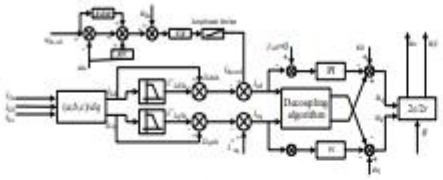

Figure 4. The control block diagram of APF in *dq* coordinate.

In order to seriously affect the effectiveness of the control strategy proposed in this paper, a simulation comparison of the PI control, the connection of the current-limiting resistor and the sliding mode variable structure control under *dq* coordinates were performed. Among them, PI controller parameters K_p=2, K_I=10, sliding mode controller parameters β=0.03, K_p=6.5, K_I=1900. Set the APF grid-connecting time to 0.04s. The DC-side voltage change curve in the three control modes is shown in the figure below.

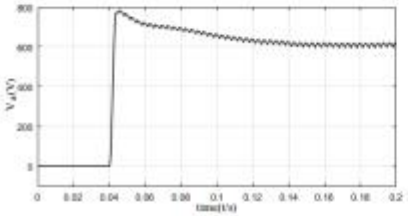

Figure 5. Effect of PI controller.

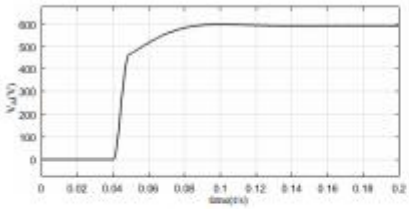

Figure 6. Connected current limiting resistor start control.

Figure 5 shows that the APF DC-side voltage adopts PI control. Before reaching the set value, a larger surge voltage will be generated. Correspondingly, a larger surge current will be generated in the AC-side power grid, which affects the compensation effect. Figure 6 is a waveform diagram of the APF DC side voltage with a current limiting resistor. The operation process is from uncontrolled rectification to controllable rectification. Although it can suppress the impulse voltage, it makes the APF start-up time too long, from charging to the DC side voltage. The preset time is approximately 0.06s.

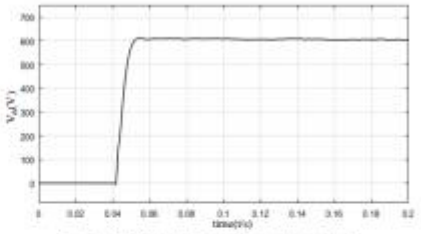

Figure 7. Sliding mode variable structure control.

Figure 7 shows the control method proposed in this paper. Due to its short command current link, the DC side voltage command current can control the IGBT faster. It has a shorter grid connection time than the method proposed in reference [8, 9].

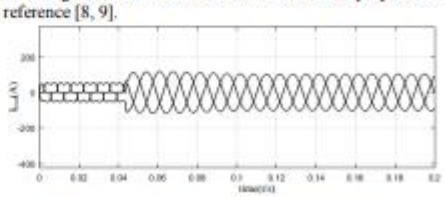

Figure 8. Current of AC side under sliding mode variable structure control.

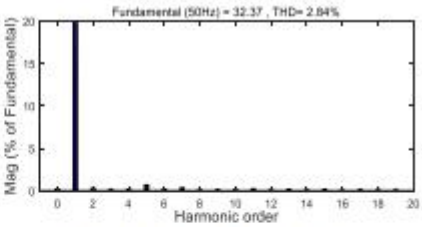

Figure 9. Total harmonic distortion of APF.

Figure 8 shows the compensation effect of the grid-side current corresponding to the method described in this paper. The FFT analysis of it is shown in Figure 9. The total harmonic distortion is 2.84%, which has an excellent harmonic compensation effect.

VI. Conclusion

Aiming at the problem of the impulse voltage and the long charging time when the APF is connected to the grid, this paper proposes a short-circuit voltage control of the APF DC side with a command current generation circuit link at *dq* coordinates. The side voltage is controlled by a sliding mode variable structure. Through simulation and comparison with traditional PI controllers and charging current limiting

resistors, the method described in this article can speed up the charging speed of APF DC side capacitors, improve its compensation performance, reduce the total harmonic distortion rate, and have a good Engineering application value.

REFERENCES

[1] Wang Feng, Zhang Xulong, Ji Wen. Research on Strategy of the DC-side Voltage Control of APF[J]. Power Electronics, 2017, 51(6): 40-42.

[2] Sheng Xu, An Improved Current-limiting Control Strategy for Shunt Active Power Filter[J]. IEEE, 2016:8,1306-1311.

[3] Allal El Moubarek Bouzid, Pierre Sicard, Ahmed Cheriti, Hicham Chaoui, Paul Makanga Koumba. Adaptive Hysteresis Current Control of Active Power Filters for Power Quality Improvement[C]. IEEE Electrical Power and Energy Conference (EPEC) 2017, 1-8.

[4] Li Cailin, Hai Zizhou, Cai Rujun, Zhou Zhilin. Control strategy based on specific harmonic compensation for three-phase four-wire active power filter[J]. Electrical Measurement & Instrumentation, 2017, 54(3): 83-88.

[5] Mariia Maliakova, Andrii Kalinov, Kremenchuk, Ukraine. APF Control with the Use of the Direction of the Energy Flow Determination Method in the Electric Circuit with a Nonlinear Load[C]. International Conference on Modern Electrical and Energy Systems (MEES), 2017, 10(1109): 220-223.

[6] Zhang Gaorong, Dai Xinyue. A DC Voltage Stabilizing and Balancing Control Method Based on H-Bridge Cascaded APF[J]. Electrical Measurement & Instrumentation, 2014, 51(20): 70-75.

[7] Deng Wenlang, Hu Bibi, Guo Yougui, Yuan Ting. Grading startup Control for Three-phase Voltage-source PWM rectifier[J]. Power Electronics, 2014, 48(1): 30-32.

[8] Yang Jianfeng, Yao Huashi, Shi Ge. Research on Time Optimal Control Algorithm of Parallel APF anti-Shock[J]. Journal of Systems Science and Mathematical Sciences, 2017, 39(9): 1904-1914.

[9] Liu Bo, Ben Hongqi, Bai Yinlong. A slow given method to suppress the start-up inrush current of PWM rectifier[J]. TRANSACTIONS OF CHINA ELECTROTECHNICAL SOCIETY, 2018, 33(12):2758-2766.

[10] Li Jinbin, Chen Chong. Research on DC side voltage control strategy of APF based on sliding-window iterative algorithm of DFT[J]. Electrical Measurement & Instrumentation, 2016, 53(22): 44-48.

2. Researchonelectrodeliftingsystembasedonrecursiveleastsquare methodandfuzzyPID

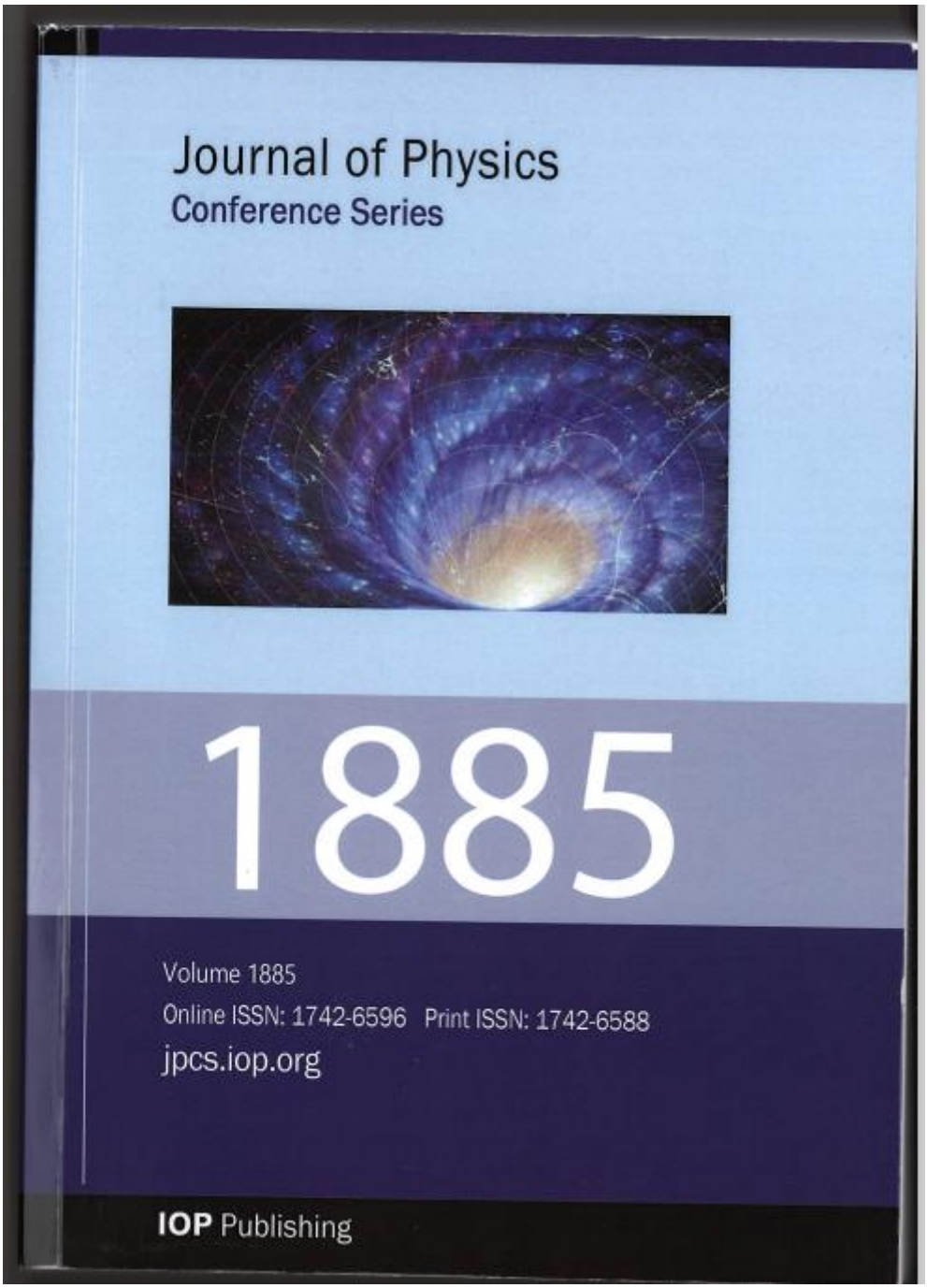

报告编号：2021-YZ-3804

论 著 检 索 报 告

委托内容： 周德东的论文收录情况

委托单位： 兰州工业学院

检索单位： 中国科学院兰州查新咨询中心

完成日期： 2021 年 7 月 2 日

中 国 科 学 院 兰 州 查 新 咨 询 中 心

二〇二一年制

一、检索要求

1、被检作者：周德东（Zhou Dedong；Zhou DD）

2、委托单位：兰州工业学院

3、论文发表年限：2021 年

4、提供待检索论文篇数：1 篇

二、检索范围

Engineering Village 2-Compendex (EI) 1884 - present 网络版

三、检索结果

1）收录：

- 有 1 篇被 EI 收录（记录见附件一）；

检索人： 检索单位： 中国科学院兰州查新咨询中心

审核人： 完成时间： 2021 年 7 月 2 日

附件：

一、EI 收录情况

<RECORD 1>

Accession number:20212110381727
Title:Research on electrode lifting system based on recursive least square method and fuzzy PID (Open Access)
Authors:Zhou, De-Dong (0); Su, Fang (0)
Source title:Journal of Physics: Conference Series
Abbreviated source title:J. Phys. Conf. Ser.
Volume:1885
Part number:4 of 5
Issue:4
Issue title:2021 7th International Conference on Manufacturing Technology and Applied Materials, ICAMMT 2021 - 3. Intelligent Mechanical Technology and Automated Manufacturing Process
Issue date:April 28, 2021
Publication year:2021
Article number:042053
Language:English
ISSN:17426588
E-ISSN:17426596
Document type:Conference article (CA)
Conference name:2021 7th International Conference on Manufacturing Technology and Applied Materials, ICAMMT 2021
Conference date:March 26, 2021 - March 28, 2021
Conference location:Sanya, China
Conference code:168830
Publisher:IOP Publishing Ltd
Abstract: The electrode of calcium carbide furnace bears the function of conduction, heat transfer and furnace condition regulation. How to keep the furnace condition in the best condition by lifting and lowering the electrode has always been a hot and difficult point in the research. In this paper, based on the analysis of the equivalent circuit of calcium carbide furnace, the system model of electrode position-current is identified by the recursive least square method, and a fuzzy PID controller based on the constant control strategy of electrode current is designed to keep the furnace condition in the best state. The simulation and application results show that the designed system has good dynamic response, anti-disturbance ability and robustness.
 © Published under licence by IOP Publishing Ltd.
Number of references:10
Main heading:Least squares approximations
Controlled terms:Calcium carbide - Electrodes - Equivalent circuits - Furnaces - Heat transfer - Manufacture - Three term control systems
Uncontrolled terms:Best state - Control strategies - Electrode current - Fuzzy PID controller - Fuzzy-PID - Lifting systems - Recursive least square methods - System modeling
Classification code:537.1 Heat Treatment Processes - 641.2 Heat Transfer - 731.1 Control Systems - 804.2 Inorganic Compounds - 921.6 Numerical Methods
DOI:10.1088/1742-6596/1885/4/042053

Database:Compendex

（End）

文本复制检测报告单(简洁)

No:BC20210927135251224939373　　检测时间:2021-09-27 13:52:51

检测文献: Research on electrode lifting system based on recursive least square method and fuzzy PID

作者: ZHOU De-dong, SU Feng

检测范围:
中国学术期刊网络出版总库
中国重要会议论文全文数据库
中国重要报纸全文数据库
中国专利全文数据库
英文数据库(涵盖期刊、博硕、会议的英文数据以及德国Springer、英国Taylor&Francis 期刊数据库等)
港澳台学术文献库
优先出版文献库
图书资源

时间范围: 1915-01-01至2021-04-27

检测结果

去除本人文献复制比: 0%

去除引用文献复制比: 0%　　总文字复制比: 0%

单篇最大文字复制比: 0%()

重复字数:	[0]	总段落数:	[1]
总字数:	[16409]	疑似段落数:	[0]
单篇最大重复字数:	[0]	前部重合字数:	[0]
疑似段落最大重合字数:	[0]	后部重合字数:	[0]
疑似段落最小重合字数:	[0]		

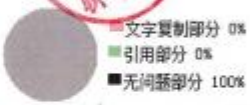

指　标:	疑似剽窃观点	疑似剽窃文字表述	一稿多投	疑似整体剽窃	过度引用	重复发表
表格: 0	公式: 没有公式	疑似文字的图片: 1(OCR)	脚注与尾注: 0			

1. Research on electrode lifting system based on recursive least square method and fuzzy PID　　总字数: 16409

相似文献列表

去除本人文献复制比: 0%(0)　　文字复制比: 0%(0)　　疑似剽窃观点: (0)

说明:

1. 总文字复制比:被检测论文总重合字数在总字数中所占的比例
2. 去除引用文献复制比:去除系统识别为引用的文献后,计算出来的重合字数在总字数中所占的比例
3. 去除本人文献复制比:去除作者本人文献后,计算出来的重合字数在总字数中所占的比例
4. 单篇最大文字复制比:被检测文献与所有相似文献比对后,重合字数占总字数的比例最大的那一篇文献的文字复制比
5. 指标是由系统根据《学术论文不端行为的界定标准》自动生成的
6. 红色文字表示文字复制部分;绿色文字表示引用部分;标灰色文字表示作者本人文献部分
7. 本报告单仅对您所选择比对资源范围内检测结果负责

amlc@cnki.net
http://check.cnki.net/
http://e.weibo.com/u/3194559873/

Research on electrode lifting system based on recursive least square method and fuzzy PID

ZHOU De-dong SU Fang

School of Electrical Engineering, Lanzhou Institute of Technology，Lanzhou Gansu,China

445291776@qq.com, suf@lzit.edu.cn

Abstract. The electrode of calcium carbide furnace bears the function of conduction, heat transfer and furnace condition regulation. How to keep the furnace condition in the best condition by lifting and lowering the electrode has always been a hot and difficult point in the research. In this paper, based on the analysis of the equivalent circuit of calcium carbide furnace, the system model of electrode position-current is identified by the recursive least square method, and a fuzzy PID controller based on the constant control strategy of electrode current is designed to keep the furnace condition in the best state. The simulation and application results show that the designed system has good dynamic response, anti-disturbance ability and robustness.

1. Introduction

At present, the electrode lifting operation of calcium carbide furnace is realized through the hydraulic transmission device. The electrode lifting operation is divided into single-phase separate operation and three-phase simultaneous operation. The secondary side of the furnace transformer is usually triangular wiring mode [1-3]. When a phase electrode is operated separately, it will affect the arc current of the other two phases, which is easy to cause three-phase imbalance. The strong coupling of the calcium carbide furnace is reflected in this point. When the three-phase electrode is operated up and down at the same time, the three-phase electrical power balance can be maintained (it is assumed that the three-phase equilibrium state is maintained before the operation of the calcium carbide furnace), and the pressure of the hydraulic station (including the energy accumulator) is required to support the simultaneous action of the three-phase electrode [4-6].

Electrode lifting range is determined by the condition of calcium carbide furnace. In normal production, the electric arc current in the furnace can be adjusted through the electrode lifting operation, and the input electric power can be changed, so as to improve the direction of the furnace condition to the furnace temperature stability change; During maintenance work, the electrode end needs to be lifted to the height of the charge surface; During the operation of the oven, the electrode end needs to be pressed to a certain height from the bottom of the furnace [7-10]. Therefore, in a sense, the position of the electrode determines the condition of the calcium carbide furnace.

It is difficult to establish a definite relationship between electrode position and arc current because of the time-varying and random characteristics of calcium carbide furnace. It is found in the field operation that the closer the electrode end is to the liquid surface of the molten pool, the greater the

electrode current is. Based on this, this paper intends to establish the system model of electrode position-current by using the method of system identification, and then design the model into the fuzzy PID control system.The first paragraph after a heading is not indented (Bodytext style).

2. Analysis of equivalent circuit of calcium carbide furnace

2.1. Short-net connection mode of calcium carbide furnace

Short network refers to the general term of all kinds of connected conductors from the outlet end of the secondary side of the calcium carbide furnace transformer to the electrode. The commonly used connection mode of short network is shown in Figure 1.

Fig. 1 (a) shows the connection mode between a three-phase furnace transformer and the electrode. The transformer is installed near a certain electrode, and due to the asymmetry of the physical structure of the three-phase short grid, the three-phase impedance is deviated, resulting in the unbalanced three-phase load. In addition, three-phase transformer is used for power supply. The non-linearity of transformer and the coupling between phases have a great influence, which leads to the decrease of electric heating efficiency and the increase of power loss of calcium carbide furnace.

Fig. 1 (b) shows the connection mode between three single-phase furnace transformers and electrodes. The transformer is symmetrically installed near the electrode and the short network is symmetrically arranged, which can effectively reduce the inductive reactance of the short network and thus eliminate the unbalance degree of the three-phase load. In addition, three single-phase transformers are used for power supply, which can greatly reduce the non-linearity of the transformer and the coupling influence between phases, thus improving the electric heating efficiency of the calcium carbide furnace and reducing the power loss. The disadvantage is that three single-phase transformers need to be equipped, and the cost is higher.

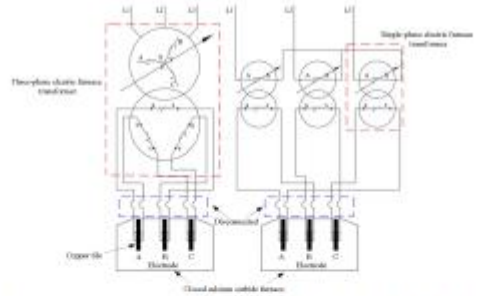

Figure 1 Short-grid connection mode of calcium carbide furnace

2.2. Equivalent circuit of calcium carbide furnace

The equivalent circuit of the secondary side winding of the electric furnace transformer, the water-cooled soft cable, the water-cooled conductive cross arm, the charge between electrodes and the working conditions in the furnace are represented by the equivalent resistance, as shown in Fig. 2.

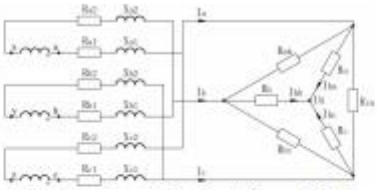

Figure 2 Equivalent circuit of calcium carbide furnace

Which, $R_{a1}+jX_{a1}$、$R_{b1}+jX_{b1}$、$R_{c1}+jX_{c1}$ and $R_{a2}+jX_{a2}$、$R_{b2}+jX_{b2}$、$R_{c2}+jX_{c2}$ are the equivalent impedance of the secondary winding, short net and electrode of the transformer, I_a、I_b and I_c are electrode currents of electrode A, B and C, respectively; R_{ab}、R_{bc} and R_{ca} are the transverse charge resistance, Form a △ connection loop; R_a、R_b and R_c Is the longitudinal charge resistance,A Y connection loop is formed for the neutral point U_0 of the molten pool; I_{ha}、I_{hb} and I_{hc} are arc currents respectively。

The neutral point U_0 of the molten pool is to facilitate the analysis of the virtual equipotential point, and the arc current flows through a circuit formed between the electrodes. Therefore, the $Y-\Delta$ conversion theory is adopted, and the longitudinal charge resistance R_a、R_b and R_c are equivalent to Δ loads, and the transformation formula is:

$$\begin{aligned} R_{ab}^{'} &= \frac{R_aR_b+R_bR_c+R_cR_a}{R_c} \\ R_{bc}^{'} &= \frac{R_aR_b+R_bR_c+R_cR_a}{R_a} \\ R_{ca}^{'} &= \frac{R_aR_b+R_bR_c+R_cR_a}{R_b} \end{aligned} \tag{1}$$

Thus, the total equivalent resistance between electrodes A, B and C is:

$$\begin{aligned} R_{AB} &= R_{ab} // R_{ab}^{'} = \frac{R_{ab}R_{ab}^{'}}{R_{ab}+R_{ab}^{'}} \\ R_{BC} &= R_{bc} // R_{bc}^{'} = \frac{R_{bc}R_{bc}^{'}}{R_{bc}+R_{bc}^{'}} \\ R_{CA} &= R_{ca} // R_{ca}^{'} = \frac{R_{ca}R_{ca}^{'}}{R_{ca}+R_{ca}^{'}} \end{aligned} \tag{2}$$

The above equivalence and conversion are carried out on the premise that the smelting condition is stable and the resistance value of each kind is equal.

2.3. Equivalent circuit of calcium carbide furnace

In the total equivalent resistance between electrodes A、B and C, the transverse charge resistance R_{ab}、R_{bc} and R_c change with the change of the smelting condition in the furnace, and the range of change is large, and there will be A jump when the material collapse. Longitudinal charge resistance A, C and C show periodic changes with the process of smelting and discharging, and the resistance value is the minimum before discharging, and gradually increases with the decrease of molten pool liquid level in discharging process. In the process of electrode discharge, the transverse charge resistance and the longitudinal charge resistance are both greatly disturbed.

The arc current accounts for most of the electrode current, and the arc current changes with the change of the total equivalent resistance between the electrodes. Therefore, in the actual control, the amplitude of the electrode current is always used as the basis for adjusting the smelting condition of calcium carbide furnace.

3. Modeling of electrode position and current identification

Calcium carbide furnace condition adjustment means transformer load regulation (voltage regulator switch), electrode rise and fall, charge resistivity changes. A voltage regulator is usually used for a wide range of load adjustment; The change of the resistivity of the charge is related to the ratio of raw materials, which is usually not used as a method of load adjustment. For small adjustment of load, electrode lifting operation is generally used.

The electrode control requirements of calcium carbide furnace are that the electrode position follows the level of molten pool liquid, that is, before the furnace, the electrode position is also high when the molten pool liquid level is high. After discharging, the electrode position of the molten pool should also drop when the liquid level drops. With the continuous smelting of calcium carbide, the liquid level of the molten pool increases gradually, and the electrode position also increases slowly. The basis of the lifting and lowering of the electrode is to keep the electrode current basically constant. However, there is no definite model between the electrode position and the electrode current. In this paper, the system identification method is adopted to establish the relationship between the two.

3.1. Recursive least square method

Recursive least square method is a method to estimate the actual output of the system at the present moment based on the past operation data. The structure diagram of electrode position-current identification system of calcium carbide furnace is shown in Fig. 3.

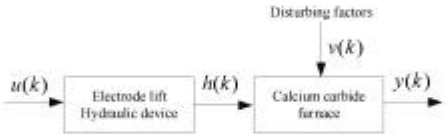

Figure 3 Structure diagram of electrode position-current identification system

In Figure 3, $u(k)$ and $u(k)$ are the discrete input and output of system model $G(z^{-1})$, representing the K-th electrode position control quantity and electrode current respectively. Noise model $N(z^{-1})$ is mainly the interference factor $v(k)$, representing the disturbed conditions such as carbide furnace collapse, discharge and electrode pressure discharge.

Recursive least square method is a method based on the ARX model, which is of the form:

$$y(k) = -a_1 y(k-1) - a_2 y(k-2) - \cdots - a_{na} y(k-na) + b_1 u(k-1) + \cdots + b_{nb} u(k-nb) + v(k) \quad (3)$$

It can also be written

$$\mathbf{A}(z^{-1})\mathbf{y}(k) = \mathbf{B}(z^{-1})\mathbf{u}(k) + \mathbf{v}(k) \quad (4)$$

Which

$$\mathbf{A}(z^{-1}) = 1 + a_1 z^{-1} + a_2 z^{-2} + \cdots + a_{na} z^{-na}$$
$$\mathbf{B}(z^{-1}) = b_1 z^{-1} + b_2 z^{-2} + \cdots + b_{nb} z^{-nb} \quad (5)$$

This model is to estimate the output value y at time k according to u values and y values before time k. Equation (4) is written in the least square format as:

$$\mathbf{y}(k) = \mathbf{h}^{\mathrm{T}}(k)\boldsymbol{\theta} + \mathbf{v}(k) \quad (6)$$

Set

$$\mathbf{e}(k)=\mathbf{y}(k)-\hat{\mathbf{y}}(k)=\mathbf{y}(k)-\mathbf{h}^{\mathrm{T}}(k)\hat{\boldsymbol{\theta}} \tag{7}$$

The least squares estimation requires the minimum sum of squares of the deviation, that is, its objective function is:

$$\mathbf{J}=\mathbf{e}(k)^{\mathrm{T}}\mathbf{e}(k)=(\mathbf{y}(k)-\mathbf{h}^{\mathrm{T}}(k)\hat{\boldsymbol{\theta}})^{\mathrm{T}}(\mathbf{y}(k)-\mathbf{h}^{\mathrm{T}}(k)\hat{\boldsymbol{\theta}}) \tag{8}$$

The least squares estimate of $\boldsymbol{\theta}$ is obtained by taking the partial derivative of $\mathbf{J}$ with respect to $\hat{\boldsymbol{\theta}}$, and setting $\hat{\boldsymbol{\theta}}$ equal to 0. At time k-1 and time k, the parameter estimation result of the system is:

$$\begin{cases}\hat{\boldsymbol{\theta}}(k-1)=(\mathbf{h}^{\mathrm{T}}(k-1)\mathbf{h}(k-1))^{-1}\mathbf{h}^{\mathrm{T}}(k-1)\mathbf{y}(k-1)\\ \hat{\boldsymbol{\theta}}(k)=(\mathbf{h}^{\mathrm{T}}(k)\mathbf{h}(k))^{-1}\mathbf{h}^{\mathrm{T}}(k)\mathbf{y}(k)\end{cases} \tag{9}$$

Which, $\hat{\boldsymbol{\theta}}(k)$ and $\hat{\boldsymbol{\theta}}(k-1)$ are estimated values of least squares parameters that can be calculated and obtained according to the first k and the first $k-1$ observation/sampling data respectively. The key to the calculation is the recursive calculation of matrix inverse. The calculation derivation process can be seen in Literature [10], and the final calculation formula is:

$$\begin{cases}\hat{\boldsymbol{\theta}}(k)=\hat{\boldsymbol{\theta}}(k-1)+\mathbf{P}(k)\boldsymbol{\phi}(k-1)[y(k)-\boldsymbol{\phi}^{\mathrm{T}}(k-1)\hat{\boldsymbol{\theta}}(k-1)]\\ \mathbf{P}(k)=[\mathbf{I}-\dfrac{\mathbf{P}(k-1)\boldsymbol{\phi}(k-1)\boldsymbol{\phi}^{\mathrm{T}}(k-1)}{1+\boldsymbol{\phi}^{\mathrm{T}}(k-1)\mathbf{P}(k-1)\boldsymbol{\phi}(k-1)}]\mathbf{P}(k-1)\end{cases} \tag{10}$$

The order of calculation is $\mathbf{P}(k)$ first, then $\hat{\boldsymbol{\theta}}(k)$.

3.2. System parameter estimation

The operation data of a calcium carbide furnace collected on site are shown in Table 1.

Table 1 Sample data

Electrode position (mm)			Electrode current (kA)		
A	B	C	A	B	C
167	161	170	74.0	74.1	73.8
189	184	186	73.2	74.6	73.4
215	195	184	72.5	72.8	72.7
235	228	230	70.9	71.4	69.7
244	247	239	68.0	67.1	66.6
257	260	255	65.7	64.3	63.8
268	271	270	62.2	61.6	63.3
281	280	284	57.5	58.6	58.9
294	294	297	52.6	53.2	54.3
301	305	308	48.6	48.2	49.3

The data shown in Table 1 are all recorded when the smelting condition of calcium carbide furnace is relatively stable, which is characterized by basic balance of three phases.

System parameter estimation steps :(1) Collection/pretreatment of sample data; (2) Determine the model structure and order; (3) Recursive least square method was used to estimate model parameters; (4) Carry out reliability test on the identification model and compare the corresponding data of the test method; (5) The electrode position-current model parameters of three-phase electrodes A, B and C were identified by this method.

3.3. Electrode position-current model

According to the above model identification method, the relationship model between three-phase electrode position and electrode current of calcium carbide furnace can be written as follows:

$$\begin{bmatrix} I_A(t) \\ I_B(t) \\ I_C(t) \end{bmatrix} = \mathbf{A}^{\mathrm{T}}(z^{-1})\mathbf{B}(z^{-1}) \begin{bmatrix} h_A(t-nk) \\ h_B(t-nk) \\ h_C(t-nk) \end{bmatrix} \tag{11}$$

Which, z^{-1} is the delay operator, nk is the delay of the model, $I_A(t)$、$I_B(t)$ and $I_C(t)$ are the current of three-phase electrode at time, $h_A(t-nk)$、$h_B(t-nk)$、$h_C(t-nk)$ denotes the position of three-phase electrode at time t, $\mathbf{A}(z^{-1})$、$\mathbf{B}(z^{-1})$ are the model parameter matrices.

$$\mathbf{A}(z^{-1}) = \begin{bmatrix} A_a(z^{-1}) \\ A_b(z^{-1}) \\ A_c(z^{-1}) \end{bmatrix}$$

$$\mathbf{B}(z^{-1}) = \begin{bmatrix} B_{a0}(z^{-1}) & B_{a2}(z^{-1}) & B_{a3}(z^{-1}) \\ B_{b1}(z^{-1}) & B_{b2}(z^{-1}) & B_{b3}(z^{-1}) \\ B_{c1}(z^{-1}) & B_{c2}(z^{-1}) & B_{c3}(z^{-1}) \end{bmatrix}$$

The identification model was selected as ARX model with order 2, that is, $na = nb = 2$. In Matlab, parameters for off-line identification based on measured data are as follows:

$$\mathbf{A}(z^{-1}) = \begin{bmatrix} 1.02 & -0.12 \\ 0.98 & -0.09 \\ 0.99 & -0.11 \end{bmatrix} \begin{bmatrix} I_A(t-1) & I_A(t-2) \\ I_B(t-1) & I_B(t-2) \\ I_C(t-1) & I_C(t-2) \end{bmatrix}$$

$$\mathbf{B}(z^{-1}) = \begin{bmatrix} -1.18 & 1.57 & -0.42 \\ -0.88 & 1.12 & -0.26 \\ 0.26 & -0.25 & 0 \end{bmatrix} \begin{bmatrix} h_A(t) \\ h_A(t-1) \\ h_A(t-2) \end{bmatrix} +$$

$$\begin{bmatrix} 0.22 & -0.21 & 0 \\ -1.11 & 1.53 & -0.42 \\ -0.93 & 1.30 & -0.39 \end{bmatrix} \begin{bmatrix} h_B(t) \\ h_B(t-1) \\ h_B(t-2) \end{bmatrix} +$$

$$\begin{bmatrix} -0.84 & 1.17 & -0.33 \\ 0.19 & -0.20 & 0 \\ -1.10 & 1.47 & -0.41 \end{bmatrix} \begin{bmatrix} h_C(t) \\ h_C(t-1) \\ h_C(t-2) \end{bmatrix}$$

4. Control system design

In this paper, the idea of constant electrode current is used to control the rise and fall of the electrode. The fuzzy PID control system is shown in Fig. 4.

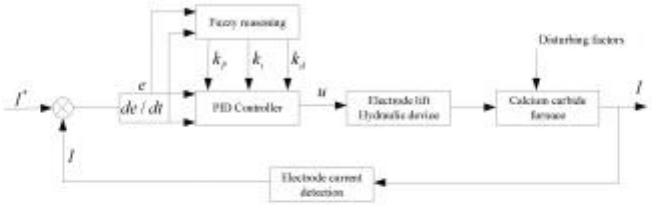

Figure 4 Schematic diagram of fuzzy PID control system

4.1. Recursive least square method

The input variables are electrode current error e and error change rate ec. Fuzzy rules, fuzzy reasoning and defuzzification are formulated. PID parameters k_p、k_i、k_d are adjusted in real time to meet the control requirements of time-varying and randomness of the furnace condition of carbide furnace.

The fuzzy set of input variables e and ec is e, $NM, NS, Z, PS, PM, PB\}$, and the corresponding domain is $e, ec = [-3, -2, -1, 0, 1, 2, 3]$. The fuzzy set of output variable k_p、k_i and k_d v is $k_p, k_i, k_d = \{NB, NM, NS, Z, PS, PM, \quad PB\}$, and the corresponding domain scope is $k_p = [-0.3 \quad 0.3]$、$k_i = [-0.06 \quad 0.06]$、$k_d = [-3 \quad 3]$.

The fuzzy rules formulated are shown in Table 2.

Table 2: Fuzzy rule table

kp ki kd		ec						
		NB	NM	NS	Z	PS	PM	PB
e	NB	PB NB PS	PB NB NS	PM NM NB	PM NM NB	PS NS NB	Z Z NM	Z Z PS
	NM	PB NB PS	PB NB NS	PM NM NB	PS NS NM	PS NS NM	Z Z NS	NS Z Z
	NS	PM NB Z	PM NM NS	PM NS NM	PS NS NM	Z Z NS	NS PS NS	NS PS Z
	Z	PM NM Z	PM NM NS	PS NS NS	Z Z NS	NS PS NS	NM PM NS	NM PM Z
	PS	PS NM Z	PS NS Z	Z Z Z	NS PS Z	NS PS Z	NM PM Z	NM PB Z
	PM	PS Z PB	Z Z NS	NS PS PS	NM PS PS	NM PM PS	NM PB PS	NB PB PB
	PB	Z Z PB	Z Z PM	NM PS PM	NM PM PM	NM PM PS	NB PB PS	NB PB PB

Fuzzy Reasoning *Zadeh* approximate reasoning method is used to derive fuzzy system. To defuzzify, select *Centroid*, the center of gravity method, and obtain the output control quantity, so as to obtain the parameter adjustment quantity of k_p、 k_i and k_d of the fuzzy PID control system.

$$\begin{cases} k_p = k_p^{'} + \{e_i, ec_i\}_p \\ k_i = k_i^{'} + \{e_i, ec_i\}_i \\ k_d = k_d^{'} + \{e_i, ec_i\}_d \end{cases} \quad (12)$$

4.2. Recursive least square method

The application object is a closed calcium carbide furnace, the capacity of which is 21000kVA, the high voltage side is powered by 110kV, the electrode lifting operation is driven by hydraulic device. The control system is composed of upper industrial computer and PLC (S7-1200 series). The two are connected by Profeibus-DP field bus. The fuzzy PID controller designed according to the control idea in this paper runs in the way of timing interrupt in PLC. The system operation data is recorded every 30s and stored in the WinCC database installed by the upper IPC.

After the control system was put into operation for about 40min, the furnace condition was relatively stable. The recorded three-phase electrode position and electrode current data were drawn into a curve, as shown in Fig. 5.

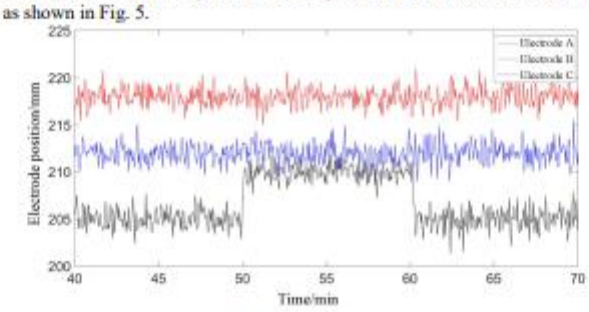

（a）Electrode position

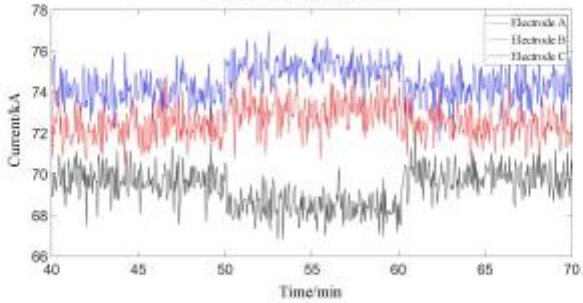

（b）Electrode current

Figure 5: Electrode position and electrode current curve

In Fig.5, the positions of electrode A, B and C are 212mm, 218mm and 205mm respectively, and the corresponding electrode currents are 74kA, 72.3kA and 69.7kA respectively. When the operating time is about 50min, the operating electrode C rises 5mm, resulting in A slight increase in the current of electrode A and B, and A slight decrease in the current of electrode C. When the operating time is about 60min, the operating electrode C drops 5mm, and the current of electrode A, B and C basically returns to the original value.

5. conclusion

(1) The fuzzy PID control system based on the constant control strategy of electrode current designed in this paper, through simulation and application, shows that the system has good dynamic response, anti-disturbance ability and robustness.

(2)Starting from the equivalent circuit of calcium carbide furnace, the electrode position-current system model identified by the recursive least square method is suitable for the relationship between electrode position and electrode current of calcium carbide furnace. By adjusting the electrode position, the electrode current can be changed, and then the furnace temperature can be controlled, so that the furnace condition can be maintained in a better state.

(3) Calcium-carbide furnace condition is very complex, time-varying and random characteristics are obvious, in the occurrence of such as collapse, discharge or electrode pressure release and other large disturbance, the performance of the control system becomes worse, the need for manual intervention. However, the furnace condition is relatively stable during most period of smelting process, so the control system is applicable.

References

[1] Xiong,M.Y., Yue H.L.(2010)Practical Manual of New Technology and New Process of Production and Processing of Calcium Carbide, Development and Utilization of Products and Pollution Prevention and Rectify. Chemical Industry Press，Beijing.

[2] Cgen, L.(2016) Application of Adaptive PID Control in Electrode Lifting Control. Automation Technology and Application,35(05):20-23+30.

[3] Zhou,X.F. (2015) Design of Embedded Automatic Control System for Electrode Lifting in Carbide Furnace . Journal of Baotou Vocational and Technical College,16(03):22-24.

[4] Fu,C., Zhang,S.J, Jin, X.M, Huang,W.(2018) Integrated control and optimization strategy for the whole process of calcium carbide production. Automation Instrumentation,39(08):23-26.

[5] Zhang,L., He,Z., Zhang,S.J., Chen,W. (2015)Research and Application of Soft Sensor Measurement for Electrode Length of Large Closed Calcium Carbide Furnace. Automation and Instrumentation,30(12):20-23.

[6] Chen,L. (2015)Application of PLC Control in Electrode Lifting Control of Calcium Carbide Furnace . Chemical Industry Automation & Instrumentation,42(12): 1378-1380 +1390.

[7] Li,Y.L.(2013) Electrode of closed calcium carbide furnace. Science and Technology Innovation and Application,(19):1-2.

[8] Yin, L.J., Cai, Z.Y.(2020)Research on Synthetic Test Control Method Based on Recursive Least Squares Algorithm. Electrical Appliances and Energy Efficiency Management Technology,2020(04):11-17.

[9] Xu, Y., Jin,W.J.LEI, X.(2019) Dynamic model identification of photovoltaic inverters based on recursive least squares . Acta Energitica Solaris Sinica,40 (10):2797-2805.

[10] Hou,Y.B., Zhou, L., Wang,L.Q., Song,V.F.(2019) System Identification. Xidian University Press, Xi 'an.

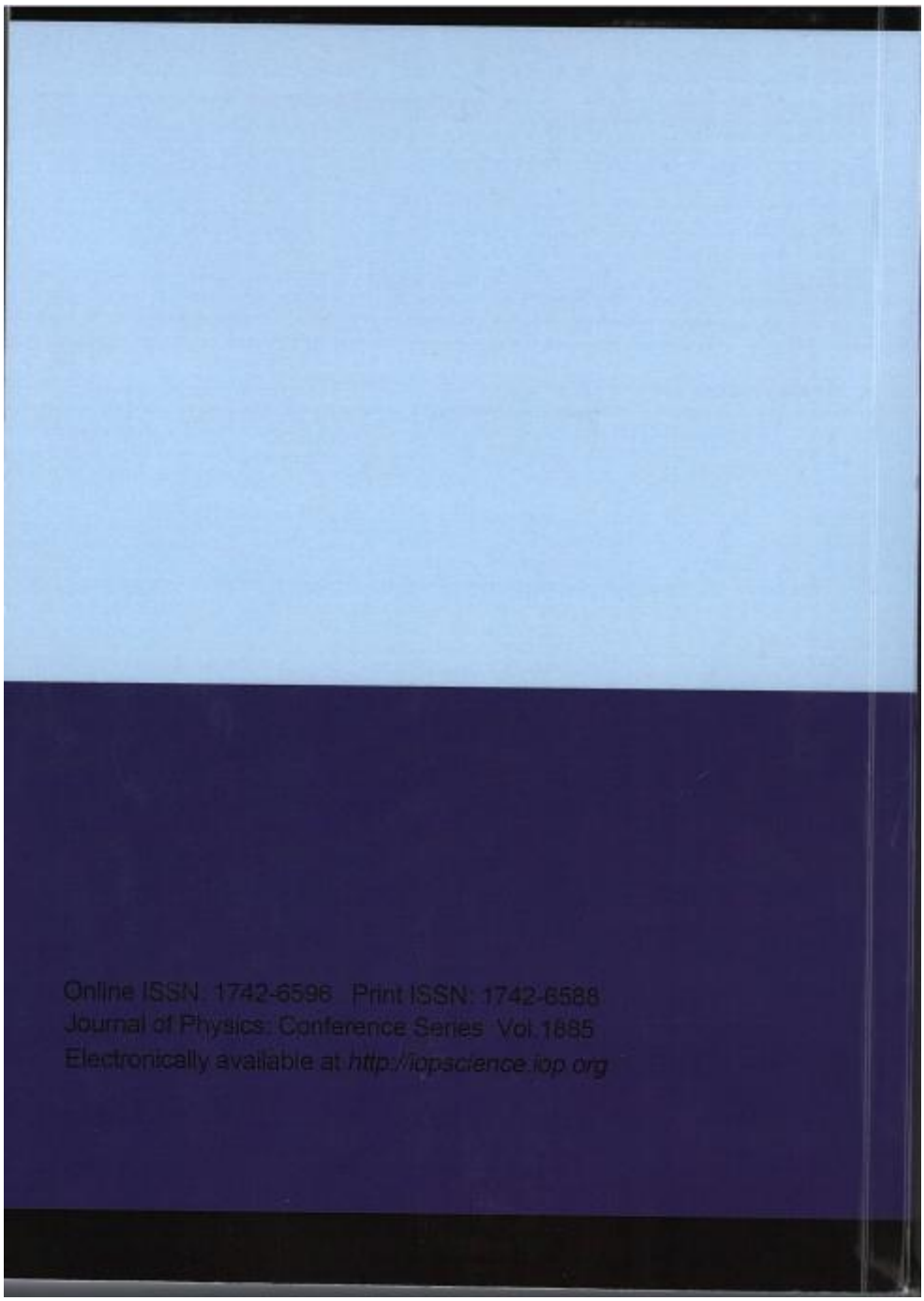
Online ISSN: 1742-6596 Print ISSN: 1742-6588
Journal of Physics: Conference Series Vol.1885
Electronically available at http://iopscience.iop.org

3. application of text error correction algorithm in railway speech recognition

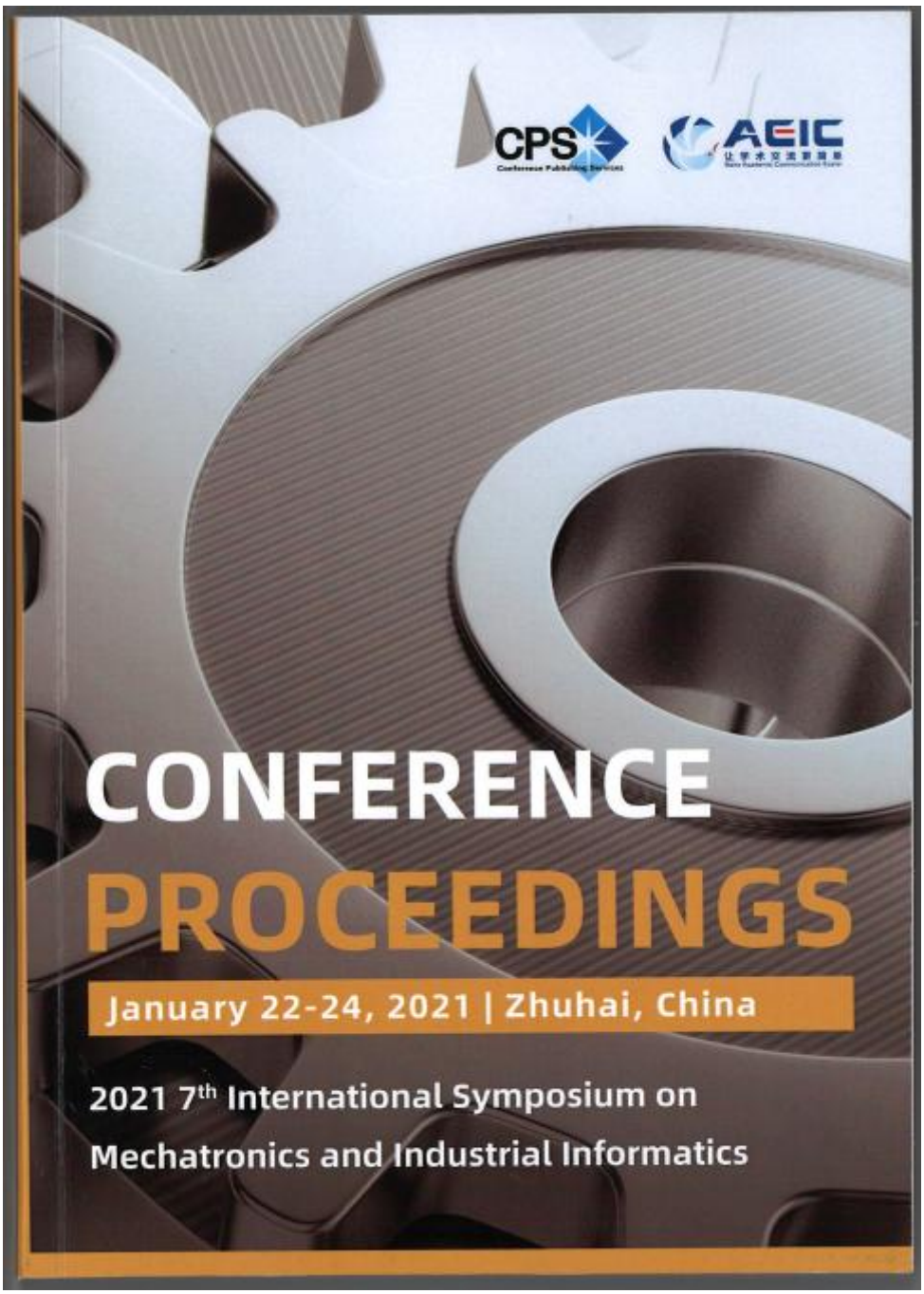

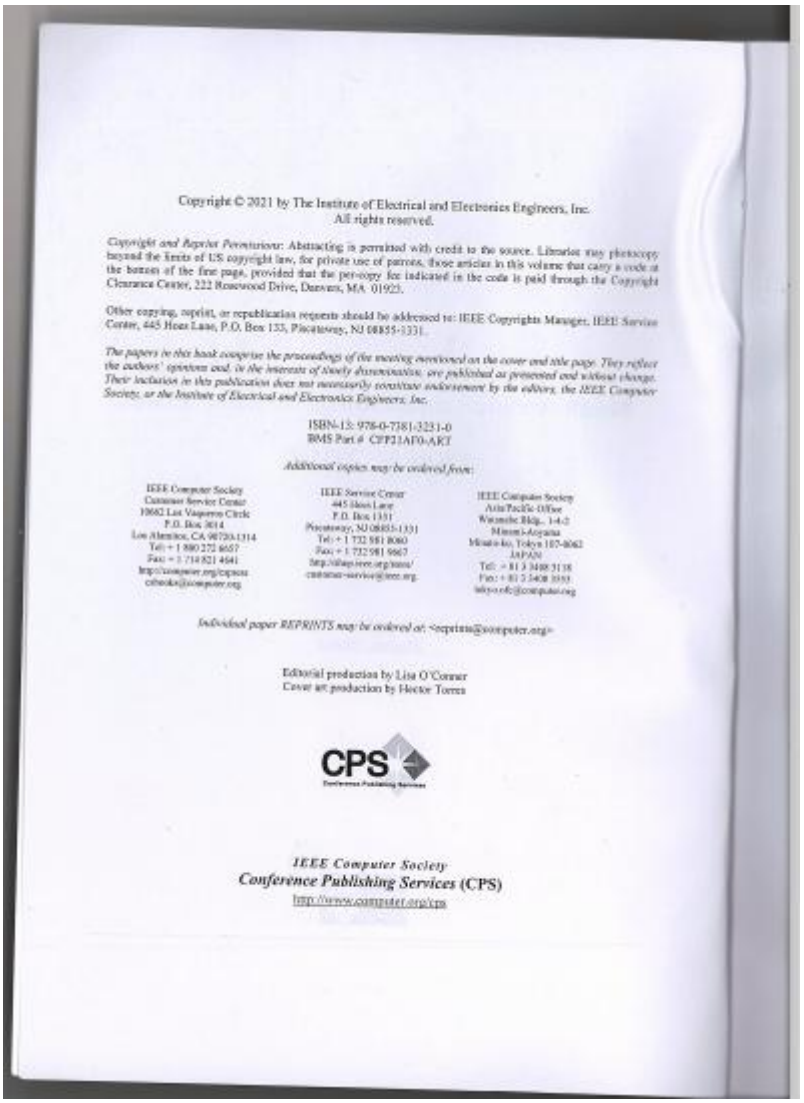

ISBN-13: 978-0-7381-3231-0
BMS Part # CFP21AF0-ART

Additional copies may be ordered from:

IEEE Computer Society
Customer Service Center
10662 Los Vaqueros Circle
P.O. Box 3014
Los Alamitos, CA 90720-1314
Tel: + 1 800 272 6657
Fax: + 1 714 821 4641
http://computer.org/cspress
csbooks@computer.org

IEEE Service Center
445 Hoes Lane
P.O. Box 1331
Piscataway, NJ 08855-1331
Tel: + 1 732 981 8060
Fax: + 1 732 981 9667
http://shop.ieee.org/store/
customer-service@ieee.org

IEEE Computer Society
Asia/Pacific Office
Watanabe Bldg., 1-4-2
Minami-Aoyama
Minato-ku, Tokyo 107-8062
JAPAN
Tel: + 81 3 3408 3118
Fax: + 81 3 3408 3553
tokyo.ofc@computer.org

Individual paper REPRINTS may be ordered at: <reprints@computer.org>

Editorial production by Lisa O'Conner
Cover art production by Hector Torres

IEEE Computer Society
***Conference Publishing Services* (CPS)**
http://www.computer.org/cps

报告编号：2021-YZ-3179

论 著 检 索 报 告

委托内容： 周德东的论文收录情况

委托单位： 兰州工业学院

检索单位： 中国科学院兰州查新咨询中心

完成日期： 2021 年 5 月 26 日

中 国 科 学 院 兰 州 查 新 咨 询 中 心

二〇二一年制

一、检索要求

1、被检作者：周德东（Zhou Dedong；Zhou DD）

2、委托单位：兰州工业学院

3、论文发表年限：2021 年

4、提供待检索论文篇数：2 篇

二、检索范围

Engineering Village 2-Compendex (EI) 1884 - present 网络版

三、检索结果

1）收录：

- 有 2 篇被 EI 收录（记录见附件一）。

检索人：焦蒙 检索单位： 中国科学院兰州查新咨询中心

审核人： 完成时间： 2021 年 5 月 26 日

附件：

一、EI 收录情况

<RECORD 1>

Accession number:20211910316377
Title:Application of Text Error Correction Algorithm in Railway Speech Recognition
Authors:Zhou, Dedong (1); Su, Fang (1)
Author affiliation:(1) Lanzhou Institute of Technology, School of Electrical Engineering, Lan Zhou, China
Source title:Proceedings - 2021 7th International Symposium on Mechatronics and Industrial Informatics, ISMII 2021
Abbreviated source title:Proc. - Int. Symp. Mechatronics Ind. Informatics, ISMII
Part number:1 of 1
Issue title:Proceedings - 2021 7th International Symposium on Mechatronics and Industrial Informatics, ISMII 2021
Issue date:January 2021
Publication year:2021
Pages:176-179
Article number:9407567
Language:English
ISBN-13:9780738132310
Document type:Conference article (CA)
Conference name:7th International Symposium on Mechatronics and Industrial Informatics, ISMII 2021
Conference date:January 22, 2021 - January 24, 2021
Conference location:Virtual, Zhuhai, China
Conference code:168557
Publisher:Institute of Electrical and Electronics Engineers Inc.
Abstract: This paper proposes an error detection and error correction algorithm for speech recognition text based on statistics and understanding, in order to optimize speech recognition results. Through experiments, the accuracy rate of the algorithm proposed in this paper is 82.1%, which can effectively correct the errors in the text after speech recognition and realize the application of speech recognition technology in the field of railway signals. This paper has solved the problem of low recognition rate of professional language in the field of railway signal by speech recognition systems.
 © 2021 IEEE.
Number of references:6
Main heading:Speech recognition
Controlled terms:Character recognition - Error correction - Error statistics - Industrial informatics - Railroads - Speech
Uncontrolled terms:Accuracy rate - Error correction algorithms - Railway signal - Speech recognition systems - Speech recognition technology
Classification code:751.5 Speech - 922.2 Mathematical Statistics
Numerical data indexing:Percentage 8.21e+01%
DOI:10.1109/ISMII52409.2021.00044

Database:Compendex
Compilation and indexing terms, Copyright 2021 Elsevier Inc.

<RECORD 2>

Accession number:20211910327845
Title:A phase plane analysis method for complex nonlinear phenomena of macroscopic traffic flow
Authors:Zhou, Dedong (1); Su, Fang (1)
Author affiliation:(1) Lanzhou Institute of Technology, Lanzhou, 730050, China
Source title:Proceedings - 2021 13th International Conference on Measuring Technology and Mechatronics Automation, ICMTMA 2021
Abbreviated source title:Proc. - Int. Conf. Meas. Technol. Mechatronics Autom., ICMTMA
Part number:1 of 1
Issue title:Proceedings - 2021 13th International Conference on Measuring Technology and Mechatronics Automation, ICMTMA 2021
Issue date:January 2021
Publication year:2021
Pages:781-786
Article number:9410065

Language:English
ISBN-13:9781665438926
Document type:Conference article (CA)
Conference name:13th International Conference on Measuring Technology and Mechatronics Automation, ICMTMA 2021
Conference date:January 16, 2021 - January 17, 2021
Conference location:Beihai, China
Conference code:168564
Sponsor:Changsha University of Science and Technology; Huaiyin Institute of Technology
Publisher:Institute of Electrical and Electronics Engineers Inc.
Abstract: In order to analysis the complex nonlinear traffic phenomena, a new phase plane analysis method is presented in this paper by transforming the traffic flow problem into system stability problem. Variable substitution is introduced into this paper as the key method which matches traffic congestion with the unstable system. The new proposed method is used to describe various nonlinear phenomena due to different input and output conditions on ramps through an existing continuum model. The results show that the new phase plane analysis method can describe the traffic phenomena as well as the traditional methods. Moreover, the variation of density or velocity with time or sections can be described more clearly by the new method.
 © 2021 IEEE.
Number of references:10
Main heading:Traffic congestion
Controlled terms:Continuum mechanics - Nonlinear analysis - System stability
Uncontrolled terms:Continuum Modeling - Input and outputs - Macroscopic traffic flows - Non-linear phenomena - Phase-plane analysis - Stability problem - Traffic phenomenon - Variable substitution
Classification code:931.1 Mechanics - 961 Systems Science
DOI:10.1109/ICMTMA52658.2021.00175

Database:Compendex
Compilation and indexing terms, Copyright 2021 Elsevier Inc.

（End）

文本复制检测报告单(简洁)

No:BC202109271347412237908411　　检测时间:2021-09-27 13:47:41

检测文献: Application of Text Error Correction Algorithm in Railway Speech Recognition

作者: Dedong Zhou, Fang Su

检测范围:
中国学术期刊网络出版总库
中国重要会议论文全文数据库
中国重要报纸全文数据库
中国专利全文数据库
英文数据库(涵盖期刊、博硕、会议的英文数据以及德国Springer、英国Taylor&Francis 期刊数据库等)
港澳台学术文献库
优先出版文献库
图书资源

时间范围: 1915-01-01至2021-01-21

检测结果

去除本人文献复制比: 0.7%

去除引用文献复制比: 0.7%　　总文字复制比: [illegible]

单篇最大文字复制比: 0.6% (A Semantic Web Service Matching Algorithm based on the Nearest Ancestor Node)

重复字数:	[96]	总段落数:	[1]
总字数:	[14343]	疑似段落数:	[1]
单篇最大重复字数:	[79]	前部重合字数:	[0]
疑似段落最大重合字数:	[96]	后部重合字数:	[96]
疑似段落最小重合字数:	[96]		

文字复制部分 0.7%
引用部分 0%
无问题部分 99.3%

指 标: 疑似剽窃观点　疑似剽窃文字表述　一稿多投　疑似整体剽窃　过度引用　重复发表

表格: 0　公式: 检测中　疑似文字的图片: 0　脚注与尾注: 0

1. Application of Text Error Correction Algorithm in Railway Speech Recognition　　总字数: 14343

相似文献列表

去除本人文献复制比: 0.7%(96)　文字复制比: 0.7%(96)　疑似剽窃观点: (0)

1	A Semantic Web Service Matching Algorithm based on the Nearest Ancestor Node	0.6% (79)
	- 《Proceedings of 2010 2nd International Conference on Intellectual Technology in Industrial Practice (ITIP2010) Volume 2》 - 2010-09-08	是否引证: 否
2	A Study on Application of Design of Experiments in GL Company	0.1% (04)
	- 《Proceedings of 2009 IEEE the 16th International Conference on Industrial Engineering and Engineering Management(Vol.1)》 - 2009-10-21	是否引证: 否
3	Study on the diffusion kinetics of adsorption of heavy rare earth with Cyanex272-P507 impregnated resin	0.1% (08)
	廖春发;聂华平;熊云芬;梁勇;杨少华; - 《Journal of Rare Earths》 - 2010-12-15	是否引证: 否

说明:

1. 总文字复制比: 被检测论文总重合字数在总字数中所占的比例
2. 去除引用文献复制比: 去除系统识别为引用的文献后，计算出来的重合字数在总字数中所占的比例
3. 去除本人文献复制比: 去除作者本人文献后，计算出来的重合字数在总字数中所占的比例
4. 单篇最大文字复制比: 被检测文献与所有相似文献比对后，重合字数占总字数的比例最大的那一篇文献的文字复制比
5. 指标是由系统根据《学术论文不端行为的界定标准》自动生成的
6. 红色文字表示文字复制部分;绿色文字表示引用部分;棕灰色文字表示作者本人文献部分
7. 本报告单仅对您所选择比对资源范围内检测结果负责

Application of Text Error Correction Algorithm in Railway Speech Recognition

1st Dedong Zhou
School of electrical engineering
Lanzhou Institute of Technology
Lan Zhou, China
445291776@qq.com

2nd Fang Su
School of electrical engineering
Lanzhou Institute of Technology
Lan Zhou, China
362820344@qq.com

***Abstract*— This paper proposes an error detection and error correction algorithm for speech recognition text based on statistics and understanding, in order to optimize speech recognition results. Through experiments, the accuracy rate of the algorithm proposed in this paper is 82.1%, which can effectively correct the errors in the text after speech recognition and realize the application of speech recognition technology in the field of railway signals. This paper has solved the problem of low recognition rate of professional language in the field of railway signal by speech recognition systems.**

Keywords- speech recognition; railway signal; error detection and error correction; statistics

I. INTRODUCTION

Speech recognition because of background noise, the expression and accent of the speaker are not normative and machines lack expertise in the field, As a result, it is difficult to apply in the professional field. The application of speech recognition technology in railway signal field has not been widely developed, Aiming at the problem of low recognition rate of professional words in the field of railway signal by speech recognition system, this paper adopts a text error checking and error correcting method which is suitable for railway signal field after speech recognition, thus the result of speech recognition is optimized and the application of speech recognition technology in railway signal system is completed.

At present, aiming at text error checking and error correction methods, literature [1] proposed an automatic error checking model of text based on the combination of binary and ternary statistical models and rules, literature [2] proposes an integration model based on integration algorithm and short - and long-term memory network, this method improves the accuracy of text error checking and correction by improving semantic feature detection, literature [3] proposes a text error checking and correction method based on neural network and attention mechanism, which can realize text error checking and correction for semantic errors, literature [4] proposes a multi-level text error-checking reasoning model based on knowledge base for errors at three levels of word, grammar and semantics, literature [5] proposes a text error checking method based on dynamic text window, which combines the weight dynamically allocated error-correcting word set to correct errors. The above algorithms and models have a good effect on the grammatical and semantic level of text, but the background information of the text is missing, this paper proposes a text error detection algorithm based on statistics and understanding based on the original research, aiming at the defects of text error detection after speech recognition in a specific field. by establishing the n-meta grammar model of words and words based on statistics and combining the grammar, semantics and context knowledge base based on understanding, the text after speech recognition is checked and corrected.

II. COMPREHENSIVE ERROR CORRECTION MODEL

By analyzing and comparing the text after speech recognition and the standard text of railway signal, this paper proposes a text correction system after speech recognition of railway signal terms.

The text error-correction system after speech recognition mainly has two tasks: text error-checking after speech recognition and text error-correcting after speech recognition. The error checking of text depends on the construction of n-element grammar model, grammar knowledge base, semantic knowledge base and context knowledge base, while the construction of pinyin dictionary and N-element grammar model affects the result of error correction. This paper first trains corpus to construct n-element grammar model and knowledge base to check errors, then uses pinyin dictionary to correct errors, and finally evaluates the error correction results. Its system framework is shown in Figure 1 below.

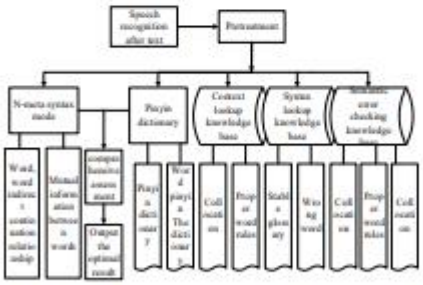

Figure 1. Block diagram of text correction system after speech recognition

978-0-7381-3231-0/21/$31.00 ©2021 IEEE
DOI 10.1109/ISMII52409.2021.00044

III. Research on Error Checking Methods

A. Error checking the N-gram model

The n-element grammar model uses the probability distribution p(s) of string s to reflect the frequency of string s as a sentence. For a string s=w1w2…wi…wn consists of n primitives w (primitives can be words, words, phrases, etc.), The calculation of p (s) is shown in Formula (1):

$$p(s) = p(w_1)p(w_2 \mid w_1)\cdots p(w_n \mid w_1 \cdots w_{n-1}) = \prod_{i=1}^{n} p(w_i \mid w_1 \cdots w_{i-1}) \quad (1)$$

In practical application, n=2 or n=3 is taken. When n=2, the n-gram model is called Bigram model, that is, the binary grammar model, the model assumes that the probability of the occurrence of the cell w_i is only related to the preceding word w_{i-1}, the calculation of $p(s)$ is shown in Equation 2. When n=3, the n-gram model is called the Trigram model, It is the ternary syntax model, the model assumes that the probability of the occurrence of the word unit w_i is only related to the first two words $w_{i-1}w_{i-2}$. The calculation of $p(s)$ is shown in Equation 3.

$$p(s) = p(w_1)\prod_{i=2}^{n} p(w_i \mid w_{i-1}) \quad (2)$$

$$p(s) = p(w_1)p(w_2 \mid w_1)\prod_{i=3}^{n} p(w_i \mid w_{i-1}w_{i-2}) \quad (3)$$

The idea of n-element grammar model error checking is to judge the correctness of text after speech recognition by using such information as the continuous relation, mutual information and co-occurrence between adjacent words and words or between words. The co-occurrence frequency of string $w_{i-1}w_i$ can be counted by word frequency statistics to train the model, due to the data sparsity problem in n-element grammar model of small vocabulary training, the corresponding data smoothing strategy is adopted to solve the problem, Literature [6] obtained witten-Bell interpolation smoothing by comparing several language model smoothing algorithms, which can make the recognition rate of n-element grammar model reach 88.4%, which is 18.18% higher than that of the general model. therefore, this system adopts Witten-Bell interpolation smoothing algorithm for data smoothing before training model.

The binary syntax model provides the basis for determining whether the words w_{i-1} and w_i continue. Assume that the occurrence frequency of the word string $w_{i-1}w_i$ is $N(w_{i-1})$ $N(w_i)$, the occurrence frequency of the word string $w_{i-1}w_i$ is $N(w_{i-1}w_i)$, the occurrence frequency of the word string $w_{i-2}w_{i-1}w_i$ is $N(w_{i-2}w_{i-1}w_i)$, then $P(w_i|w_{i-1}) = N(w_{i-1}w_i)/N(w_{i-1})$, $P(w_i|w_{i-2}w_{i-1}) = N(w_{i-2}w_{i-1}w_i)/N(w_{i-1})$. Using the indirect relation of words to check the mistakes, If $p(s)$ between w_i and w_{i-1} or between w_i and w_{i+1} meets a certain threshold α_1, it can judge whether w_i is connected with w_{i-1} or w_{i+1}, so as to judge whether w_i is wrong.

Mutual information is a measure to calculate the common information between two random variables. The definition of mutual information between words or words is shown in Formula 4 below:

$$I(w_{i-1}w_i) = \log_2 \frac{p(w_{i-1}w_i)}{p(w_{i-1})p(w_i)} \quad (4)$$

In Equation (4), if I $(w_{i-1}w_i)$ meets a certain threshold a2, it is considered that the connection between the word w_i and w_{i-1} is reliable, and the probability of making mistakes on w_i is very small. The n-element grammar model uses the continuation relation and mutual information joint error checking definition, as shown in Equation (5):

$$\begin{cases} w_{i-1} \text{ and } w_i \text{ are reliably connected} & p(w_{i-1}w_i) \geq \alpha_1 \text{ or } I(w_{i-1}w_i) \geq \alpha_2 \\ w_{i-1} \text{ and } w_i \text{ are not reliably connected} & p(w_{i-1}w_i) < \alpha_1 \text{ and } I(w_{i-1}w_i) < \alpha_2 \end{cases} \quad (5)$$

When w_{i-1} and w_i, and w_{i+1} are reliably connected, it can be determined that w_i is correct, and w_i can be used as a reliable word to determine the meaning of a sentence, as n-meta grammar model is based on statistical method, it can only detect partial errors in sentences and lacks textual semantic, grammatical and contextual information. To find errors in the whole sentence, it needs to check the errors in depth according to the above three aspects.

B. Knowledge base for error checking based on understanding

The comprehense-based knowledge base error checking mainly includes the construction of semantic knowledge base, grammatical knowledge base and contextual knowledge base. By preprocessing the text after speech recognition and matching it with the text in the knowledge base, errors can be found and marked.:

(1) Syntax knowledge base error checking

Check wrong grammar knowledge base mainly studies the stability of the speech recognition, speech recognition stability calculation is by training a lot of voice, statistical comparison through the text after speech recognition system to recognize and standard text to get frequent error and can be stable identify words, create easy wrong words glossary table and stability and stability of words in the table can be as key words of the sentence semantic and contextual information. If a word in the stable word list appears in the text after speech recognition, it can be confirmed that the word is recognized correctly, and if it is a word in the error-prone word list, the word will be marked. Speech recognition stability R is defined as follows, and the value of R is the real number between [0,1].

$$\text{Speech recognitio n stability R} = \frac{\text{correct number of recognitio n}}{\text{total number of recognitio n training}} \quad (6)$$

(2) Semantic knowledge base error checking

Semantic knowledge base error checking is mainly realized by establishing keyword and common word lists and stop-word lists. TF-IDF word frequency statistics method is adopted to calculate the word frequency (TF) and reverse file frequency (IDF) of the words after word segmentation in the whole corpus, by calculating TF-IDF, the keyword base and common word base of text meaning can be determined. For some auxiliary words, prepositions and conjunctions such as "Yes, no, no "and other words frequently appearing in the text, the defunct word base can be established, in text preprocessing, the speed of error checking is improved by deleting stopped words from the

defunct word thesaurus, and the error checking of semantic knowledge base is measured by the semantic measurement value, The semantic metric S is the real number between [0,1]. Based on the TF-IDF word frequency weight calculation, the collected data can be divided into the following key words of work terms: dispatcher, assistant on duty, adjacent station on duty, driver, cadre on duty, public works, electrical affairs, operator.

(3) Contextual knowledge base error checking

The purpose of context knowledge base error checking is to consider the context information and build the word collocation library and word rule library. Contextual knowledge base error-detection mainly aimed at the translocation, improper collocation and words of railway parlance mistakes such as the special words, such as "open" and "signal" match, "flipping" and "switch" is tie-in, but in the process of speech recognition will be identified as "open switch", contextual knowledge base mainly by calculating the degree of coordination between the word and the word, the corpus of the collocation of words frequently coordination degree, by calculation to determine speech recognition results are correct. The E calculation method of context coordination degree of words w_i and w_j is as follows:

$$E(w_i, w_j) = \frac{P(w_i, w_j) \mid sameE}{[P(w_i) + P(w_j)] \mid sameE} \quad (7)$$

In equation (6), P(wi, wj)|sameE represents the probability of the occurrence of words wi and wj in the same context, and the determination of the same context can be judged according to the determination of classification in the semantic knowledge base above. [P(wi)+P(wj)]|sameE represents the probability and the occurrence of the words wi and wj in the same context, and the context coordination degree E is the real number between [0,1].

The contextual knowledge base is trained through the collected corpus to obtain the word collocation table and word rule table respectively. To enlarge the scale of knowledge base, online search engines can be used to obtain corpus in the field of expertise.

C. *Error checking methods based on statistics and understanding*

In this paper, the error checking method based on statistics and understanding is implemented by using n-Gram model and knowledge base of context, semantics and grammar, the error checking process is shown in Figure 2.

Figure 2. Flow chart of text error checking after speech recognition

IV. STUDY ON ERROR CORRECTION METHODS

This paper adopts the error correction method based on pinyin dictionary. The construction of pinyin dictionary is to compare the identified text with the correct text, and take pinyin as the index to save the same pinyin and similar pinyin words into the pinyin dictionary. The realization process of error correction method based on pinyin dictionary is shown in Figure 3 below.

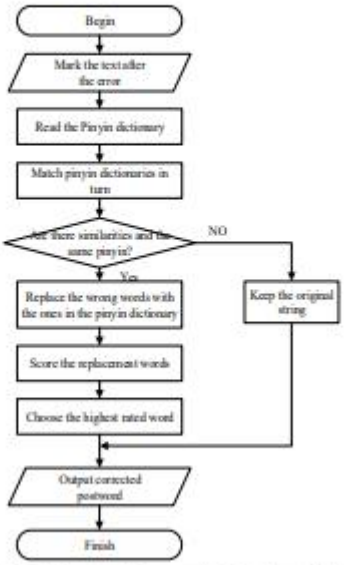

Figure 3. Text error correction process after Speech recognition based on Pinyin dictionary

Figure 3 after the speech recognition based on pinyin dictionary text error correction method, after marking the wrong text, match the corresponding same and similar pinyin words from the pinyin dictionary, and then grade and evaluate the matched words in turn, correct the error by replacing the error word with the highest rated word, and retain the original string if there is no match.

V. Experiment and Result Analysis

300 texts collected from the railway signal field on the website and in the field were input into the speech recognition system, and the text after speech recognition was used as the test corpus, with a total of error words 308. The error checking and correction methods of the text after speech recognition proposed in this paper were tested, and the experimental results were shown in Table 1.

TABLE I. Table 1 Experimental results

Name	Statistical data
Errors Total	308
Number of text errors found	260
Error correction suggestions	258
Reasonable number of error correction suggestions	211
Error correction accuracy	82.1%

According to the above results, the method of text error checking and error correcting in the field of railway signal after speech recognition proposed in this paper can effectively optimize the 211 errors in the text after speech recognition, achieving the error correcting accuracy rate of 82.1%, which indicates that the method proposed in this paper can effectively optimize the errors in the text after speech recognition in the field of railway signal.

VI. Conclusion

This paper presents a text correction method based on statistics and understanding, and verifies the performance of this method by the railway signal text collected on site and web page. The method presented in this paper can effectively achieve the result optimization of post-speech text, which is of great significance for the application of speech recognition technology in the field of railway signal, and also provides a key step for the human-computer interaction in this field.

References

[1] Xu Quansheng, Chen Ying. Research on Automatic Error checking of Chinese Text based on the combination of binary and ternary statistical models and rules [J]. Scientific and Technological Information (Academic Research), 2006(36): 677-678.

[2] Tao Yongcai, Wu Wenle, Hai Chaoyang, Shi Lei, Wei Lin. A text proofreading model combining LSTM and integrated algorithm [J]. Miniature microcomputer system, 2020, 41(05): 967-971.

[3] Hao Yanan, Qiao Gangzhu, Tan Ying. Chinese text proofreading method based on neural network and Attention mechanism [J]. Computer System application, 2019, 28(10): 190-195..

[4] Wu Lin, Zhang Yangsen. Multilevel Chinese text error-checking inference Model based on knowledge base [J]. Computer Engineerin, 2012, 38(20): 21-25.

[5] Huang Gajuan, Wang Scurry, Zhang Yangsen. Chinese text error correction method based on dynamic text window and Dynamic weight allocation [J/OL]. Journal of Zhengzhou University (Science Edition): 1-6[2020-06-08]. https://doi.org/10.13705/j.issn.1671-6841. 2019393.

[6] Yang Lin, ZHANG Jianping, Yan Yonghong. Comparative Study on Smoothing Algorithm of Chinese Language Model in specific field [J]. Computer Engineering and Application, 2006(32): 14-16.

4. A phase plane analysis method for complex nonlinear phenomena of macroscopic traffic flow

ISBN-13: 978-0-7381-4642-3
ISSN: 2157-1481
BMS Part# CFP2113G-CDR

Additional copies may be ordered from:

IEEE Computer Society
Customer Service Center
10662 Los Vaqueros Circle
P.O. Box 3014
Los Alamitos, CA 90720-1314
Tel: + 1 800 272 6657
Fax: + 1 714 821 4641
http://computer.org/cspress
csbooks@computer.org

IEEE Service Center
445 Hoes Lane
P.O. Box 1331
Piscataway, NJ 08855-1331
Tel: + 1 732 981 0060
Fax: + 1 732 981 9667
http://shop.ieee.org/store/
customer-service@ieee.org

IEEE Computer Society
Asia/Pacific Office
Watanabe Bldg., 1-4-2
Minami-Aoyama
Minato-ku, Tokyo 107-0062
JAPAN
Tel: + 81 3 3408 3118
Fax: + 81 3 3408 3553
tokyo.ofc@computer.org

Editorial production by Juan Guerrero
Cover art production by Annie Jiu

IEEE COMPUTER SOCIETY
CONFERENCE
PUBLISHING
SERVICES

IEEE Computer Society
***Conference Publishing Services* (CPS)**
http://www.computer.org/cps

文本复制检测报告单(简洁)

No:BC20210927134514323046730S　　检测时间:2021-09-27 13:45:14

检测文献: A phase plane analysis method for complex nonlinear phenomena of macroscopic traffic flow
作者: Dedong Zhou, Fang Su

检测范围:
中国学术期刊网络出版总库
中国重要会议论文全文数据库
中国重要报纸全文数据库
中国专利全文数据库
英文数据库(涵盖期刊、博硕、会议的英文数据以及德国Springer、英国Taylor&Francis 期刊数据库等)
港澳台学术文献库
优先出版文献库
图书资源

时间范围: 1915-01-01至2021-01-15

检测结果

去除本人文献复制比: 6.2%
去除引用文献复制比: 6.2%　　总文字复制比: 6.2%
单篇最大文字复制比: 2.6% (Nonlinear analysis of traffic jams in an anisotropic continuum model)

重复字数:	[916]	总段落数:	[1]
总字数:	[14667]	疑似段落数:	[1]
单篇最大重复字数:	[375]	前部重合字数:	[370]
疑似段落最大重合字数:	[916]	后部重合字数:	[546]
疑似段落最小重合字数:	[916]		

指　标:　疑似剽窃观点　疑似剽窃文字表述　一稿多投　疑似整体剽窃　过度引用　重复发表

表格: 0　公式: 0　疑似文字的图片: 0　脚注与尾注: 0

1. A phase plane analysis method for complex nonlinear phenomena of macroscopic traffic flow　　总字数: 14667

相似文献列表

去除本人文献复制比: 6.2%(916)　　文字复制比: 6.2%(916)　　疑似剽窃观点: (0)

1	Nonlinear analysis of traffic jams in an anisotropic continuum model Arvind Kumar Gupta;Sapna Sharma; - 《Chinese Physics B》 - 2010-11-15	2.6% (375) 是否引证: 否
2	Phase Plane Analysis Method of Nonlinear Traffic Phenomena Wenhuan Ai;;Zhongke Shi;;Dawei Liu;;Hung-Yuan Chung - 《Journal of Control Science and Engineering》 - 2015-09-20	1.3% (215) 是否引证: 否
3	A Remark on Using Gravitational Lensing Probability as a Probe of the Central Regions of CDM Halos - 《Chinese Journal of Astronomy and Astrophysics》 - 2002-10-30	1.3% (184) 是否引证: 否
4	应用于高速光通信中的Turbo乘积码的HIHO译码算法(英文) 史治平;周亮;范祥;杨阳; - 《中国通信》 - 2012-06-15	1.3% (176) 是否引证: 否
5	A new family of two-dimensional triple-codeweight asymmetric optical orthogonal code for OCDMA networks 殷洪玺;梁霞;马乐;覃丽巧; - 《Chinese Optics Letters》 - 2009-02-10	1.1% (164) 是否引证: 否
6	Conditional quantum CNOT gate between two four-level atoms 樊洋 - 《Chinese Optics Letters》 - 2005-03-20	1.0% (148) 是否引证: 否
7	Review and Analysis on the Meridian Research of China over the Past Sixty Years 杨英娜;韩金祥; - 《Chinese Journal of Integrative Medicine》 - 2015-05-15	0.9% (127) 是否引证: 否
8	Uncertainty Principles for the Segal-Bargmann Transform Fethi SOLTANI; - 《Journal of Mathematical Research with Applications》 - 2017-09-15	0.9% (127) 是否引证: 否
9	Effects of Agkistrodon in Different Dosage Forms on Collagen-Induced Arthritis in Rats 包洁;谢志平;陈震鸿;孙静;范永升; - 《Chinese Journal of Integrative Medicine》 - 2016-11-16	0.9% (126) 是否引证: 否
10	Wet Cupping Therapy Improves Local Blood Perfusion and Analgesic Effects in Patients with Nerve-Root Type Cervical Spondylosis MENG Xiang-wen;WANG Ying;PIAO Sheng-ai;LV Wen-tao;ZHU Cheng-hui;MU Ming-yuan;LI Dan-dan;LIU Hua-peng;GUO Yi; - 《Chinese Journal of Integrative Medicine》 - 2018-11-06	0.9% (126) 是否引证: 否
11	Efficacy of Xuebijing Injection(血必净注射液)on Cardiopulmonary Bypass-Associated Pulmonary Injury:A Prospective,Single-center,Double Blinded,Randomized Controlled Trial GAO Wei;LI Na;CUI Xiao-guang; - 《Chinese Journal of Integrative Medicine》 - 2018-11-06	0.9% (126) 是否引证: 否
12	Effect of Xuefu Zhuyu Capsule (血府逐瘀胶囊) on Angiogenesis in Hindlimb Ischemic Rats SHI Wei-li;LU Peng-fei;GAO Dong;SONG Jun;CHEN Ke-ji; - 《Chinese Journal of Integrative Medicine》 - 2019-12-30	0.9% (124) 是否引证: 否
13	Correlation between Chinese Medicine Constitution and Skin Types: A Study on 187 Japanese Women Seika Kanozawa;ZHU Yan-bo;WANG Qi; - 《Chinese Journal of Integrative Medicine》 - 2020-03-15	0.9% (124) 是否引证: 否
14	Brain Functional connectivity network studies of acupuncture:a systematic review on resting-state fMRI Rong-lin Cai;Guo-ming Shen;Hao Wang;Yuan-yuan Guan; - 《Journal of Integrative Medicine》 - 2018-01-15	0.8% (123) 是否引证: 否
15	A novel strategy of smart manipulation by micro-scale oscillatory networks of the reactionary zones for enhanced extreme thrust control of the next-generation solid propulsion systems Alexander N.Lukin; - 《Defence Technology》 - 2018-10-15	0.8% (123) 是否引证: 否
16	Surface modification of ammonium nitrate by coating with surfactant materials to reduce hygroscopicity Baha I.Elzaki;Yue Jun Zhang; - 《Defence Technology》 - 2019-08-15	0.8% (123) 是否引证: 否
17	Modeling and simulation of bullet-barrel interaction process for the damaged gun barrel Chao Shen;Ke-dong Zhou;Ye Lu;Jun-song Li; - 《Defence Technology》 - 2019-12-15	0.8% (122) 是否引证: 否
18	Hypergeometric Series Solution to a Class of Second-Order Boundary Value Problems via Laplace Transform with Applications to Nanofluids Abdelhalim Ebaid;Abdul-Majid Wazwaz;Elham Alali;Basem S.Masaedeh; - 《Communications in Theoretical Physics》 - 2017-03-01	0.8% (121) 是否引证: 否

说明:

1. 总文字复制比: 被检测论文总重合字数在总字数中所占的比例
2. 去除引用文献复制比: 去除系统识别为引用的文献后，计算出来的重合字数在总字数中所占的比例
3. 去除本人文献复制比: 去除作者本人文献后，计算出来的重合字数在总字数中所占的比例
4. 单篇最大文字复制比: 被检测文献与所有相似文献比对后，重合字数占总字数的比例最大的那一篇文献的文字复制比
5. 指标是由系统根据《学术论文不端行为的界定标准》自动生成的
6. 红色文字表示文字复制部分;绿色文字表示引用部分;棕灰色文字表示作者本人文献部分
7. 本报告单仅对您所选择比对资源范围内检测结果负责

cnki.net
http://check.cnki.net/
http://e.weibo.com/u/3194559873/

2021 13th International Conference on Measuring Technology and Mechatronics Automation (ICMTMA)

A phase plane analysis method for complex nonlinear phenomena of macroscopic traffic flow

Dedong Zhou, Fang Su
1. Lanzhou Institute of Technology, Lanzhou 730050, China
E-mail: 445291776@qq.com, 362820344@qq.com

***Abstract*—In order to analysis the complex nonlinear traffic phenomena, a new phase plane analysis method is presented in this paper by transforming the traffic flow problem into system stability problem. Variable substitution is introduced into this paper as the key method which matches traffic congestion with the unstable system. The new proposed method is used to describe various nonlinear phenomena due to different input and output conditions on ramps through an existing continuum model. The results show that the new phase plane analysis method can describe the traffic phenomena as well as the traditional methods. Moreover, the variation of density or velocity with time or sections can be described more clearly by the new method.**

Keywords- phase plane method; traffic phenomena; continuum model; traffic flow

I. INTRODUCTION

An important branch of the research on traffic flow is the quantitative study of traffic phenomena based on the traffic flow models. In recent years, many physical models have been proposed [1-3].Most of them are hydrodynamic models which provide macroscopic description of traffic flow. The study of continuum traffic phenomena began with the LWR model developed independently by Lighthill and Whitham [4] and Richards [5]. In this model, vehicles have often been considered as interacting particles and traffic flow can be considered as a one-dimensional compressible flow of these particles. In the past decades，researchers have made many efforts to improve the LWR model, they developed many higher order models which use a dynamic equation to make speed to replace the equilibrium relationship. Subsequent studies [6-9] of the models have explained many observed features of the free flow and traffic jams in highways.

In this paper, we use a new method to describe a variety of nonlinear traffic flow phenomena which are raised by different input and output on ramp. We use some variable substitution to convert the traffic flow model into a functional stability model. From this model many well-known nonlinear phenomena may be analyzed. The theory is applied to analyze all kinds of nonlinear phenomena with a single ramp generated by different initial densities and vehicle generation rates which were rarely studied in the past.

II. VARIABLE SUBSTITUTION BASED ON THE GK MODEL

Gupta and Katiyar [10] proposed an anisotropic continuum model, which is referred to as GK model. It has been mostly studied nowadays and has the following form:

$$\begin{cases}\dfrac{\partial \rho}{\partial t}+\dfrac{\partial(\rho v)}{\partial x}=0\\ \dfrac{\partial v}{\partial t}+v\dfrac{\partial v}{\partial x}=a\left[V_e(\rho)-v\right]+\varepsilon V_e'(\rho)\left(\frac{1}{2\rho}\frac{\partial \rho}{\partial x}+\frac{1}{4\rho^2}\frac{\partial^2 \rho}{\partial x^2}-\frac{1}{2\rho^3}\left(\frac{\partial \rho}{\partial x}\right)^2\right)+\beta\rho\left(\rho\frac{\partial v}{\partial x}\right)\end{cases} \quad (1)$$

where ρ is the density; v is the velocity; x and t represent space and time respectively; a is the driver's sensitivity which equals the inverse of the driver's reaction time; $V_e[\rho(x,t)]$ is the optimal velocity function and has the following form:

$$V_e[\rho]=v_f\left\{\left[1+\exp\left(\frac{\rho/\rho_m-0.25}{0.06}\right)\right]^{-a}-3.72\times10^{-4}\right\} \quad (2)$$

$V_e'(\rho)=\dfrac{dV_e(\rho)}{d\rho}$, β is a non-negative dimensionless parameter and $\varepsilon(\rho)\geq 0$ is the traffic sound speed given by:

$$c=\sqrt{\frac{V_e'(\rho)}{2\varepsilon}} \quad (3)$$

here v_f is the free-flow speed, ρ_m is the maximum or jam density.

In the present paper, a simple transformation is employed as follows:

$$\begin{cases}\sigma=\dfrac{1}{v}\\ \eta=\dfrac{1}{\rho_m v}\end{cases} \quad (4)$$

Substituting the variables into equation (1), we have a new traffic flow model as follows:

$$\begin{cases}\sigma^2\dfrac{\partial \eta}{\partial t}+(\eta-\rho_m\sigma^2)\dfrac{\partial \sigma}{\partial x}+\sigma\dfrac{\partial \eta}{\partial x}=0\\ \dfrac{\partial \sigma}{\partial t}+\left(\dfrac{1}{\sigma}-2\beta\sqrt{\dfrac{V_e'(\eta)}{2\varepsilon}}\right)\dfrac{\partial \sigma}{\partial x}-a\sigma+a\sigma^2V_e(\eta)\\ +a\sigma^2V_e'(\eta)\left(\dfrac{1}{2\rho_m^2}\dfrac{\partial \eta}{\partial x}+\dfrac{1}{8\rho_m^3}\dfrac{\partial^2 \eta}{\partial x^2}-\dfrac{1}{2\rho_m^4}\left(\dfrac{\partial \eta}{\partial x}\right)^2\right)+1=0\end{cases} \quad (5)$$

Where $S=\rho_m\eta-1$.

Similarly, substituting the variables into equation (2), the equilibrium velocity $v_e(\eta)$ is as following:

2157-1481/21/$31.00 ©2021 IEEE
DOI 10.1109/ICMTMA52658.2021.00175

$$V_e(\eta)=v_f\left\{\left[1+\exp\left(\frac{0.75-\frac{1}{\eta\rho_m}}{0.06}\right)\right]^{-a}-3.72\times10^{-4}\right\} \quad (6)$$

According to the variable substitution $\sigma=\frac{1}{v}$ and $\eta=\frac{1}{\rho_m v}$, we can see that as long as the vehicles velocity goes to zero or the vehicle density becomes saturated, the state variable σ or η will approach infinity. So we can use the phase plane diagrams about the variable η or σ to describe clearly the relationship between traffic jams and system instability. When the traffic becomes congested, the state variable ρ and v both tend to a specific value. However, through such variable substitutions, the state variable η or σ both tend to infinity. As long as there is traffic jam formation, the value of η or σ will approach infinity. So the problem of traffic flow could be converted into that of system stability. Some stability theories and mathematical tools can be applied directly to solve the traffic problems. If we use the new model by such variable substitution, we can see from the phase plane that there is a one-to-one relationship between the traffic congestion and the unstable system. The new traffic flow model can analyze various traffic phenomena directly and can also analyze the chaotic fluctuations of traffic flow.

III. THE ANALYSIS OF DIFFERENT INPUT AND OUTPUT TRAFFIC PHENOMENA USING THE NEW METHOD

By analyzing the model, we first carried out numerical tests for the phenomena of fixed vehicle generation rate but increasing initial homogeneous density with a single ramp, which is rarely studied in the past. To study the effects of ramps, we added the source and the drain terms on the right-hand side of the continuity equation in (5) as follows.

$$\sigma^2\frac{\partial \eta}{\partial t}+(\eta-\rho_m\sigma^2)\frac{\partial \sigma}{\partial x}+\sigma\frac{\partial \eta}{\partial x}=r_{in}(t)-r_{out}(t) \quad (7)$$

where $r_{in}(t)$ and $r_{out}(t)$ represent the external flux through an on-ramp and through an off-ramp, respectively. We have also taken the test road section as 32.2 km long and set a ramp in the middle of the road section. The vehicle generation rate was set to 0.0001veh/m/s, that was to say, the number of vehicles through an on-ramp was 0.0001 more than that through an off -ramp every meter per second. The initial density ρ_0 was 0.027veh/m. Other parameter values were the same as in Section 3 and the results were shown in Fig. 1(a)-(c).

It is clear from figure 1(a) that since the vehicle generation rate is a small constant and the initial density of the whole road is also very small, the vehicles come from the on-ramp can drive quickly downstream and will not have any effect on the upstream traffic. Vehicles in upstream of the road can drive forward still keeping the original speed even when they move to the ramp. So the density of the ramp increases just because of vehicles inflows and the increments attenuate downstream gradually when the entered vehicles continually drive downstream. The density of the off-ramp remains the initial uniform density of 0.027veh / m at the beginning. Then it is increasing with the vehicles entered from the ramp and reaches the value of the ramp density ultimately. The number of vehicles goes in and out the ramp can be equilibrium approximately after a while because of the constant vehicle generation rate and the density increments is almost not changed finally.

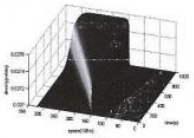
(a)

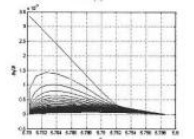
(b)

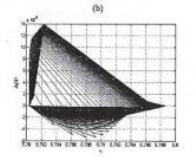
(c)

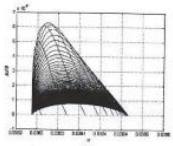

(d)

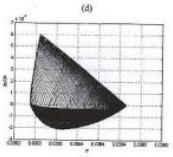

(e)

Figure 1. The density temporal evolution and phase plane diagrams with initial homogeneous traffic of amplitude ρ_0 =0.027veh/m (a) the temporal evolution of vehicle density; (b) the phase plane diagram of $\left(\eta, \partial\eta/\partial t\right)$; (c) the phase plane diagram of $\left(\eta, \partial\eta/\partial x\right)$; (d) the phase plane diagram of $\left(\sigma, \partial\sigma/\partial t\right)$; (e) the phase plane diagram of $\left(\sigma, \partial\sigma/\partial x\right)$

It can be seen from an overall point of view that no curves toward infinity are found in figures 1(b)-(e). That mean, the system is stable and the whole road section is not blocked. The phase plane diagrams also highlight the variation of the traffic flow. Figure 1(b) is the combination of variation curves of η on each road section during the first 16 minutes. The trajectories of it show that all curves change from left to right. That is to say, the value of η which is proportional to the vehicle density keeps on increasing. So, it reflects the phenomenon that the densities of downstream sections increase gradually. The more the curve is changed, the greater is the density fluctuation. Moreover, the phase plane diagrams can also clearly reflect the speed of density change on each section. We observed the trajectory of each road and found that the density increasing velocity on ramp section decreases gradually, but on the other road sections first increases and then decreases.

The traffic of the whole road sections will eventually tend towards stability. Figure 1(c) could be considered as a group of curves which describes the change of η per second on the whole road. All of them move from the starting point (5.7803,0) , then increase along the approximate triangular trajectory and return back to the starting point. Correspondingly, the value of η increases at first and finally decreases again. It illustrates that at a given time the density increases at the ramp then decreases when vehicles entered from the ramp continually drive downstream. Moreover, the phase plane diagrams can describe more clearly the size and speed of density variation on the whole road at different times. When we draw the trajectory of it one by one, we can see at the initial time the density increment of the whole road is small then it is increasing with time because the vehicles continually entered from the ramp. After a while, the number of vehicles goes in and out the ramp can be equilibrium approximately. So the density variation of the whole road will remain the same. Similarly, figures 1 (d) and (e) reflect the same phenomena based on the velocity variation with time and displacement because the state variable σ is inversely proportional to the vehicle velocity.

If we increased the initial density to 0.037veh / m and remained other conditions such as the value of vehicle generation rate unchanged, the temporal evolution of vehicle density and phase plane diagrams could be compared as in Fig.2(a)-(e).

In Fig. 2(a), as the initial density increases, the vehicles come from the on-ramp will have an effect on the upstream traffic. Vehicles in upstream of the road need to decelerate when they move to the ramp and can't drive keeping the original speed. So the density in upstream of the road near the ramp will increase gradually. On the other hand, the initial density in downstream of the road also increases and the vehicles come from the on-ramp can't move downstream quickly, so some of them stay on the ramp, it makes the density increment on the ramp is a lot larger than that with a small initial density. The increment will decrease very fast as vehicles in downstream road sections move forward.

Figure 2(b) is the combination of variation curves of η on each road section during the first 16 minutes. All curves in the figure change from left to right. That is to say, the value of η which is proportional to the vehicle density keeps on increasing. So, it mainly reflects the phenomenon that the density of each road section near the ramp increased gradually with time when vehicles continually entered from the ramp. Figure 2(c) could be considered as a group of curves which describe the change of π per second on the whole road. All curves are closed curves which increase firstly then decrease again. It illustrates that the upstream density near the ramp increases gradually and the downstream density decreases as vehicles move forward. Similarly, figures 2(d) - (e) reflect the same phenomena based on the velocity variation with time and displacement. Moreover, both the value and the change rate

of η and σ in figures 2(b)-(e) increase more significantly than in the figure 1 whose initial density is small.

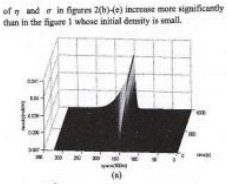

(a)

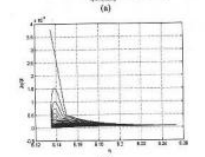

(b)

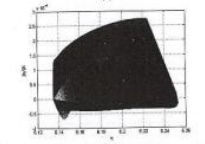

(c)

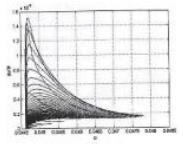

(d)

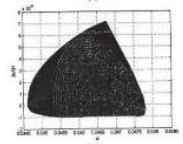

(e)

Figure 2. The density temporal evolution and phase plane diagrams with initial homogeneous traffic of amplitude ρ_0 =0.037veh/m (a) the temporal evolution of vehicle density; (b) the phase plane diagram of $\left(\eta, \partial\eta/\partial x\right)$; (c) the phase plane diagram of $\left(\eta, \partial\eta/\partial t\right)$; (d) the phase plane diagram of $\left(\sigma, \partial\sigma/\partial t\right)$; (e) the phase plane diagram of $\left(\sigma, \partial\sigma/\partial x\right)$

If we continually increased the initial density to 0.047veh/m and remained other conditions such as the value of vehicle generation rate unchanged, the temporal evolution of vehicle density and phase plane diagrams could be compared as in fig.3(a)-(e).

Since the initial density is just above the down-critical unstable density, a small quantity of vehicles come from the ramp can be seen as a small localized perturbation on the initial homogeneous traffic flow and the amplitude of it grows in time, which eventually forms the stop-and-go traffic. The fluctuation amplitude of traffic flow is so large that the small vehicle generation rate on ramp can't make an appreciable effect on the density of the whole road. Figures 3 (b)-(e) all consist of a number of circles and clearly highlight the fluctuations of density and velocity with

time or displacement. So they also describe the stop-and-go traffic phenomenon.

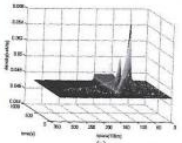

(a)

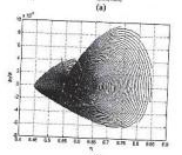

(b)

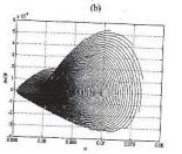

(c)

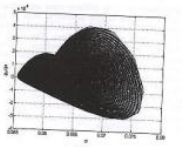

(d)

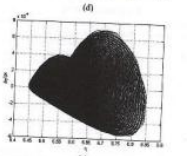

(e)

Figure 3. The density temporal evolution and phase plane diagrams with initial homogeneous traffic of amplitude ρ_0 =0.047veh/m (a) the temporal evolution of vehicle density; (b) the phase plane diagram of $\left(\eta, \partial\eta/\partial t\right)$; (c) the phase plane diagram of $\left(\sigma, \partial\sigma/\partial t\right)$; (d) the phase plane diagram of $\left(\sigma, \partial\sigma/\partial x\right)$; (e) the phase plane diagram of $\left(\eta, \partial\eta/\partial x\right)$

IV. Conclusions

In this paper, we adopt the variable substitution of original traffic flow models to convert traffic flow problems into system stability problems, just as the stability of discrete systems in the unit circle is expanded to the whole complex plane. Thus we can carry out the stability analysis directly by traffic flow models. Using the phase plane diagrams we can also describe all kinds of nonlinear phenomena observed in traffic flow. This will provide theoretical basis for traffic control and decision. In order to specify this new method, we first build a new traffic flow model through substituting the variable in the GK model. Then the relationship between traffic congestion and the stability of the system can be obtained. So we can determine whether there will be traffic congestion or other abnormal phenomena from a global stability point. There is less study

on the phenomena raised by different input and output on ramps. We use the new method to describe some of them with fixed vehicle generation rate but increasing initial homogeneous density with a single ramp. The results are also consistent with the diverse nonlinear dynamics phenomena observed in realistic traffic flow. Furthermore, the phase plane diagrams employed the new model highlight the instability of the system. When the traffic became slow and congested, some curves tending to infinite can be seen from the phase plane diagrams and they account for a large proportion in the graphs while most small amplitude density fluctuations under stable traffic conditions just centered in a small area near the initial value.

Acknowledgements

The authors would like to thank the anonymous referees and the editor for their valuable opinions. This work is partially supported by the National Natural Science Foundation of China under the Grant No. 61863033 and the China Postdoctoral Science Foundation Funded Project (Project No.: 2018M633653XB) and the " Qizhi " Personnel Training Support Project of Lanzhou Institute of Technology (Grant No. 2018QZ-11) and the National Natural Science Foundation of China under the Grant No. 11965019.

References

[1] D.W. Liu, Z.K. Shi, W.H. Ai. Enhanced stability of car-following model upon incorporation of short-term driving memory [J]. Communications in Nonlinear Science and Numerical Simulation, 2016, 47: 139-150.

[2] D.W. Liu, Z.K. Shi, W.H. Ai. A new car-following model accounting for impact of wrong wind [J]. Mathematical Problems in Engineering, 2017, 1:1-12.

[3] D.W. Liu, Z.K. Shi, W.H. Ai. An improved car-following model from the perspective of driver' s forecast behavior [J]. International Journal of Modern Physics C,2017,28(4).

[4] M. J. Lighthill and G. B. Whitham. On kinematic waves: II. A theory of traffic flow on long crowded roads [C]. Proceedings of the Royal Society of London, 1955, 229:317 - 345.

[5] P. I. Richards. Shock waves on the highway [J]. Operations Research, 1956, 4: 42 - 51.

[6] W.H. Ai, Z.K. Shi, D.W. Liu. Bifurcation Analysis of a speed gradient continuum traffic flow model [J]. Physica A: Statistical Mechanics and its Applications, 2015, 437: 418-429.

[7] W.H. Ai, Z.K. Shi, D.W. Liu. Bifurcation Analysis Method of Nonlinear Traffic Phenomena [J]. International Journal of Modern Physics C, 2015, 26, 1550111.

[8] C.X. Ma, K.C. He. Green wave traffic control system optimization based on adaptive genetic-artificial fish swarm algorithm [J]. Neural Computing and Applications, 2019, 31(7):2073-2083.

[9] B. Yang, J. Kostkova, J. Flusser, T. Suk, R. Bujack. Rotation invariants of vector fields from orthogonal moments [J]. Pattern Recognition, 2018, 74: 110-121.

[10] A.K. Gupta, V.K. Katiyar, Analyses of shock waves and jams in traffic flow, J. Phys. A. 38 (2005) 4069-4083.

5. Research on Compound Control Strategy of Dynamic Voltage Restorer

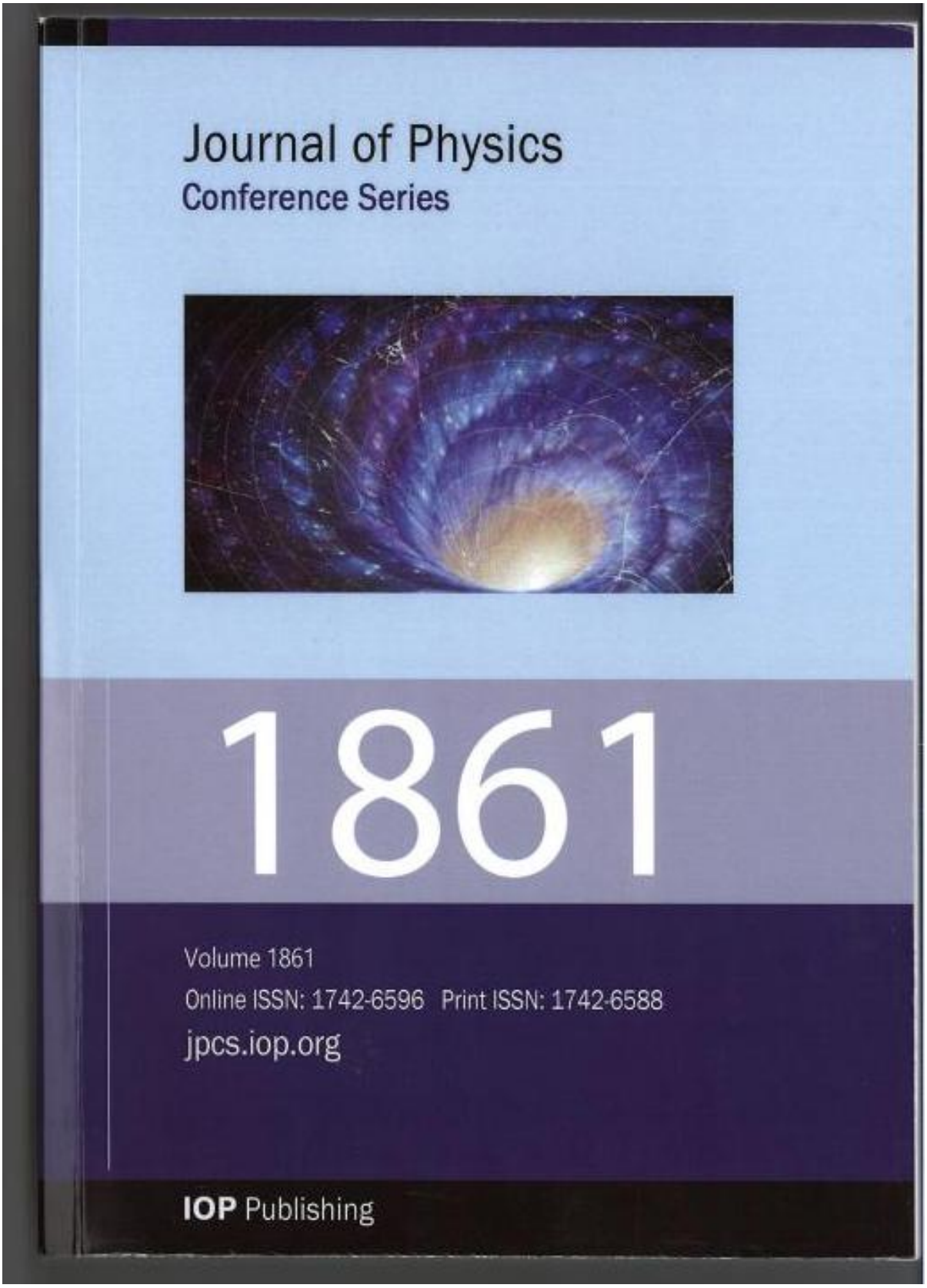

Table of Contents

Research on Compound Control Strategy of Dynamic Voltage Restorer

Zhicheng Guo*

School of Electrical Engineering,Lanzhou Institute of Technology,Lanzhou 730050, China

email: guozc@lzit.edu.cn

Abstract. Dynamic voltage restorer (DVR) is an economical and effective device to suppress the voltage drop of the power grid. This paper establishes the equivalent circuit and mathematical model of the DVR. Aiming at the shortcomings of feedforward control and feedback control, a composite control strategy is adopted, feedforward control is introduced on the basis of feedback control, and the load adaptability and stability of composite control Perform analysis. Finally, MATLAB is used for simulation verification, and the results show that the compound control can meet the requirements of the DVR control system.

1. Introduction

The power distribution network structure of the power system is becoming more and more complex, especially the investment of large-load electrical equipment, so that there are various dynamic power quality problems in the power grid such as power supply interruption, harmonics, flicker, and voltage sag. Dynamic voltage restorer (DVR) is currently one of the most economical and effective means to solve the dynamic power quality problem of voltage sag [1-2]. The DVR itself is equivalent to a controlled voltage source, which can insert a voltage of any amplitude and phase between the power supply and the sensitive load [3]. When the power supply voltage is distorted, the purpose of stabilizing the sensitive load voltage is achieved by changing the voltage of the DVR. In DVR, control strategy is a key factor, it is directly related to the DVR compensation effect.

At present, the linear control strategy of DVR mainly includes feedforward control, various feedback control and so on. Feedforward control has the characteristics of simple control and fast response, but there will be voltage amplitude attenuation and phase shift in the impedance of coupling transformer and filter. It is an open-loop control mode without feedback link, so the output can not follow the input completely, so it is difficult to achieve complete compensation, and the adaptability to the load is not strong[4-5]. The feedback control has strong load adaptability, but the parameter design is difficult, and the limitation of control coefficient value will affect the compensation effect. Considering the advantages of the two, this paper adopts the compound control strategy of feedforward control on the basis of feedback.

2. DVR system structure

The DVR system structure is shown in Fig.1. The inverter adopts a three single-phase H-bridge structure, which is composed of three single-phase full bridges. The control system controls the inverter circuit and reverses the energy storage of the battery on the DC side. It becomes a three-phase AC output, and after filtering out higher harmonics through an LC filter, it is finally injected into the

grid through a series transformer. Through appropriate control strategy, the output voltage of DVR can track the change of command voltage in real time. Finally, the compensation voltage is generated to offset the voltage drop in the power supply side voltage, so as to improve the power quality of the system.

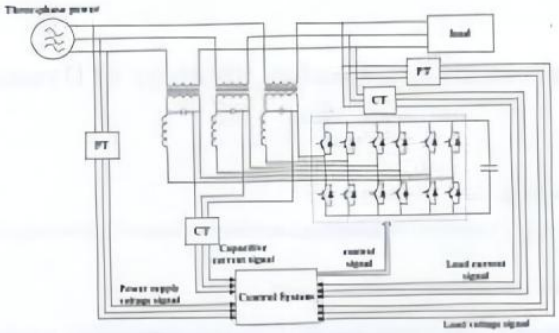

Fig.1 DVR system structure block diagram

According to the working principle of DVR, the equivalent circuit diagram of DVR [6] is shown in Fig.2.

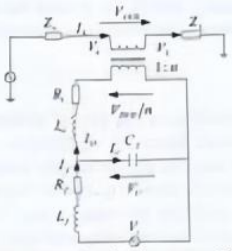

Fig.2 Equivalent circuit diagram of DVR

In the figure, V_s is the system side voltage; V_{DVR} is the compensation voltage output by the DVR; V_L is the load voltage; V_i is the output voltage of the DVR inverter; V_C is the voltage across the filter capacitor; I_O is the primary current of the transformer; I_f is the filter inductance Current; I_C is the current of the filter capacitor; L_f, C_f and R_f represent the inductance, capacitance and line resistance of the filter circuit, L_t and R_t represent the winding resistance and leakage inductance of the transformer, respectively, Z_L is the load resistance, and the transformation ratio of the transformer is 1: n.

According to Kirchhoff's law, the state equation of the equivalent circuit diagram can be obtained as:

$$V_i = L_f \frac{dI_f}{dt} + I_f R_f + V_C \tag{1}$$

$$V_C = L_t \frac{dI_O}{dt} + I_O R_t + \frac{V_{DVR}}{n} \tag{2}$$

$$V_L = V_s + V_{DVR} \tag{3}$$

$$I_C = C_f \frac{dV_C}{dt} \tag{4}$$

$$I_f = I_C + I_O \tag{5}$$

$$I_O = nI_L \tag{6}$$

3. DVR control strategy

3.1. Feedforward control strategy

The feedforward control mode has the advantages of fast response speed, high stability, simple control method, etc., so this control method is used in quite a few occasions. In the feedforward control method of DVR, a linear link with a gain of k_m is used instead of the inverter. According to equations (1) to (6), the block diagram of the feedforward control strategy is shown in Fig. 3. In the figure, $V_L^*(s)$ is the reference value of the load voltage, and the load voltage $V_L(s)$ can be expressed as:

$$V_L = G_{LO}V_L^* + G_{SO}V_S \tag{7}$$

$$G_{LO}(s) = \frac{nk_m(L_2 s + R_2)}{a_1 s^3 + a_2 s^2 + a_3 s + a_4} \tag{8}$$

$$G_{SO}(s) = \frac{L_1 L_f C_f s^3 + (L_f R_1 + L_1 R_f)C_f s^2 + (R_f R_1 C_f + (1-n)L_1)s + (1-n)R_1}{a_1 s^3 + a_2 s^2 + a_3 s + a_4} \tag{9}$$

Among them $a_1 = (L_1 + n^2 L_2)L_f C_f$; $a_2 = (L_1 + n^2 L_2)R_f C_f + (R_1 + n^2 R_2)L_f C_f$;

$a_3 = R_f C_f (R_1 + n^2 R_2) + n^2 L_f + n^2 L_2 + L_1$; $a_4 = n^2 R_f + n^2 R_2 + R_1$

G_{LO} represents the transfer function from the reference voltage $V_L^*(s)$ to the load voltage $V_L(S)$, and G_{SO} represents the transfer function from the system voltage V_S to the load voltage $V_L(S)$. It can be seen from the formula (7) that in an ideal situation, only V_L can track V_L^* well, and it is not affected by the disturbance of V_S in a certain frequency range to ensure the correct output of V_L.

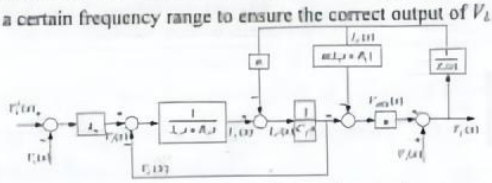

Fig.3 Block diagram of DVR feedforward control system

In order to verify the load adaptability of the feedforward control system, the transfer function of load current to load voltage can be expressed as:

$$G_{ai}(s) = -\frac{n^2 L_1 L_f C_f s^3 + n^2 (L_1 R_f + L_f R_1)C_f s^2 + n^2 (L_f + L_1 + R_1 R_f C_f)s + n^2 R_1}{L_f C_f s^2 + R_f C_f s + 1} \tag{10}$$

From the transfer function, the Bode diagrams of G_{LO}, G_{SO}, and G_{ai} can be obtained, as shown in Fig.4.

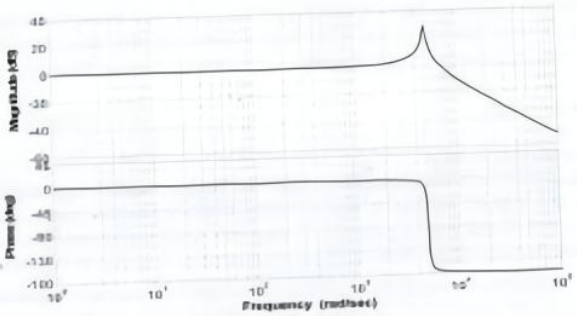

(a) G_{LO} Bode diagram

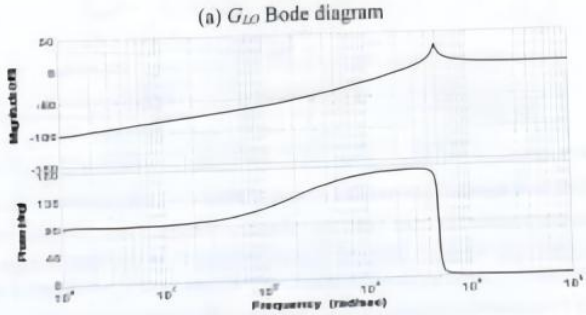

(b) G_{SO} Bode diagram

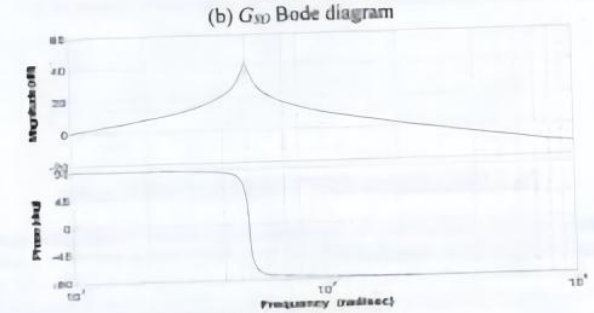

(c) G_{OI} Bode diagram

Fig.4 Bode diagram of G_{LO}, G_{SO}, G_{OI}

It can be seen from Fig.4(a) that although the system is stable, the phase margin is relatively small, and the damping is small, which is prone to oscillation. From Fig.4(b), it can be seen that the system's disturbance to the grid voltage is inhibited in the low frequency band, while it will cause interference to the system in the high frequency band. It can be seen from Fig.4(c) that the feedforward control has a weak attenuation effect on the load current interference, so the load adaptability of the feedforward control is relatively poor.

From the above analysis, it can be seen that a simple feedforward control strategy cannot meet the requirements of DVR performance, and it is difficult to obtain good compensation effects and good load adaptability.

3.2. Compound control strategy

The compound control strategy is to introduce feedforward control on the basis of feedback control. Feedforward control can significantly improve the dynamic response speed of the system and shorten the time for the compensation voltage to be issued; the feedback control adopts double closed-loop feedback control, the inner loop is the feedback link of the instantaneous value of the filter capacitor current, and the outer loop is the instantaneous value feedback link of the load voltage. Closed-loop feedback control can not only improve the stability of the system, but also improve the dynamic performance and adaptability of the system to the load. In particular, the integral part of the PI controller can effectively reduce the stability error of the system. Compound control combines their advantages, and its system control block diagram is shown in Fig.5.

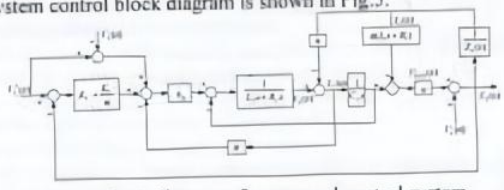

Fig.5 Block diagram of compound control system

From Fig.5, the load voltage in the compound control mode can be expressed as:

$$V_L = G_{LO}V_L^* + G_{SO}V_s \tag{11}$$

In the above formula, G_{LO} represents the transfer function from the reference voltage V_L^* to the load voltage V_L, and G_{SO} represents the transfer function from the system voltage V_S to the load voltage V_L.

$$G_{LO} = \frac{nR_L k_m[R_{Cf}C_f(1+k_v)\tau s^2 + (k_v\tau + \tau + R_{Lf}C_f)s + 1]}{b_1 s^4 + b_2 s^3 + b_3 s^2 + b_4 s + b_5} \tag{12}$$

$$G_{SO} = \frac{R_L\tau s[L_f C_f s^2 + (\alpha k_m + R_{Cf} + R_{Lf} - nk_m R_{Cf})C_f s + (1 - nk_m)]}{b_1 s^4 + b_2 s^3 + b_3 s^2 + b_4 s + b_5} \tag{13}$$

Among them: $b_1 = n^2\tau L_f L_1 C_1$; $b_2 = n^2\tau(\alpha k_m + R_{Lf} + R_{Cf})L_1 C_f + \tau(n^2 R_{Cf} + n^2 R_1 + R_L)L_f C_f$;

$$b_3 = n^2\tau(L_1 + L_f) + \tau(n^2 R_1 + R_L)(\alpha k_m + R_{Lf} + R_{Cf})C_f + n\tau R_{Cf}C_f(k_m k_v R_L + nR_{Lf}) \tag{B}$$

$$b_4 = \tau(n^2 R_1 + R_L) + nk_m R_L(R_{Cf}C_f + \tau k_v) + n^2\tau R_{Lf}$$

$$b_5 = nk_m R_L$$

In order to verify the load adaptability of the system, the transfer function of load current to load voltage is:

$$G_{oi}(s) = \frac{L_f C_f s^3 + (R_{Lf}C_f + k_m\alpha C_f)s^2 + (1 + k_v k_m n)s + k_m n/\tau}{L_f C_f s^4 + (L_f C_f R_L + R_{Cf}C_f L_1 + L_1 k_m \alpha C_f)s^3 + (L_f + R_{Cf}C_f R_L + k_m\alpha C_f R_1 + L_1)s^2 + (R_{Cf} + R_L)s} \tag{14}$$

From the transfer function, the Bode diagrams of G_{LO}, G_{SO}, and G_{OI} can be obtained, as shown in Fig.6.

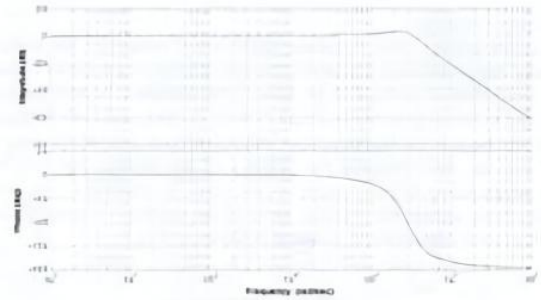

(a) G_{LO} Bode diagram

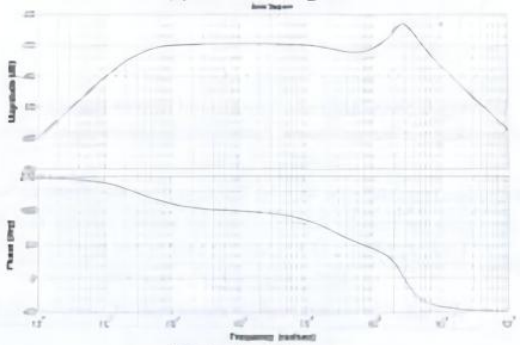

(b) G_{SO} Bode diagram

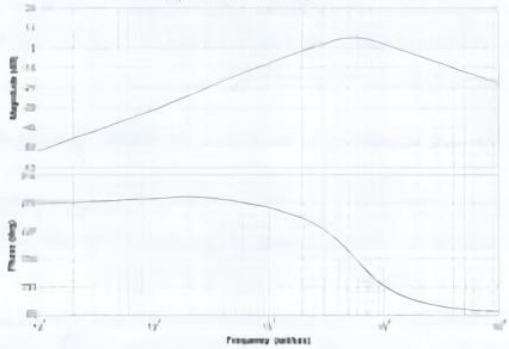

(c) G_{OI} Bode diagram

Fig.6 Bode diagram of G_{LO}, G_{SO}, G_{OI}

It can be seen from Fig.6(a) that the load voltage V_L has a large stability margin to the reference voltage V_L^*, and the load voltage can track the reference voltage well in the low frequency band, and has a better suppression of high-frequency signals. From Fig.6(b), it can be seen that the G_{SO} gain is small in all frequency bands, indicating that the system has a good suppression effect on the

disturbance of the grid voltage. Comparing Fig.6(c) with Fig.4(c), the gain of G_{cl} is relatively small in all frequency ranges, indicating that the system has better load adaptability.

It can be seen from the above analysis that the composite control combines the advantages of feedforward control and feedback control, and can improve the dynamic performance, followability and stability of the DVR system.

4. Simulation verification and analysis

Use Matlab/Simulink to simulate and verify the compound control strategy adopted in this paper. According to the DVR system structure shown in Fig.1, a simulation model is established for simulation verification.

(1) Voltage sag tracking compensation experiment

In the experiment, a pure resistive load is selected to verify the following compensation performance of the control system when the voltage drops. As shown in Fig.7, at t=0.045s, a voltage drop occurs. After a short dynamic process, the output of the DVR is that the load voltage returns to the level before the drop, and the steady-state error is small.

(2) Suppress system voltage interference experiment

The control system must have a certain suppression effect on the disturbance of the grid voltage and ensure the stable accuracy of the DVR output voltage.

As shown in Fig.8, the grid voltage contains a certain amplitude of the 3rd, 5th, and 7th harmonics, and a voltage drop occurs at t=0.045s. After a short dynamic process, the load voltage returns to the level before the drop. And the control system has a strong inhibitory effect on the harmonic disturbance of the grid voltage. Therefore, DVR can effectively compensate for voltage drops and harmonic disturbances.

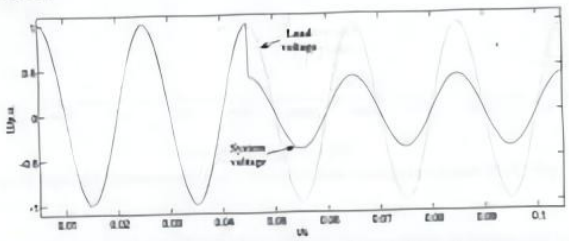

Fig.7 DVR tracking compensation voltage drop

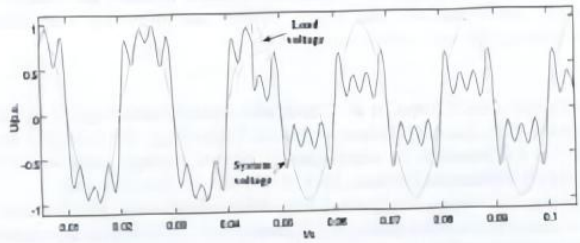

Fig.8 Compensate for voltage harmonics and drops

(3) Load adaptability experiment

In the experiment, a resistive and inductive load is selected to compare the compensation effects of the compound control and the double closed-loop feedback control when the voltage drops. Fig.9(a) is

the compensation effect when double closed-loop feedback is used, and Fig.9(b) is the compensation effect when the compound control is used. It can be seen from the figure that compound control method is superior to double closed loop feedback control in overshoot, dynamic response time, compensation effect, etc.

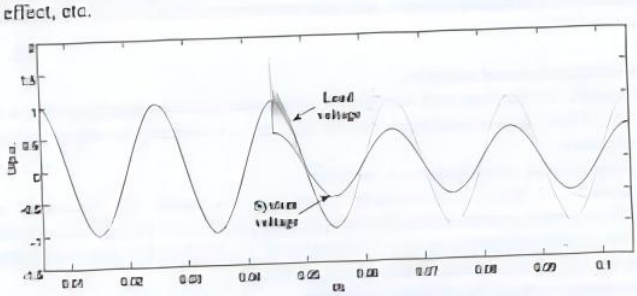

(a) Double closed loop feedbac

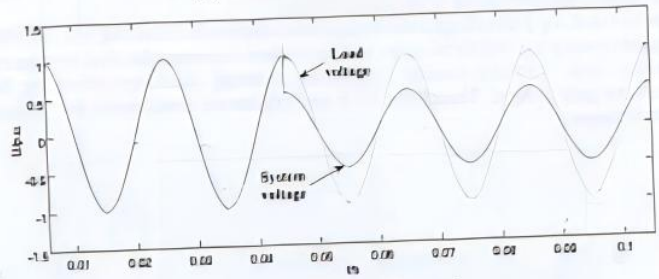

(b) Compound control

Fig.9 DVR band-resistance inductive load compensation voltage drop

5. Conclusion

Based on the brief introduction of the working principle of DVR, this paper proposes a compound control strategy composed of feedforward control, voltage instantaneous value feedback control and filter capacitor current instantaneous value feedback control, deduces the transfer function of the system, analyzes the Bode diagram, and finally verifies the rationality and effectiveness of the compound control strategy through matlab simulation.

References

[1] Shi Ye, Wu Zaijun, Dou Xiaobo, et al. Compound control technology of single-phase dynamic voltage restorer[J]. Journal of Electrotechnical Technology, 2015, 35(17): 85-95(in Chinese).

[2] Shi Jianping, Du Li. Research on compensation control strategy based on DVR in distributed power grid [J]. Electronic Devices, 2018, 41(3): 631-637(in Chinese).

[3] Huang Yonghong, Xu Junjun, Liu Guohai. Non-series transformer type dynamic voltage restorer based on compound control strategy[J].Transactions of China Electrotechnical Society, 2015, 30(12):253-259 (in Chinese).

[4] Guan Huchang. Research on control strategy of dynamic voltage restorer[J]. Automation and Instrumentation, 2017 (06): 26-27 (in Chinese).

[5] Li Jin, Chen Yuanhua, Hu Leilei. Research on the parallel system of dynamic voltage restorer and its control strategy [J]. Energy and Conservation, 2016, (04): 2-4 (in Chinese).

[6] Ma Zhenhua, Zhang Lanyu, Ouyang Jin. Research on control strategy and simulation based on dynamic voltage restorer[J]. Ningxia Electric Power, 2016, (02): 10-18 (in Chinese).

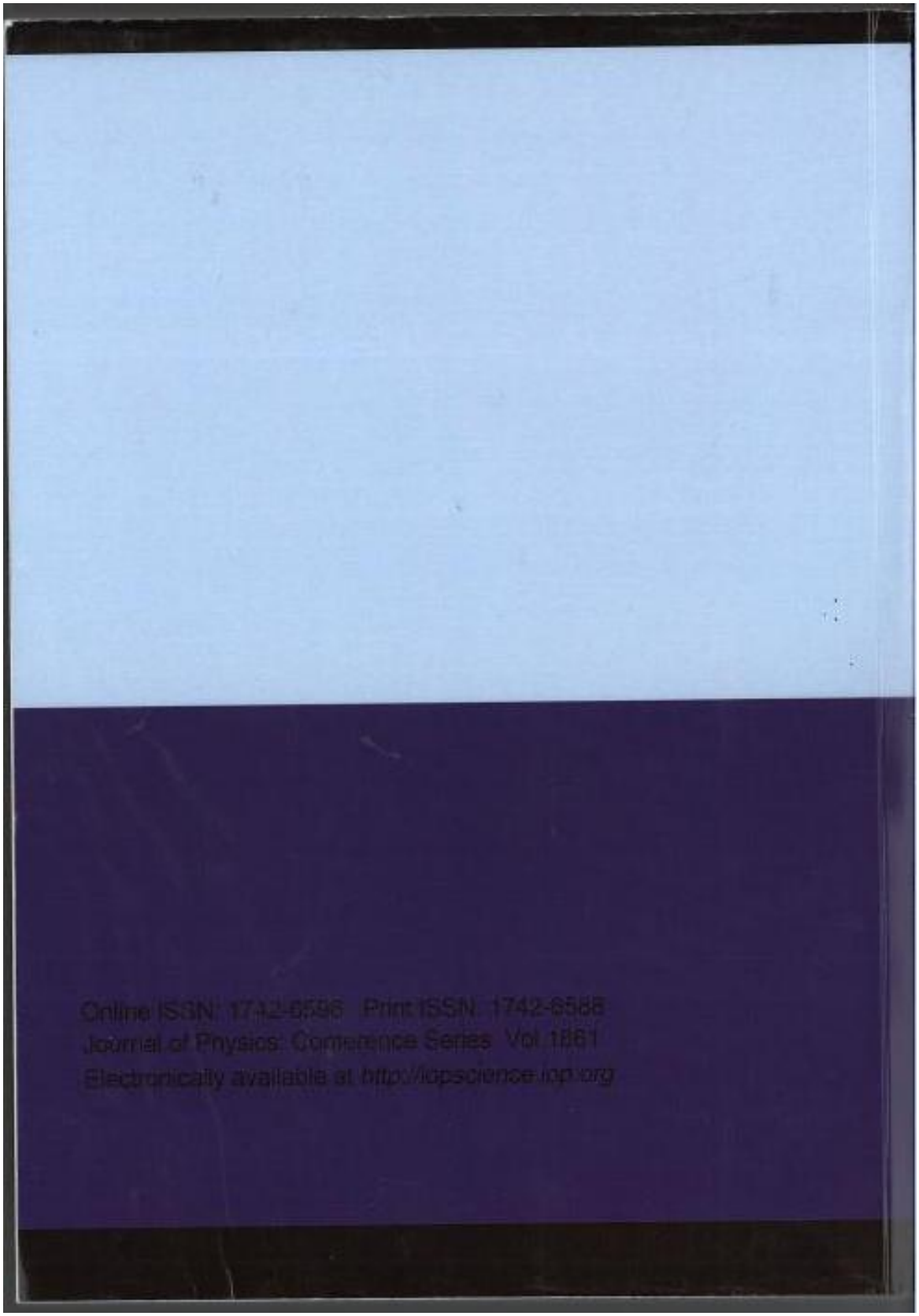
Online ISSN: 1742-6596 Print ISSN: 1742-6588
Journal of Physics: Conference Series Vol 1861
Electronically available at http://iopscience.iop.org

6. Design of Temperature Control System for MTBE Combined Plant Based on Variable Universe Fuzzy Control

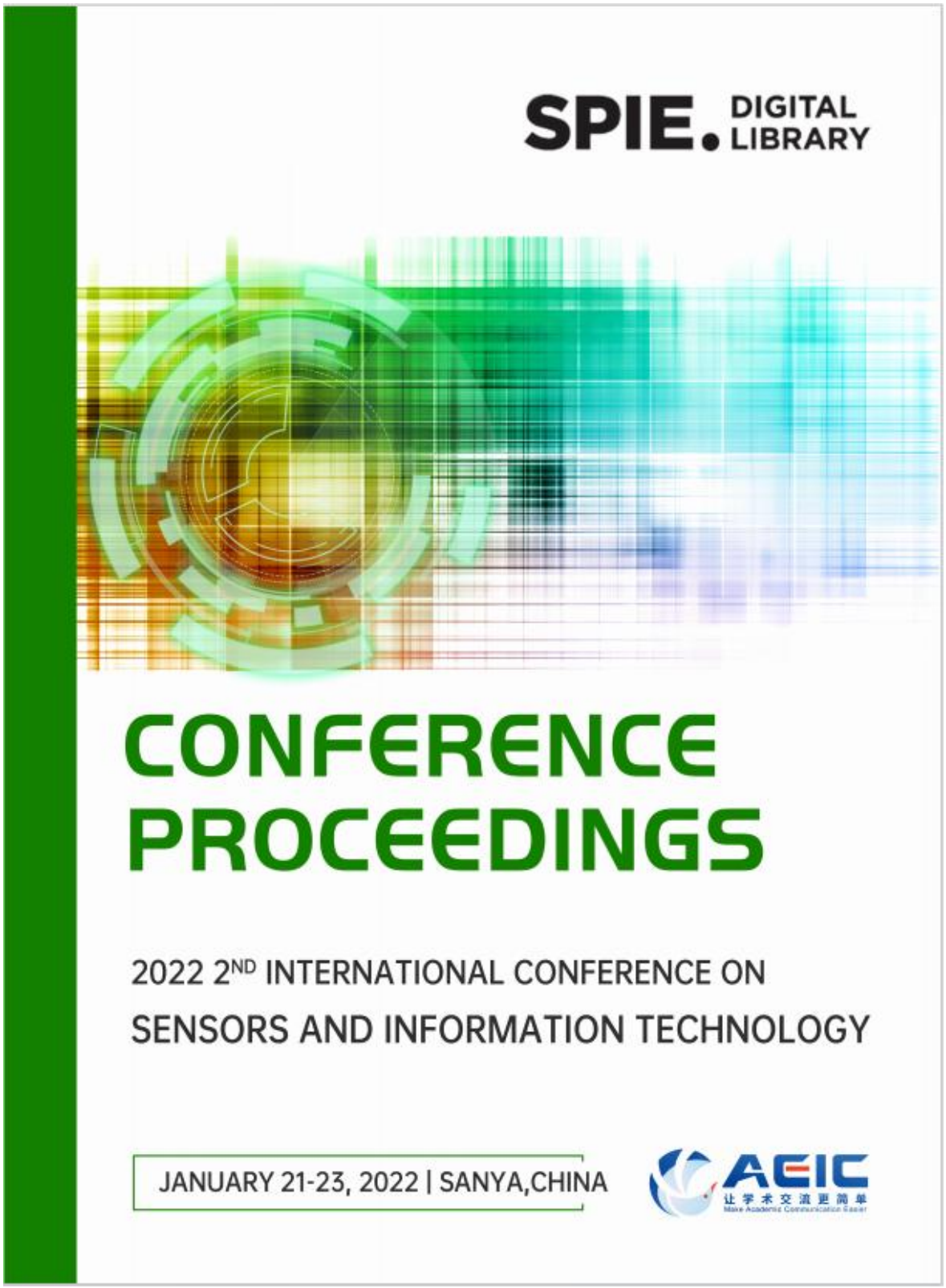

The papers in this volume were part of the technical conference cited on the cover and title page. Papers were selected and subject to review by the editors and conference program committee. Some conference presentations may not be available for publication. Additional papers and presentation recordings may be available online in the SPIE Digital Library at SPIEDigitalLibrary.org.

The papers reflect the work and thoughts of the authors and are published herein as submitted. The publisher is not responsible for the validity of the information or for any outcomes resulting from reliance thereon.

Please use the following format to cite material from these proceedings:
Author(s), "Title of Paper," in *Second International Conference on Sensors and Information Technology (ICSI 2022)*, edited by Lijia Pan, Proc. of SPIE 12248, Seven-digit Article CID Number (DD/MM/YYYY); (DOI URL).

ISSN: 0277-786X
ISSN: 1996-756X (electronic)

ISBN: 9781510654860
ISBN: 9781510654877 (electronic)

Published by
SPIE
P.O. Box 10, Bellingham, Washington 98227-0010 USA
Telephone +1 360 676 3290 (Pacific Time)
SPIE.org

Printed in the United States of America by Curran Associates, Inc., under license from SPIE.

Publication of record for individual papers is online in the SPIE Digital Library.

SPIE. DIGITAL LIBRARY
SPIEDigitalLibrary.org

Paper Numbering: A unique citation identifier (CID) number is assigned to each article in the Proceedings of SPIE at the time of publication. Utilization of CIDs allows articles to be fully citable as soon as they are published online, and connects the same identifier to all online and print versions of the publication. SPIE uses a seven-digit CID article numbering system structured as follows:

- The first five digits correspond to the SPIE volume number.
- The last two digits indicate publication order within the volume using a Base 36 numbering system employing both numerals and letters. These two-number sets start with 00, 01, 02, 03, 04, 05, 06, 07, 08, 09, 0A, 0B ... 0Z, followed by 10-1Z, 20-2Z, etc. The CID Number appears on each page of the manuscript.

Contents

Proc. of SPIE Vol. 12248 1224801-3

论 著 检 索 报 告

委托内容： 周德东的论文收录情况

委托单位： 兰州工业学院

检索单位： 中国科学院兰州查新咨询中心

完成日期： 2022 年 10 月 18 日

中 国 科 学 院 兰 州 查 新 咨 询 中 心

二〇二一年制

一、检索要求

1. 被检作者：周德东（Zhou Dedong；Zhou DD）
2. 委托单位：兰州工业学院
3. 论文发表年限：2022 年
4. 提供待检索论文篇数：2 篇

二、检索范围

Engineering Village 2-Compendex (EI) 1884 - present 网络版

三、检索结果

(1) 收录。

- 有 2 篇被 EI 收录（记录见附件一）。

检索人：

检索单位：

审核人：

完成时间：

附件：

一、EI 收录情况

<RECORD 1>

Accession number 20223712724674
Title Proportioning analysis and PLC control system design of calcium carbide furnace
Authors Zhou, De-Dong (1); Dang, Yuan (1)
Author affiliation (1) School of Electrical Engineering, Lanzhou Institute of Technology, Lanzhu, Lanzhou, China
Source title Proceedings of SPIE - The International Society for Optical Engineering
Abbreviated source title Proc SPIE Int Soc Opt Eng
Volume 12246
Part number 1 of 1
Issue title Second International Conference on Sensors and Information Technology, ICSI 2022
Issue date 2022
Publication year 2022
Article number 1224601
Language English
ISSN 0277786X
E-ISSN 19057853
CODEN PSISDG
ISBN 13 978 1510654983
Document type Conference article (CA)
Conference name 2nd International Conference on Sensors and Information Technology, ICSI 2022
Conference date January 21, 2022 - January 23, 2022
Conference location Sanya, China
Conference code 182083
Sponsor Academic Exchange Information Center (AEIC)
Publisher SPIE
Abstract There are some technical problems in the preparation of mixed charge for calcium carbide furnace, such as cumbersome operation, inaccurate ratio and uneven mixing. Based on the analysis of burden proportioning calculation, working principle of batching equipment and batching operation requirements, this paper designs a control system based on frequency converter, PLC and HMI by using frequency converter frequency modulation and master-slave following method, which well meets the requirements of accurate proportion, mixing uniformity and multi-batch operation of calcium carbide furnace mixture. The practical application in the production field shows that the designed control system has the advantages of accurate burden ratio, simple operation, high production efficiency and reliability.</br> © 2022 SPIE.
Number of references 10
Main heading Mixing
Controlled terms Control systems - Frequency converters - Furnaces - Production efficiency
Uncontrolled terms Batch operation - Batching equipment - Calcium carbide furnace - Control system designs - Master slave - Mixed ingredient - Mixing uniformities - Multiple batch - PLC - PLC control systems
Classification codes 731.1 Control Systems - 802.3 Chemical Operations - 913 Production Planning and Control; Manufacturing - 913.4 Manufacturing
DOI 10.1117/12.2637881

Database Compendex
Compilation and indexing terms, Copyright 2022 Elsevier Inc.

<RECORD 2>

Accession number 20223712724670
Title Design of Temperature Control System for MTBE Combined Plant Based on Variable Universe Fuzzy Control
Authors Zhou, De-Dong (1); Shi, Dong-Dong (1)
Author affiliation (1) School of Electrical Engineering, Lanzhou Institute of Technology, Lanzhu, Lanzhou, China
Corresponding author Shi, Dong-Dong(shidongdong@lzjtu.com)
Source title Proceedings of SPIE - The International Society for Optical Engineering
Abbreviated source title Proc SPIE Int Soc Opt Eng
Volume 12246
Part number 1 of 1
Issue title Second International Conference on Sensors and Information Technology, ICSI 2022
Issue date 2022

Publication year 2022
Article number 1224603
Language English
ISSN 0277786X
E-ISSN 19057853
CODEN PSISDG
ISBN 13 978 1510654983
Document type Conference article (CA)
Conference name 2nd International Conference on Sensors and Information Technology, ICSI 2022
Conference date January 21, 2022 - January 23, 2022
Conference location Sanya, China
Conference code 182083
Sponsor Academic Exchange Information Center (AEIC)
Publisher SPIE
Abstract To meet the requirements of temperature controlling of MTBE complex unit, MTBE complex unit temperature control system is designed. The principle of MTBE complex unit temperature control system is introduced. Aiming at the characteristics of the controlled object, the mathematical model of the system is constructed and analyzed. By adopting the method of Feedforward and variable-region fuzzy control system, the structure of system hardware and software are designed. Results of experiment indicate that the designed temperature control system has the strong anti-interference performance and robustness. It can meet the requirement of accuracy and stability of MTBE complex unit temperature control system.</br> © 2022 SPIE.
Number of references 9
Main heading Temperature control
Controlled terms Feedforward control - Fuzzy control
Uncontrolled terms Complex units - Controlled objects - Feed forward - Fuzzy control system - Hardware structures - Software structures - Temperature control systems - Temperature controlling - Variable regions - Variable universe fuzzy controls
Classification code 731 Automatic Control Principles and Applications - 731.3 Specific Variables Control
DOI 10.1117/12.2637881

Database Compendex
Compilation and indexing terms, Copyright 2022 Elsevier Inc.

（End）

文本复制检测报告单(简洁)

No:BC20220928103409923766145　　检测时间:2022-09-28 10:34:59

检测文献: Design of Temperature Control System for MTBE Combined Plant Based on Variable Universe Fuzzy Control

作者: 周德东

检测范围: 中国学术期刊网络出版总库
中国重要会议论文全文数据库
中国重要报纸全文数据库
中国专利全文数据库
英文数据库(涵盖期刊、博硕、会议的英文数据以及德国Springer、英国Taylor&Francis 期刊数据库等)
港澳台学术文献库
优先出版文献库
图书资源

时间范围: 1900-01-01至2022-05-18

检测结果

去除本人文献复制比: 2.2%

去除引用文献复制比: 2.2%　　总文字复制比: 2.2%

单篇最大文字复制比: 1%(Simulation and Research of Fuzzy PID Used in the Biomass Fuel Boiler Temperature Control System)

重复字数:	[399]	总段落数:	[1]
总字数:	[17917]	疑似段落数:	[1]
单篇最大重复字数:	[173]	前部重合字数:	[249]
疑似段落最大重合字数:	[399]	后部重合字数:	[150]
疑似段落最小重合字数:	[399]		

指　标:　疑似剽窃观点　疑似剽窃文字表述　一稿多投　疑似整体剽窃　过度引用　重复发表

表格: 0　公式: 没有公式　疑似文字的图片: 0　脚注与尾注: 0

1. Design of Temperature Control System for MTBE Combined Plant Based on Variable Universe Fuzzy Control

总字数: 17917

相似文献列表

去除本人文献复制比: 2.2%(399)　文字复制比: 2.2%(399)　疑似剽窃观点: (0)

1	Simulation and Research of Fuzzy PID Used in the Biomass Fuel Boiler Temperature Control System - 《Proceedings of 2011 IEEE International Conference on Intelligent Computing and Intelligent Systems(ICIS 2011) vol.01》 - 2011-11-18	1.9% (173) 是否引证：否
2	Researches on Variable Temperature Drying Technology and on-Line Control for High Moisture Content Paddy - 《Proceedings of 2011 international Conference on New Technology of Agricultural Engineering(ICAE 2011)》 - 2011-05-27	1.9% (173) 是否引证：否
3	Two Intersections Traffic Signal Control Method Based on ADHDP Lin Cao;Bin Hu;Xiong Dong;Gang Xiong;Fenghua Zhu;Zhen Shen;Dong Shen;Yulong Liu; - 《Proceedings of 2016 IEEE International Conference on Vehicular Electronics and Safety》 - 2016-07-10	1.3% (123) 是否引证：否
4	Neural Networks Adaptive Control of Aircraft Engine Based on Genetic Algorithm Hongmei Zhang;Ziyun Dong;Guangyun Xu; - 《第26届中国控制与决策会议论文集》 - 2014-05-31	0.7% (128) 是否引证：否
5	A Novel Modified PID Controller Applied to Temperature Control with Self-Tuning Ability Enxiang Yu;Yundou Hu; - 《第28届中国控制与决策会议论文集（下）》 - 2016-05-28	0.7% (107) 是否引证：否
6	Study on the Evaluation of Comprehensive Effect of Logistics Facility Planning Based on Fuzzy Logic Control - 《Proceedings of 2010 International Conference on Management Science and Engineering (MSE 2010) (Volume 1)》 - 2010-10-17	0.7% (107) 是否引证：否

7	The Resin Abrasives Products Hardening Furnace Temperature Control System Design Based on Fuzzy Self-tuning PID - 《Proceedings of 2010 International Conference on Computer,Mechatronics, Control and Electronic Engineering (CMCE 2010) Volume 3》 - 2010-08-24	0.6% (107) 是否引证：否
8	Based on Transcendental Knowledge of Neuron Model to Achieve PH Detection and Control - 《2010 Second International Conference on Communication Systems, Networks and Applications (ICCSNA 2010) (Volume 1)》 - 2010-06-29	0.5% (81) 是否引证：否
9	Research on Sintering Blending Cost Optimization Design for Quality Loss - 《Proceedings of 2011 IEEE the 18th International Conference on Industrial Engineering and Engineering Management(Volume 2)》 - 2011-09-03	0.4% (69) 是否引证：否
10	The Design of Greenhouse Environment Control System Based on Variable Universe Fuzzy Control Algorithm - 《Computer and Computing Technologies in Agriculture V(Part I)》 - 2011-10-01	0.3% (58) 是否引证：否
11	Control Strategy and Experimental Research on Girder Holster Steering System Based on RBF Neural Network PID - 《Proceedings of 2009 9th International Conference on Electronic Measurement & Instruments (ICEMI' 2009) Vol.3》 - 2009-08-16	0.3% (58) 是否引证：否

说明:

1. 总文字复制比：被检测论文总重合字数在总字数中所占的比例
2. 去除引用文献复制比：去除系统识别为引用的文献后，计算出来的重合字数在总字数中所占的比例
3. 去除本人文献复制比：去除作者本人文献后，计算出来的重合字数在总字数中所占的比例
4. 单篇最大文字复制比：被检测文献与所有相似文献比对后，重合字数占总字数的比例最大的那一篇文献的文字复制比
5. 指标是由系统根据《学术论文不端行为的界定标准》自动生成的
6. 红色文字表示文字复制部分;绿色文字表示引用部分;棕灰色文字表示系统依据作者姓名识别的本人其他文献部分
7. 本报告单仅对您所选择比对资源范围内检测结果负责

anlc@cnki.net
https://check.cnki.net/
http://e.weibo.com/u/3194559873/

Design of Temperature Control System for MTBE Combined Plant Based on Variable Universe Fuzzy Control

ZHOU De-dong, SHI Dong-dong*
School of Electrical Engineering, Lanzhou Institute of Technology，Lanzhou Gansu, China
* Corresponding author: 963898691@qq.com

Abstract

To meet the requirements of temperature controlling of MTBE complex unit, MTBE complex unit temperature control system is designed. The principle of MTBE complex unit temperature control system is introduced. Aiming at the characteristics of the controlled object, the mathematical model of the system is constructed and analyzed. By adopting the method of Feedforward and variable region fuzzy control system, the structure of system hardware and software are designed. Results of experiment indicate that the designed temperature control system has the strong anti-interference performance and robustness. It can meet the requirement of accuracy and stability of MTBE complex unit temperature control system.

Key words: Temperature control; Fuzzy control; Feedforward control; Hardware structure; Software structure

1. Introduction

MTBE (methyl tertiary butyl ether), is a colorless, transparent, low viscosity, high octane liquid. Due to its good mutual solubility with gasoline, it can improve the antiknock property of gasoline and improve the quality of gasoline, so it is often used as a gasoline additive to replace tetraethyl lead, and it is an ideal blending component for producing clean gasoline. At present, domestic petrochemical enterprises generate MTBE products through etherification reaction of isobutene components and methanol in MTBE synthesis devices. Temperature and liquid level in the device are the key control parameters, and their fluctuations directly affect the qualification rate of products.

At present, domestic petrochemical MTBE combined devices often use PID controller for control. Although PID control has a simple structure, due to the fixed parameters, the control overshoot is large, the adjustment ability is weak, and it is more dependent on the mathematical model of the controlled object. However, the MTBE system is a complex system with nonlinear, time-varying, and large lag. It is difficult to establish an accurate mathematical model. The control effect of the traditional PID control method is not ideal, resulting in a low automatic control utilization rate, large fluctuations in process parameters, and poor control. Low quality, unstable operation, reduced use efficiency, and increased energy consumption have brought many problems to the environment and enterprises [1-3]. The variable universe fuzzy control is developed on the basis of the traditional fuzzy control theory. Compared with the PID control strategy, it does not need to establish an accurate mathematical model of the control system. It has a wide range of applications, fast response speed, and high control accuracy. It has good stability and reliability, and has certain advantages such as robustness to time-varying loads. In order to meet the temperature control requirements of petrochemical MTBE combined plant, this paper studies and designs a temperature control system based on feedforward and variable universe fuzzy control methods [4-6].

2. How the system works

The structure of the petrochemical MTBE combined device is shown in Figure 1. The material enters the combined device from the top feed port, while the steam enters the combined device from the steam inlet. In the combined device, the steam heats the material through heat exchange to make it fully react. The material separated by heating flows out from the discharge port at the bottom of the tower. During this process, the liquid level and temperature in the tower are required to be kept stable.

Second International Conference on Sensors and Information Technology (ICSI 2022),
edited by Lijia Pan, Proc. of SPIE Vol. 12248, 122480D · © 2022 SPIE
0277-786X · doi: 10.1117/12.2637641

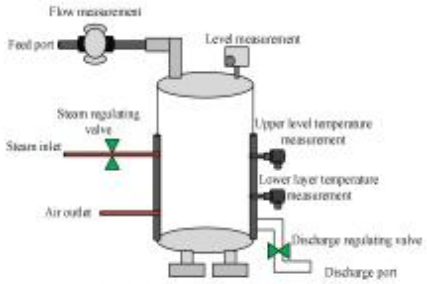

Figurel : Structure of petrochemical MTBE unit

2.1 System Mathematical Model

The temperature control system of the petrochemical MTBE combined plant can be approximately represented by the first-order inertial pure lag link, and its transfer function is:

$$G(s)=\frac{K}{Ts+1}e^{-\tau s} \quad (1)$$

In the above formula, is the static gain of the controlled object; is the time constant of the controlled object; is the pure lag time constant of the controlled object. The temperature control system of the combined device is a common deterministic, nonlinear, large time-varying, and large lag system. According to the above temperature control system, the transfer function of the combined device temperature control system is:

$$G(s)=\frac{0.7}{75s+1}e^{-10s} \quad (2)$$

2.2 Control algorithm

It can be seen from Figure 1 that the flow rate of the feed port in the combined device may change at any time, and this change is a strong disturbance to the temperature in the combined device, which increases the complexity of the system and the difficulty of control. For this kind of nonlinear, large time-varying, and large lag control object, the traditional PID control is difficult to satisfy the static and dynamic indexes of the system. As an important branch of intelligent control, fuzzy control has the advantages of simple operation, fast response speed, good control effect and good robustness without requiring precise mathematical model of the control object. In order to satisfy the anti-disturbance and following performance of the temperature control system, this paper adopts variable universe fuzzy control. In addition, in order to enhance the system stability and control accuracy, this paper adopts the feedforward control and variable universe fuzzy control based on the principle of structure invariance. Compound control method. Such a hybrid control strategy not only overcomes the shortcomings of traditional PID control, but also easily realizes digital control. The control structure of the temperature controller of the combined device is shown in Figure 2. Where is the disturbance amount, the disturbance amount in the combined device temperature control system is the change of the feed inlet flow; is the system given temperature; is the transfer function of the feed-forward compensation device; and is the forward path transfer function of the feedback part is the system output .

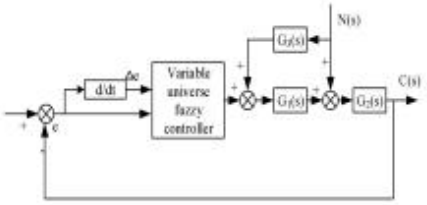

Figure 2: Combined unit temperature controller control structure

3. System hardware design

3.1 System Hardware Composition

The hardware composition of the system is shown in Figure3. The system mainly includes controller, keyboard, lower temperature transmitter, liquid level transmitter, liquid crystal, upper temperature transmitter, flow transmitter, DAC conversion circuit, RS232 communication, power Drive circuit and other components [7-9]. Among them, the controller is the core control unit. The temperature transmitter, liquid level transmitter and flow transmitter respectively collect the temperature of the upper and lower layers of the liquid in the combined device, the flow rate of the feed port and the liquid level information, and process it through the signal conditioning circuit. After that, it is sent to ADC for processing. After the controller analyzes the data, it combines the feedforward and variable universe fuzzy compound control algorithm to output the control signals of the steam inlet electric control valve and the outlet electric control valve to keep the liquid temperature and level in the combined device relatively stable. The control signal output by the controller is converted into an analog voltage signal through the DAC, and then acts on the electric regulating valve after passing through the power drive circuit. Liquid crystal display, keyboard, communication circuit are mainly used for human-computer interaction.

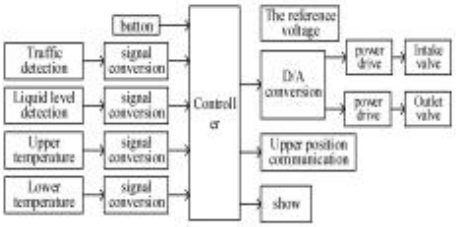

Figure 3: System hardware structure

3.2 Selection of Controller

The controller must use Freescale's 16-bit microcontroller MC9S12XS128. It uses a 16M external crystal oscillator, and the highest frequency is multiplied to 96M through a phase-locked loop; it has a 128K Flash program space, 8-channel 16-bit timer, 8-channel 24-bit interrupt timer, 8-channel 12-bit precision and 8-channel PWM wave output AD converter; at the same time, it integrates communication interfaces such as CAN, SPI, SCI and UART; the on-chip hardware resources are rich, which can meet the system design requirements.

3.3 Signal conditioning circuit

The temperature of the upper layer, the temperature of the lower layer, the flow rate of the feed inlet and the liquid level in the combined device output a 4~20mA current signal through the corresponding transmitter, and the signal that can be processed by the A/D converter on the single chip chip is a voltage of 0~5V. Therefore, it is necessary to replace the 4~20mA current signal with a 0~5V voltage signal, and filter out the interference. In this design, the precision current loop receiver RCV420 produced by TI Company in the United States is used to accurately convert the 4~20mA input

current signal into a 0~5V output voltage signal. In order to filter out the external electrical interference received by the output signal of the transmitter during the transmission process, the converted 0~5v voltage signal is filtered before it is sent to the on-chip A/D of the single-chip microcomputer. The signal conditioning circuit is shown in Figure 4. shown. The operational amplifier TL082 is used to form a second-order low-pass filter, and the filter cutoff frequency is determined according to the size of the resistors R4, R30, and the capacitors C48 and C66. Since the input pin of the A/D of the microcontroller cannot withstand excessive voltage, a high-speed switching diode BAV99 is used to limit the overvoltage under abnormal conditions.

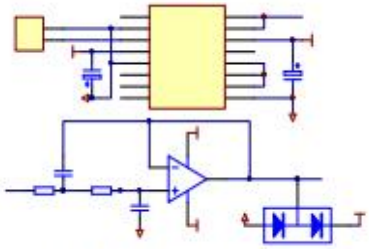

Figure 4: Signal Conditioning Circuit

3.4 DAC conversion circuit

Since the output of the single-chip microcomputer is a digital quantity and the electric regulating valve can only accept the analog quantity, the control signal output by the single-chip microcomputer needs to be converted by DAC. The DAC conversion circuit is shown in Figure 5. The power supply of the electric regulating valve is DC 24V, and the control signal is 0~10V. Therefore, the 4-channel voltage output type 12-bit D/A converter DAC7715 produced by TI Company in the United States is used to realize DAC conversion. The REF01 output voltage is used as the reference voltage of the DAC conversion circuit, which is 10V. The DAC7715 has an SPI serial interface, which can easily communicate with the microcontroller.

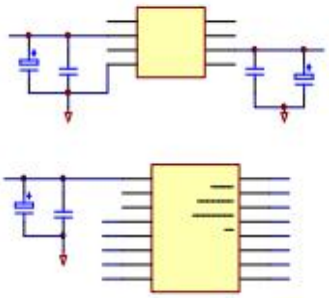

Figure 5: DAC conversion circuit

3.5 Power drive circuit

The 0~10V voltage signal output by DAC7715 is not enough to directly drive the electric regulating valve, so it needs a driving circuit to complete it. This paper adopts the high-voltage and high-current operational amplifier OPA548 produced by TI Company in the United States to form a successful amplifier circuit. OPA548 has low power consumption, wide power supply range, good output voltage swing, continuous output current of 3A, and maximum current of 5A, which can fully meet the needs of system design. Its hardware circuit is shown in Figure 6. First, the 0~10V voltage signal output by DAC7715 is followed by a voltage follower composed of op amp TL082. Its output is

used as the input of OPA548, and the voltage output by OPA548 from pin 6 acts directly. on the electric control valve.

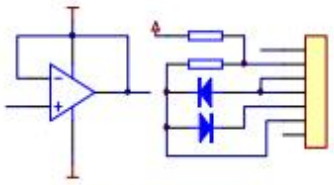

Figure 6: Power Driver Circuit

3.6 Communication circuit

The single-chip microcomputer not only needs to complete the data acquisition and control of the temperature control system of the combined device, but also needs to exchange information with the host computer. Freescale's MC9S12XS128 microcontroller integrates a serial communication interface. Using it can easily expand the RS232 communication circuit, as shown in Figure 7.

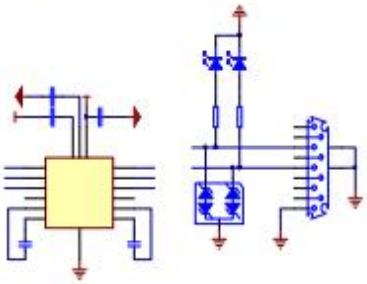

Figure 7: RS232 Communication Circuit

4. Software Design

The system software is mainly composed of initialization program, digital filter program, ADC conversion program, control algorithm program, DAC conversion program, RS232 communication program, and liquid crystal display program. The temperature regulation adopts the compound control algorithm combining feedforward and variable paper fuzzy. The flow chart of the overall system control is shown in Figure 8.

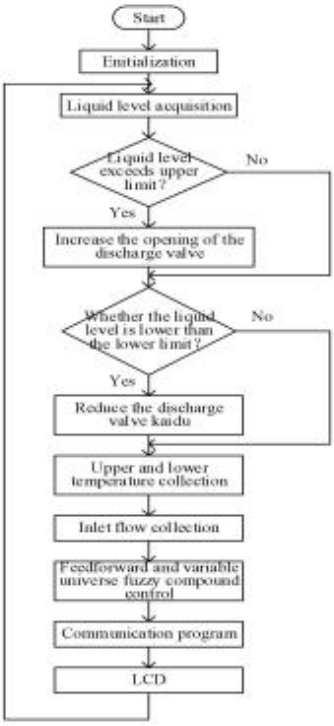

Figure 8: system control flow chart

5. Experimental results

The temperature control system of the combined device designed in this paper is used to collect the liquid level, temperature and material flow in the combined device; Control of liquid level and temperature; Test the communication and monitoring functions between the upper computer and the local control unit. The test results are shown in Figure 9. It can be observed from the figure that the temperature change is controlled within the range of 68 ± 3 ℃, meeting the requirements of technical indicators.

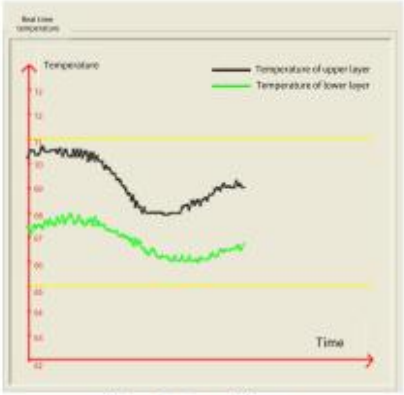

Figure 9: test result diagram

6. Conclusion

This paper introduces the working principle of the temperature control system of the petrochemical MTBE combined plant, establishes and analyzes the mathematical model of the system, and introduces the composite control method of feedforward control and variable universe fuzzy control for the shortcomings of PID control, while maintaining the fuzzy control rules. Under the premise that the form remains unchanged, by selecting the appropriate domain expansion factor, the initial domain of the fuzzy controller changes with the change of the error. When the error is small, the domain of discourse shrinks accordingly, and when the error increases , the universe of discourse is expanded accordingly to improve the accuracy of the control system. The hardware and software design and experimental research of the system are also carried out in this paper. From the experimental research results, it can be seen that the method has good control effect, strong anti-interference ability, can effectively suppress temperature fluctuations, and has good robustness. Requirements for control accuracy and stability.

Reference

[1] Ye Jianchu, Gao Xueshun, Jin Zhenyu, et al. Quality improvement technology for co-production of MTBE by isobutane co-oxidation method [J]. Chemical

[2] Sun Zhongqi, Dai Liankui. Control system of blended gasoline octane number based on nonlinear predictor [J]. Chemical Automation and Instrumentation, 2019, (08): 615-621.

[3] Zhang Guisheng. Optimization analysis of catalytic distillation column of MTBE unit[J].ChemicalManagement,2019,(06):43-44

[4] Lv Shuyan, Chen Hua. Research on performance optimization of boiler main steam temperature control system [J]. Computer Simulation, 2017, 34(1): 109-112.

[5] Wang Jian, Xie Nan. Intelligent temperature control strategy for greenhouse tomato based on fuzzy theory of variable universe [J]. China Agricultural Science and Technology Herald, 2018,21(3):71-79.

[6] Lin Qianjin, Yang Bo, Yu Yue. Simulation and FPGA Optimization Implementation of Fuzzy Control Algorithm Based on Variable Universe [J]. Shanghai Aerospace, 2020, (6): 98-106.

[7] Miao Wennan. Research and Design of Unmanned Bicycle Controller Based on Fuzzy PID [J]. Electronic Measurement Technology, 2021,(12):12-17.

[8] Fan Xiaojing. Research on temperature control system of petrochemical plant heating furnace based on fuzzy algorithm [J]. New Industrialization, 2020,(02):144-147.

[9] Liu Yang, Xing Hongyan, Hou Tianhao. Research on Cascade Variable Universe Fuzzy PID Attitude Control of Quadrotor UAV [J]. Journal of Electronic Measurement and Instrumentation, 2019, 33(10): 46-52.

ISBN 978-1-510-65486-0

SPIE
ISBN:978-1-5106-5486-0
P.O. Box 10, Bellingham, Washington 98227-0010 USA
SPIE.org

7.Proportioning analysis and PLC control system design of calcium carbide furnace

The papers in this volume were part of the technical conference cited on the cover and title page. Papers were selected and subject to review by the editors and conference program committee. Some conference presentations may not be available for publication. Additional papers and presentation recordings may be available online in the SPIE Digital Library at SPIEDigitalLibrary.org.

The papers reflect the work and thoughts of the authors and are published herein as submitted. The publisher is not responsible for the validity of the information or for any outcomes resulting from reliance thereon.

Please use the following format to cite material from these proceedings:
Author(s), "Title of Paper," in *Second International Conference on Sensors and Information Technology (ICSI 2022)*, edited by Lijia Pan, Proc. of SPIE 12248, Seven-digit Article CID Number (DD/MM/YYYY); (DOI URL).

ISSN: 0277-786X
ISSN: 1996-756X (electronic)

ISBN: 9781510654860
ISBN: 9781510654877 (electronic)

Published by
SPIE
P.O. Box 10, Bellingham, Washington 98227-0010 USA
Telephone +1 360 676 3290 (Pacific Time)
SPIE.org

Printed in the United States of America by Curran Associates, Inc., under license from SPIE.

Publication of record for individual papers is online in the SPIE Digital Library.

SPIE. DIGITAL LIBRARY
SPIEDigitalLibrary.org

Paper Numbering: A unique citation identifier (CID) number is assigned to each article in the Proceedings of SPIE at the time of publication. Utilization of CIDs allows articles to be fully citable as soon as they are published online, and connects the same identifier to all online and print versions of the publication. SPIE uses a seven-digit CID article numbering system structured as follows:

- The first five digits correspond to the SPIE volume number.
- The last two digits indicate publication order within the volume using a Base 36 numbering system employing both numerals and letters. These two-number sets start with 00, 01, 02, 03, 04, 05, 06, 07, 08, 09, 0A, 0B ... 0Z, followed by 10-1Z, 20-2Z, etc. The CID Number appears on each page of the manuscript.

文本复制检测报告单(简洁)

№:BC2022092810402948738862 76　　检测时间:2022-09-28 10:40:29

检测文献: Proportioning analysis and PLC control system design of calcium carbide furnace

作者: 周德东

检测范围: 中国学术期刊网络出版总库
中国重要会议论文全文数据库
中国重要报纸全文数据库
中国专利全文数据库
英文数据库(涵盖期刊、博硕、会议的英文数据以及德国Springer、英国Taylor&Francis 期刊数据库等)
港澳台学术文献库
优先出版文献库
图书资源

时间范围: 1915-01-01至2022-05-18

检测结果

去除本人文献复制比: 0%

去除引用文献复制比: 0%　　总文字复制比: 0%

单篇最大文字复制比: 0%()

重复字数:	[0]	总段落数:	[1]
总字数:	[17511]	疑似段落数:	[0]
单篇最大重复字数:	[0]	前部重合字数:	[0]
疑似段落最大重合字数:	[0]	后部重合字数:	[0]
疑似段落最小重合字数:	[0]		

指　标: 疑似剽窃观点　疑似剽窃文字表述　一稿多投　疑似整体剽窃　过度引用　重复发表

表格: 0　公式: 没有公式　疑似文字的图片: 0　脚注与尾注: 0

1. Proportioning analysis and PLC control system design of calcium carbide furnace　总字数: 17511

相似文献列表

去除本人文献复制比: 0%(0)　文字复制比: 0%(0)　疑似剽窃观点: (0)

说明:

1. 总文字复制比: 被检测论文总重合字数在总字数中所占的比例
2. 去除引用文献复制比: 去除系统识别为引用的文献后，计算出来的重合字数在总字数中所占的比例
3. 去除本人文献复制比: 去除作者本人文献后，计算出来的重合字数在总字数中所占的比例
4. 单篇最大文字复制比: 被检测文献与所有相似文献比对后，重合字数占总字数的比例最大的那一篇文献的文字复制比
5. 指标是由系统根据《学术论文不端行为的界定标准》自动生成的
6. 红色文字表示文字复制部分;绿色文字表示引用部分;棕灰色文字表示系统依据作者姓名识别的本人其他文献部分
7. 本报告单仅对您所选择比对资源范围内检测结果负责

amlc@cnki.net
https://check.cnki.net/
http://e.weibo.com/u/3194559873/

PROCEEDINGS OF SPIE

SPIEDigitalLibrary.org/conference-proceedings-of-spie

Proportioning analysis and PLC control system design of calcium carbide furnace

Zhou, De-dong, Dang, Yuan

De-dong Zhou, Yuan Dang, "Proportioning analysis and PLC control system design of calcium carbide furnace," Proc. SPIE 12248, Second International Conference on Sensors and Information Technology (ICSI 2022), 122480H (13 May 2022); doi: 10.1117/12.2637651

SPIE. Event: 2nd International Conference on Sensors and Information Technology (ICSI 2022), 2022, Nanjing, China

Proportioning analysis and PLC control system design of calcium carbide furnace

ZHOU De-dong DANG Yuan

School of Electrical Engineering, Lanzhou Institute of Technology , Lanzhou Gansu,China
445291776@qq.com, 352231344@qq.com

ABSTRACT

There are some technical problems in the preparation of mixed charge for calcium carbide furnace, such as cumbersome operation, inaccurate ratio and uneven mixing. Based on the analysis of burden proportioning calculation, working principle of batching equipment and batching operation requirements, this paper designs a control system based on frequency converter, PLC and HMI by using frequency converter frequency modulation and master-slave following method, which well meets the requirements of accurate preparation, mixing uniformity and multi batch operation of calcium carbide furnace mixture. The practical application in the production field shows that the designed control system has the advantages of accurate burden ratio, simple operation, high production efficiency and reliability.

Key words: Calcium carbide furnace; Mixed ingredients; Multiple batches; Frequency converter; PLC

1. INTRODUCTION

Calcium carbide furnace is a special equipment for high-temperature smelting using the mixture of quicklime, coke and anthracite as raw materials through the arc current between the electrodes. Its working mode is continuous feeding and intermittent discharge. The calcium carbide (calcium carbide, CaC2) flowing out of the furnace is an important chemical industry. Basic raw materials [1]. The by-product produced in the smelting process is coal gas (CO), which is mixed in the flue gas of the calcium carbide furnace and sent to the lime kiln as fuel for calcination after purification treatments such as sedimentation and dust removal.

The raw materials of calcium carbide furnace are dried, crushed and screened through processing equipment, and are prepared into block materials of a certain particle size, which are transferred to the corresponding raw material storage tanks with a forklift. [2-4]. In the production of calcium carbide, 100 parts quicklime and 56~65 parts of carbon-containing raw materials are used to prepare mixed charge for calcium carbide furnace[5]. When the carbon-containing raw material is coke alone, the charge resistance is extremely low, and the electrode rises too high, which will cause the manufacturing capacity of the electric furnace to decrease, the power consumption to increase, and the quality of calcium carbide is not good; when the carbon-containing raw material is anthracite alone, the furnace resistance is more independent The coke time is much higher, and the electrode often goes deep into the furnace, causing serious electrode consumption[6-8]. Therefore, the carbon-containing raw materials used in the three-phase calcium carbide furnace are mostly a mixture of coke and anthracite [9]. In the carbon-containing raw materials, when the content of coke is large, the lower limit of the ratio is 56 parts, and when the content of anthracite is large, the upper limit of the ratio is 65 parts.

Ingredients are an important link in the production of calcium carbide. The precise ratio of raw materials and the uniformity of the mixed charge are the prerequisites for ensuring the quality of calcium carbide, saving energy and reducing consumption. However, in the actual production of calcium carbide, there are many factors that affect the ratio of the mixed charge, mainly manual operation, the uniformity of raw material particles, the working characteristics of the batching equipment and the deviation of the weighing system, etc[10]. In order to overcome these unfavorable factors, this article intends to design a high-precision, multi-batch batching control system based on inverter and PLC control.

2. CALCIUM CARBIDE FURNACE BATCHING CONTROL ANALYSIS

2.1 Calculation of the proportion of ingredients

The calculation of the ratio of the mixed charge of the calcium carbide furnace depends on the capacity of the calcium carbide furnace. For the large-capacity calcium carbide furnace, its capacity is large, the furnace temperature is high, and the raw material ratio is different, which has little effect on the reaction in the furnace. Therefore, the large-capacity

Second International Conference on Sensors and Information Technology (ICSI 2022), edited by Lijia Pan, Proc. of SPIE Vol. 12248, 122480H · © 2022 SPIE 0277-786X · doi: 10.1117/12.2637651

calcium carbide furnace has not very strict requirements for the raw material ratio; Calcium carbide furnace, when the moisture content of coke fluctuates greatly, it will have a greater impact on the quality of calcium carbide and the power consumption of the electric furnace. Therefore, it is necessary to accurately calculate the ratio of raw materials. The commonly used raw material ratio calculation methods for calcium carbide furnace are divided into anhydrous coke calculation method and water-containing coke calculation method.

$$\begin{cases} X = \dfrac{K_1 + K_2 \times K_d + \Delta C}{K_2 + K_g \times K_d + G_g + \Delta C_a} \times 100 & (1) \\ Y = X + (1 - W) & (2) \end{cases}$$

Formula (1) is an anhydrous coke calculation method, where X is the amount of anhydrous coke required for 100 parts of quicklime, K1=56.25, K2=87.5, Kc is the fixed carbon% contained in coke, Kg is the CaO% contained in quicklime, Kd is the calcium carbide component (CaC2)%, Gg is the weight of free calcium oxide, ΔC is the loss of coke, and ΔCa is the loss of quicklime.

Formula (2) is the calculation method for water-containing coke, where Y is the amount of water-containing coke required for 100 parts of quicklime, X is the amount of anhydrous coke required for 100 parts of quicklime, and W is the water content% of the coke. In actual production, follow the data listed in Table 1 to guide production.

Table 1: Reference table of raw material ratio of calcium carbide furnace

W%	Y	W%	Y	W%	Y	W%	Y
1	54.4	6	57.3	11	60.5	16	64.1
2	55.0	7	57.9	12	61.2	17	64.9
3	55.5	8	58.5	13	61.9	18	65.7
4	56.1	9	59.2	14	62.6	19	66.5
5	56.7	10	59.8	15	63.4	20	67.3

2.2 Batching equipment

The batching equipment of calcium carbide furnace includes raw material storage tank and discharger, batching tank and discharger, batching tank weighing equipment, and drum belt conveyor. A schematic diagram of the relative position of the batching equipment is shown in Figure 1.

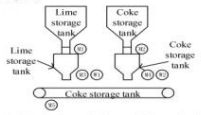

Figure 1: Schematic diagram of calcium carbide furnace ingredients

In Figure 1, M1 and M2 represent the unloaders of lime and coke storage tanks, M3 and M4 represent the unloaders of lime and coke batching tanks, M5 represents the drum belt conveyor, and W1 and W2 represent the scales of lime and coke batching tanks respectively. Heavy equipment.

The unloader of the storage tank and the batching tank is composed of a discharging device, an electric vibrator and its driving motor. The driving motor of the electric vibrator is powered by a general frequency converter. Adjusting the frequency of the inverter can change the discharge volume. The higher the frequency, the more the discharge volume. When the frequency is zero, the discharging device stops discharging. A tension sensor is installed at the supporting hook of the batching tank. As a weighing device, the amount of raw materials in the batching tank can be accurately

sensed by the sensor and its transmitter. The drum belt conveyor conveys the prepared charge to the calcium carbide furnace charging and distributing process.

2.3 Ingredients operation requirements

The operation requirements for the batching process of calcium carbide furnace are precise preparation, uniform mixing, and multi-batch operation. Precise preparation refers to calculating the weight of coke GC online according to the preset weight GCa of lime and the ratio value Y:

$$G_c = \frac{G_{Ca} \times Y}{100} \quad (3)$$

The operating procedure is that when the preset weight GCa (or calculated weight GC) differs greatly from the actual weight of the ingredients, the variable frequency speed control system runs at a high frequency value and feeds quickly to improve the efficiency of the ingredients; when the two weights are close, the variable frequency system Reduce the operating frequency and feed slowly to prevent overweight; when the two weights are equal, the frequency conversion system stops running and ends the batching.

If the charge of the calcium carbide furnace is not uniformly mixed, it will seriously affect the smelting conditions and power consumption of the electric furnace. In order to achieve uniform mixing of the charge, when unloading, two batching tanks are required to start unloading at the same time and finish unloading at the same time.

Multi-batch batching is based on the level of the material in each barrel, and the operator determines the batching batch for each barrel. Multi-batch operation can simplify the operation of the operator.

3. CALCIUM CARBIDE FURNACE BATCHING CONTROL SYSTEM DESIGN

3.1 Control system hardware design

Calcium carbide furnace batching control system consists of frequency converter, PLC, HMI man-machine interface (touch screen) and related electrical equipment. The schematic diagram of the batching control system is shown in Figure 2

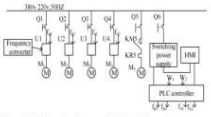

Figure 2: Schematic diagram of the batching control system

In Figure 2, Q1-U1-M1 and Q2-U2-M2 are the frequency conversion drive systems of the lime and coke storage tank dischargers, respectively, and Q3-U3-M3 and Q4-U4-M4 are the lime and coke batching tank dischargers respectively. The frequency conversion drive system of the inverter, Q5-KM5-KR5-M5 is the drive control system of the roller belt conveyor.

The frequency given value of the U1~U4 inverter comes from the analog output of the PLC, which are fp1, fp2, fX1 and fX2 respectively. The signal type is 0~20mA, and 0~20mA corresponds to 0~50Hz. W1 and W2 are the outputs of the weighing equipment transmitter of the batching tank. The signal type is 4~20mA, which is connected through the PLC analog input port. 4~20mA corresponds to 0~GCa or 0~GC. The man-machine interface HMI can be set to select the manual/automatic batching mode, set batching batches, set the preset weight GCa of lime, etc., and can also display the operating frequency of the inverter, the actual weight of the batching and other values.

3.2 The idea of batching control and software programming

Calcium carbide furnace ingredients are divided into manual control and automatic control. Manual control is used for equipment installation and debugging, function inspection and maintenance, and automatic control is used for normal production.

In the manual control mode, each batching equipment can be individually controlled to start and stop without logical coordination. The purpose is to identify the installation and operation status of each batching equipment. The flow chart of manual control is shown in Figure 3.

In Figure 3, the electric vibrator control of storage tank and batching tank includes single-button start-stop control, inverter RUN command output, inverter running status confirmation, inverter frequency setting (fixed value), inverter fault interlock, batching Weight accumulation, etc. When the RUN command of the inverter has been issued and the running status signal has not been fed back, the frequency given value of the inverter is zero. The control of the drum belt conveyor includes single-button start-stop control, control command output, and overload fault interlocking.

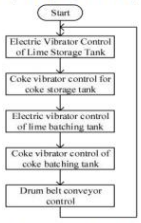

Figure 3: Manual control flow chart

In the automatic control mode, first set the batching batch, the preset weight of quicklime, and the proportioning value; then issue the "batching start" command, and each batching equipment is controlled according to the proposed batching production process with a certain logical relationship. Ingredient production can be interrupted by the "Ingredient Stop" command, or by the "Ingredient Cancel" command. The flow chart of automatic control is shown in Figure 4.

In Figure 4, after the command of "batch start" is issued, the control of the electric vibrator of the lime and coke storage tank is mainly the coarse setting and fine setting of the frequency given value of the inverter. When the weight deviation (= preset weight - actual weight) > the fine setting weight (usually set to 10~15% of the preset weight), the inverter runs at the coarse given frequency (large value); when the weight deviation When ≤ fine setting weight, the inverter runs at fine given frequency (small value). This design can effectively improve batching efficiency and weighing accuracy. The judgment condition for the end of batching is the actual weight = preset weight (or calculated weight). When the batching end signals of lime and coke appear at the same time ("AND" operation), the "unloading start" command is issued.

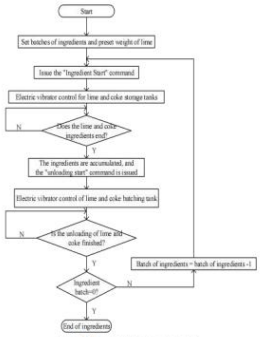

Figure 4: Flowchart of automatic control

After the "unloading start" command is issued, the control of the electric vibrator of the lime and coke batching tank is mainly the coordination of the frequency given value of the inverter, and the coordination is reflected in the simultaneous start and completion of unloading. The control idea is the master-slave-following method. Usually, lime with a large amount of material is used as the master setting, coke with a small amount of material is used as the slave setting, and the slave setting follows the master setting. This design can ensure the mixing uniformity of the charge. The judgment condition for the end of unloading is that the actual weight = 0. When the discharge end signals of lime and coke appear at the same time ("AND" operation), then judge whether the batch of batches is zero. If the batch of batches is zero, end the batch batching; otherwise, the batch number of batches will be reduced by one, and the command of "batching start" will be issued again.

3.3 Operation interface design

The operation of the calcium carbide furnace batching control system is carried out on the man-machine interface HMI, and the HMI operation display interface is shown in Figure 5.

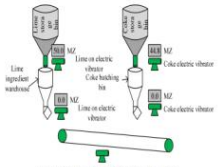

Figure 5: HMI operation display interface

In Figure 5, the electric vibrators of the lime and coke storage tanks are in operation, the icons are displayed as "green", and the operating frequencies are 50Hz and 44.8Hz, respectively. The lime and coke batching tank vibrator is stopped and the icon is shown as "grey". As long as the batching is started, the drum belt conveyor has been running, and the icon display is also "green". The HMI operation setting interface is shown in Figure 6.

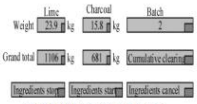

Figure 6: HMI operation setting interface

In Figure 6, the commands that can be issued are "Ingredient Start", "Ingredient Stop", "Ingredient Cancel" and "Cumulative Clear"; the variables that can be set are "Ingredient Batch", "Lime Preset Weight", "Ingredient "Coke preset weight" (can not be set, obtained by calculation); the variables that can be displayed are the current batching batch, the actual batching weight and cumulative weight of lime and coke.

4. CONCLUSION

The control system based on frequency converter, PLC and HMI human-machine interface designed in this paper can meet the requirements of precise preparation, mixing uniformity and multi-batch operation of mixed charge of calcium carbide furnace, and can be applied to production sites with harsh environments such as dust, , with high reliability. The use of this control system has solved the problems of cumbersome batching operation, inaccurate proportioning and uneven mixing in calcium carbide furnace production. It should be noted that in order to ensure the accuracy of the mixing charge ratio, the weighing equipment must be regularly repaired and calibrated.

REFERENCES

[1] Xiong Moyuan, Yue Hongliang. Calcium carbide production and processing, product development and utilization, and a practical manual for new technologies and new processes for pollution prevention and rectification [M]. Beijing: Chemical Industry Press, 2005

[2] Gong Yuqiang, Yu Shurong, Yang Haoran, Wu Mingyong. Research and design of automatic batching system for submerged arc furnace weight reduction method [J]. Industrial Instrumentation and Automation Equipment, 2021(02):21-26+40.
[3] Chen Haibong. Design and Application of Automatic Control Transformation of Submerged Arc Furnace Batching System [J]. Building Materials and Decoration, 2019(18):290-291.
[4] Cong Bin, Zhu Yu. Design and implementation of automatic control system for batching and feeding of submerged arc furnace [J]. Electronic Technology and Software Engineering, 2018(11): 144-145.
[5] Dai Jinshi. A method to improve the cumulative error of automatic batching system of submerged arc furnace [J]. Ferroalloy, 2017,48(10):35-39.
[6] Wu Mingyong, Li Jusheng, Wang Guowei, Zhang Rui. Design of automatic batching control system for submerged arc furnace[J].ChinaMetallurgy,2017,27(10):70-75.
[7] Dong Bingbin, Zhang Xing, Hu Jinrui, Zhang Kun, Duan Wangchun. Design and implementation of automatic control system for batching and feeding of submerged arc furnace [J]. Ferroalloys, 2017,48(08):31-34.
[8] Gao Gang, He Xueling. Application of frequency conversion speed regulation technology in calcium carbide smelting batching system [J]. Chemical Management, 2021(22):58-59+94.
[9] Yan Baogang. Research and Design of Calcium Carbide Furnace Batching and Feeding Control System [D]. Inner Mongolia University of Science and Technology, 2012.
[10] Li Yali. Research on PLC-based automatic batching control system [J]. Digital Technology and Application, 2018,36(01):6-7.

ISBN 978-1-510-65486-0

SPIE
ISBN:978-1-5106-5486-0
P.O. Box 10, Bellingham, Washington 98227-0010 USA
SPIE.org

8. Research on engineering testing method of automatic train control

system based on communication

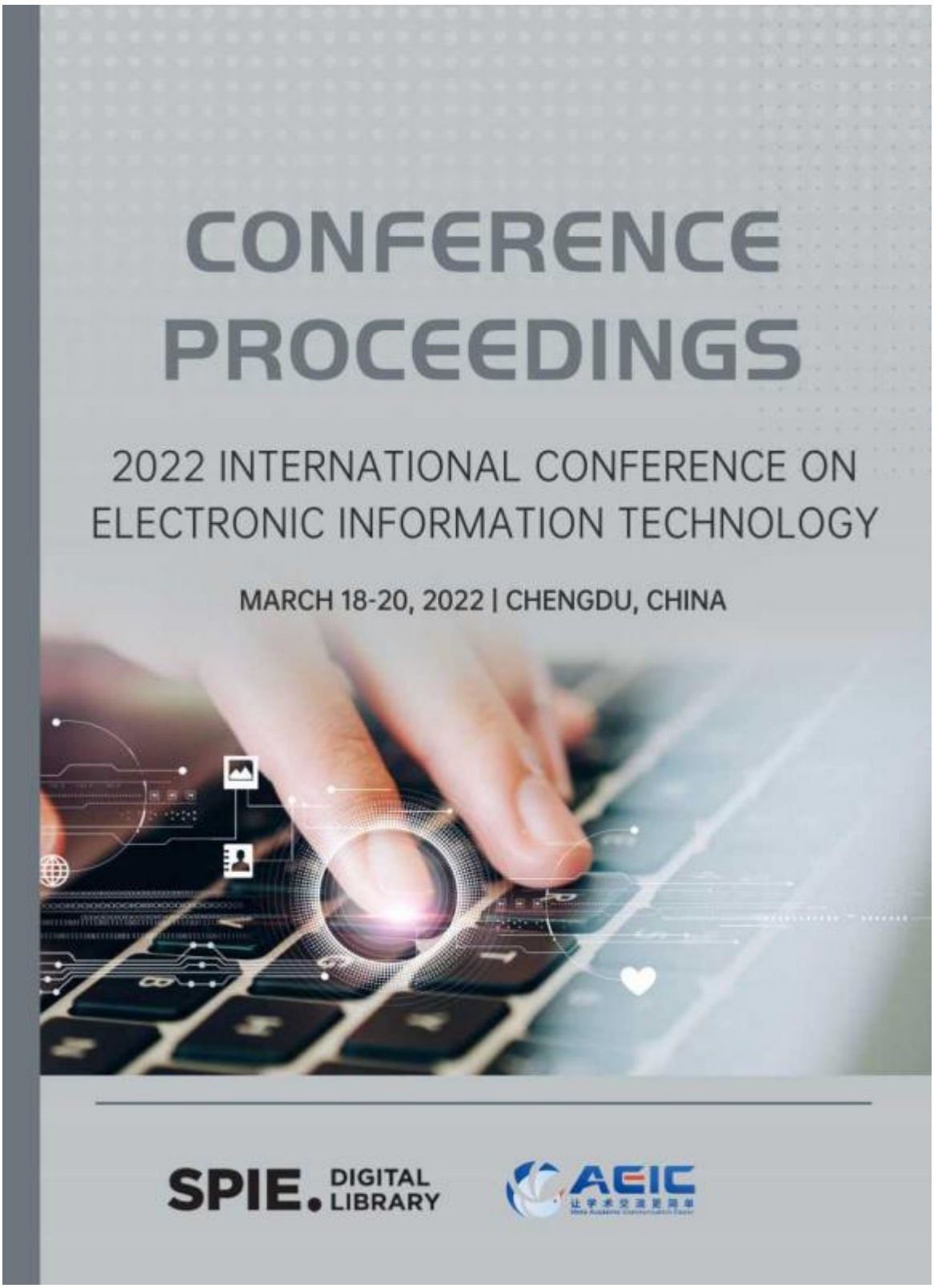

The papers in this volume were part of the technical conference cited on the cover and title page. Papers were selected and subject to review by the editors and conference program committee. Some conference presentations may not be available for publication. Additional papers and presentation recordings may be available online in the SPIE Digital Library at SPIEDigitalLibrary.org.

The papers reflect the work and thoughts of the authors and are published herein as submitted. The publisher is not responsible for the validity of the information or for any outcomes resulting from reliance thereon.

Please use the following format to cite material from these proceedings:
Author(s), "Title of Paper," in *International Conference on Electronic Information Technology (EIT 2022)*, edited by Zhangyu Li, Hilal Imane, Proc. of SPIE 12254, Seven-digit Article CID Number (DD/MM/YYYY); (DOI URL).

ISSN: 0277-786X
ISSN: 1996-756X (electronic)

ISBN: 9781510655096
ISBN: 9781510655102 (electronic)

Published by
SPIE
SPIE.org

Printed in the United States of America by Curran Associates, Inc., under license from SPIE.

Publication of record for individual papers is online in the SPIE Digital Library.

SPIE. DIGITAL LIBRARY
SPIEDigitalLibrary.org

Paper Numbering: A unique citation identifier (CID) number is assigned to each article in the Proceedings of SPIE at the time of publication. Utilization of CIDs allows articles to be fully citable as soon as they are published online, and connects the same identifier to all online and print versions of the publication. SPIE uses a seven-digit CID article numbering system structured as follows:

- The first five digits correspond to the SPIE volume number.
- The last two digits indicate publication order within the volume using a Base 36 numbering system employing both numerals and letters. These two-number sets start with 00, 01, 02, 03, 04, 05, 06, 07, 08, 09, 0A, 0B ... 0Z, followed by 10-1Z, 20-2Z, etc. The CID Number appears on each page of the manuscript.

中国科学院兰州文献情报中心科技论著查收证明书 2022-YZ-0174

查收编号：2022-YZ-0174

论 著 检 索 报 告

委托内容： 周德东的论文收录情况

委托单位： 兰州工业学院

检索单位： 中国科学院兰州文献情报中心

完成日期： 2022 年 9 月 5 日

中 国 科 学 院 兰 州 文 献 情 报 中 心

二〇二一年制

中国科学院兰州文献情报中心科技论著查收证明书 2022-YZ-0174

一、检索要求

1、被检作者：周德东（Zhou Dedong；Zhou DD）

2、委托单位：兰州工业学院

3、论文发表年限：2022 年

3、提供待检索论文篇数：1 篇

二、检索范围

Engineering Village 2-Compendex (EI) 1884 - present 网络版

三、检索结果

（1）收录：

- 有 1 篇被 EI 收录（记录见附件一）。

检索人：许萍 检索单位：中国科学院兰州文献情报中心

审核人：任珩 完成时间：2022 年 9 月 5 日

中国科学院兰州文献情报中心科技论著查收证明书 2022-YZ-0174

附件：

一、EI 收录情况

<RECORD 1>
Accession number 20223013295215
Title Research on engineering testing method of automatic train control system based on communication
Authors Zhou, De-Dong (1); Dang, Yalei (1)
Author affiliation (1) Lanzhou Institute of Technology, School of Electrical Engineering, Qilihe, Lanzhou, China
Source title Proceedings of SPIE - The International Society for Optical Engineering
Abbreviated source title Proc SPIE Int Soc Opt Eng
Volume 12294
Part number 1 of 1
Issue title International Conference on Electronic Information Technology, EIT 2022
Issue date 2022
Publication year 2022
Article number 1225412
Language English
ISSN 0277786X
E-ISSN 19963424
CODEN PSISDG
ISBN-13 9781510653085
Document type Conference article (CA)
Conference name 2022 International Conference on Electronic Information Technology, EIT 2022
Conference date March 18, 2022 - March 20, 2022
Conference location Chengdu, China
Conference code 180151
Sponsor Academic Exchange Information Center
Publisher SPIE
Abstract Aiming at the problems of backward test method, long test period and low test efficiency of communication-based train operation control system, the formalized generation method of CBTC (Communication Based Train Control) system engineering acceptance test sequence was studied. The first is to divide the test line into several test sections, the second is to analyze the constraints of the test cases and the characteristics of the test lines, the third is to design the matching algorithm and the connection algorithm, and to connect the constraints of the test cases and the characteristics of the lines into a formal language; It is to design test sequence generation software to generate several executable test sequences. Through the result analysis, the test sequence generated by this method meets the test requirements of the CBTC system, can cover all test cases, and greatly improves the test efficiency. Scopus 2022 SPIE
Number of references 7
Main heading Acceptance tests
Controlled terms Control systems - Efficiency - Formal languages - Formal methods - Railroad traffic control - Software testing
Uncontrolled terms Communication-based train control systems - Communication-based train controls - Engineering tests - Test cases - Test efficiency - Test sequence - Test lines - Testing method - Train control systems - Urban rail transit
Classification code 433.4 Railway Traffic Control - 721.1 Computer Theory, Includes Formal Logic, Automata Theory, Switching Theory, Programming Theory - 723.1 Computer Programming - 723.1.1 Computer Programming Languages - 723.5 Computer Applications - 731.1 Control Systems - 913 Production Planning and Control; Manufacturing - 913.1 Production Engineering
DOI 10.1117/12.2642661
Database Compendex
Compilation and indexing terms, Copyright 2022 Elsevier Inc.

（End）

文本复制检测报告单(简洁)

№:BC20220928102406487379882 6　　检测时间:2022-09-28 10:24:06

检测文献:　Research on engineering testing method of automatic train control system based on communication

作者:　周德东

检测范围:　中国学术期刊网络出版总库
中国重要会议论文全文数据库
中国重要报纸全文数据库
中国专利全文数据库
英文数据库(涵盖期刊、博硕、会议的英文数据以及德国Springer、英国Taylor&Francis 期刊数据库等)
港澳台学术文献库
优先出版文献库
图书资源

时间范围:　1915-01-01至2022-03-16

检测结果

去除本人文献复制比:　0%

去除引用文献复制比:　0%

单篇最大文字复制比:　0%()

总文字复制比:　0%

重复字数:	[0]	总段落数:	[2]
总字数:	[24567]	疑似段落数:	[0]
单篇最大重复字数:	[0]	前部重合字数:	[0]
疑似段落最大重合字数:	[0]	后部重合字数:	[0]
疑似段落最小重合字数:	[0]		

指　标:　疑似剽窃观点　疑似剽窃文字表述　一稿多投　疑似整体剽窃　过度引用　重复发表

表格:0　公式:　没有公式　疑似文字的图片:　0　脚注与尾注:　0

0%(0)	0%(0)	Research on engineering testing method of automatic train control system based on communication_第1部分 (总16493字)
0%(0)	0%(0)	Research on engineering testing method of automatic train control system based on communication_第2部分 (总8074字)

1. Research on engineering testing method of automatic train control system based on communication_第1部分　总字数:16493

相似文献列表

去除本人文献复制比:0%(0)　文字复制比:0%(0)　疑似剽窃观点:(0)

2. Research on engineering testing method of automatic train control system based on communication_第2部分　总字数:8074

相似文献列表

去除本人文献复制比:0%(0)　文字复制比:0%(0)　疑似剽窃观点:(0)

说明:

1. 总文字复制比:被检测论文总重合字数在总字数中所占的比例
2. 去除引用文献复制比:去除系统识别为引用的文献后,计算出来的重合字数在总字数中所占的比例
3. 去除本人文献复制比:去除作者本人文献后,计算出来的重合字数在总字数中所占的比例
4. 单篇最大文字复制比:被检测文献与所有相似文献比对后,重合字数占总字数的比例最大的那一篇文献的文字复制比
5. 指标是由系统根据《学术论文不端行为的界定标准》自动生成的
6. 红色文字表示文字复制部分;绿色文字表示引用部分;棕灰色文字表示系统依据作者姓名识别的本人其他文献部分
7. 本报告单仅对您所选择比对资源范围内检测结果负责

PROCEEDINGS OF SPIE

SPIEDigitalLibrary.org/conference-proceedings-of-spie

Research on engineering testing method of automatic train control system based on communication

Zhou, De-dong, Dang, Yuan

De-dong Zhou, Yuan Dang, "Research on engineering testing method of automatic train control system based on communication," Proc. SPIE 12254, International Conference on Electronic Information Technology (EIT 2022), 122541Z (23 May 2022); doi: 10.1117/12.2640461

SPIE.

Event: International Conference on Electronic Information Technology (EIT 2022), 2022, Chengdu, China

Research on engineering testing method of automatic train control system based on communication

De-dong ZHOU[1], Yuan DANG[1]
[1]School of Electrical Engineering, Lanzhou Institute of Technology, Lanzhou Gansu, China
f_author 445291776@qq.com, s_author 352231344@qq.com

Abstract

TAiming at the problems of backward test method, long test period and low test efficiency of communication-based train operation control system, the formalized generation method of CBTC (Communication Based Train Control) system engineering acceptance test sequence was studied. The first is to divide the test line into several test sections; the second is to analyze the constraints of the test cases and the characteristics of the test lines; the third is to design the matching algorithm and the connection algorithm, and to convert the constraints of the test cases and the characteristics of the lines into a formal language; It is to design test sequence generation software to generate several executable test sequences. Through the result analysis, the test sequence generated by this method meets the test requirements of the CBTC system, can cover all test cases, and greatly improves the test efficiency.

Key words: CBTC, test sequence, formal method, urban rail transit, engineering test

1.INTRODUCTION

Communication-based train control system (CBTC) is a kind of continuous control and monitoring of train operation using advanced communication and computer technology. It is a two-way transmission system between ground control system and train transmission information. The advantages of superior transmission mode and other advantages are the development trend of the global urban rail transit train control system. It adopts more advanced communication means, so that the station and train control center personnel can monitor the train operation in real time, and can effectively prevent accidents and accidents. Prevent all kinds of accidents caused by communication and equipment failures (Liu2020, Han2020). The CBTC system is a prerequisite for ensuring the safe operation of urban rail transit, and it is also a necessary condition for realizing interconnection between lines. Therefore, the system must be fully tested before it is put into use to ensure the safe and efficient operation of urban rail transit. the system must be fully tested before it is put into use to ensure the safe and efficient operation of urban rail transit.

Foreign research on test sequence generation methods is relatively mature, and the most widely used is the European ETCS system, which models the system and generates test sequences. It is relatively immature in China. It is mainly used in the train control system of high-speed railways, and the test sequence is generated by using intelligent algorithms and model building methods.

The formal language can be well recognized by the computer. The research on the test sequence generation method is based on the formal realization of the test case. Therefore, this paper uses the superiority of the formal language to study the test sequence generation method of CBTC system engineering, analyze the test The characteristics of the case and test section, design two logic algorithms, write test sequence generation software, and finally generate several executable test sequences with 100% coverage (Gao2018, Gario A2018, Song2018).

1.1 CBTC system test requirements and test objectives

The CBTC system has become the trend of urban rail transit development in my country and the world because of its fast transmission speed, large transmission data capacity and high real-time performance. The reliability and functional integrity of the CBTC system directly affect the safety and reliability of urban rail transit operations. For the safety of passengers' lives and property, in order to ensure that the CBTC system can meet the system safety requirements and functional requirements, it must be tested for completeness, and scientific testing methods can greatly improve the efficiency of testing and the coverage of requirements. Through the investigation of many mainstream signal equipment manufacturers in China, the current engineering acceptance test of the CBTC system still uses test cases for testing. The test efficiency is low, the engineering test environment is complex, the test cost is high, and the test is related to other

International Conference on Electronic Information Technology (EIT 2022)
edited by Zhengbo Li, Hilal Imane, Proc. of SPIE Vol. 12254, 122541Z
© 2022 SPIE · 0277-786X · doi: 10.1117/12.2640461

tasks in the rail transit industry. Simultaneous or staggered development, the test time is tight and insufficient. Therefore, it is necessary to study the generation method of CBTC system engineering acceptance test sequence.

The test work of CBTC system engineering test mainly includes: subsystem test, integration test and field test. No matter which type of test, the specific functions of the system need to be tested according to the test cases in a specific environment. This article compiles 305 test cases based on the relevant standards of a subway Line 10 and the latest interconnection specifications, and covers the latest functional requirements of the CBTC system. all needs. The completeness test of the CBTC system is carried out. The test goal is that the system passes all test cases and the system functions meet all system requirements and specifications.

1.2 Definition of Test Cases and Test Sequences

The test case is the soul of the test, and its design and compilation are one of the most important activities in the engineering acceptance test of the system. The criterion for checking whether the system can meet the specified safety standards and functional requirements is the passing of the relevant test cases (Jiang2020).

The goal of the CBTC system engineering acceptance test is to check whether the functions of the system meet the latest interconnection specifications. If each requirement in the specification is compiled into a corresponding test case, the number of test cases obtained will be very large, which is not conducive to testing, development of work. Therefore, the functions of the CBTC system are refined and refined, and the necessary functions at the bottom of the system are divided, and these necessary functions are called functional characteristics. Each requirement in the specification can find its corresponding functional feature, and each functional feature corresponds to one or more system requirements, and each functional feature is a set of system requirements. One or more test cases can be prepared for each functional feature, and testing the test cases is the verification of whether the system can meet the system requirements specification. Its relationship diagram is shown in Figure 1

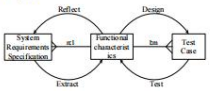

Figure1 Relationship between SRS, functional characteristics and test cases

When testing the CBTC system, if all the test cases prepared are tested in sequence, it is indeed possible to complete the test to ensure the security and reliability of the system. In order to save unnecessary time in the test phase and reduce the labor intensity and workload of testers, we will arrange some relevant test cases in the order of train operation or train state transition, and the formed aggregate is the test case. sequence (Cui2020).

The test sequence is obtained by connecting the test cases in an orderly series. A good test sequence can guide the smooth progress of the test work., greatly reduce the test time, reduce the test pressure of the tester, and at the same time, can effectively avoid the test work. Accidents caused by mistakes. How to scientifically arrange the test sequence is the focus of this study.

2.RESEARCH METHODS

There are two main methods for generating test sequences in the CBTC system, namely the model-building method and the manual arrangement method. The model method is mainly used in high-speed railway train control systems, such as high-speed railway C3-level train control systems, on-board equipment, and RBC subsystems. The scope of its application has certain limitations, and the CBTC system engineering test requires the acceptance and confirmation of the overall function of the system. Therefore, the model method is not suitable for the CBTC system engineering acceptance test. Manual arrangement method This method requires relatively mature test specifications and sufficient experience of on-site testers. It is mainly aimed at CTCS-3 train control system of high-speed railway, and is also not suitable for engineering acceptance test of CBTC system.

This paper proposes a formal language description method, which converts test lines, test trains and test cases into a

formal language that can be recognized by machines, and uses test sequence auxiliary generation tools to concatenate test cases into executable test sequences. The basic flow chart of the automatic generation method of the test sequence described by language is shown in Figure 2

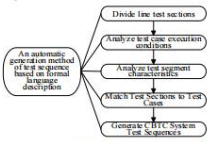

Figure 2: Basic flow chart of automatic generation of test sequences

2.1 Divide line test sections

The CBTC system engineering acceptance test case has certain requirements for the execution location. For example, the test to determine the train stop position needs to be tested near the platform; the red light protection needs to be tested outside the signal guard; the switch protection should be tested near the switch, etc. In order to better find the suitable execution location of the test case, the actual train running route needs to be divided into several sections. The following conditions need to be met when dividing the test section:

(1) the length of the test segment; Considering that it takes a certain amount of time for testers to compare and record a test case and ensure high test efficiency, the length of the test section should be moderate.

(2) the markers of the demarcation; When dividing the test section, it is better to have a physical reference mark, so that the tester can observe the boundary of the test section, which can greatly facilitate the on-site test work.

(3) The test section can be monitored in real time; the vacancy and occupation of the test section can be displayed on the ATS interface, which is convenient for the control center to command and manage the test during on-site testing.

Considering the above factors, the axle counter is selected as the dividing point of the test section to meet the above requirements, and the line is divided into several test sections according to the signal layout of a subway line 10.

2.2 Analyze test case execution constraints

Observing all the test cases in the test case library, it can be found that there are many factors restricting the execution of the test case, such as the execution location of the test case, the preset conditions of the test case, etc. These factors are called the execution constraints of the test case.

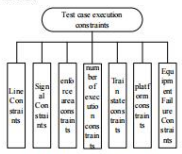

Figure 3 :Test case execution constraints

(1) Route_Constraint: The execution of the test case is the process of the train running on the line, which will involve line-related constraints, which are divided into line-related equipment constraints and line type constraints.

(2) Signal Constraint: In the CBTC system used in urban rail transit in my country, the setting of the signal is mainly used in backup modes such as point mode and interlock mode. Define the state of the semaphore and the formal language: semaphore red light, semaphore green light.

(3) Constraints of execution area: To analyze the execution area of the test case, first analyze the driving route of the train. The train starts from the garage, that is, the depot, enters the section and the station, and finally returns to the depot. The area where the train runs is the test. The execution area of the case.

(4) Constraints on the number of executions: Some test cases need to be tested multiple times on the line. In order to ensure the completeness of the test, tests must be performed in all areas that meet the conditions of the test case, such as the test train detaining and skipping functions. Every station area is tested

(5) Train state constraints, platform type constraints, and equipment failure constraints.

By analyzing the functional description, case description, test requirements, and test environment in the test case, the following constraints are established, as shown in Figure3. Formalize the execution constraints of various test cases into machine language that the computer can recognize, expressed in parentheses.l

2.3 Analyze test segment characteristics

The characteristics of the test section are various, and we only need to be able to determine the characteristic amount of the test site of the test case. By analyzing the test case library, the execution constraints of the test case are obtained, and the characteristic quantities of the test site can be determined by analyzing them, such as transponders, signals, switch sections, parking points, platform types, and routes. It is summarized and summarized, as shown in Figure 4.

Figure 4: Test section characteristics

2.4 Design matching algorithm

The test line has been divided into test sections, so how to reasonably allocate all the test cases to the test sections according to the execution constraints of the test cases is the focus of this section. By analyzing the test location constraints of each test case, a set of constraint relation expressions can be obtained. Similarly, by analyzing each test section, a set of corresponding test section line characteristic expressions can be obtained. The line feature expression of each test section is matched, and if the match is successful, it will be put into the corresponding test section. The specific implementation process is given as an example.

For example, a train recovered from a fault completes the position initialization test case on a straight line. A train at the CTC control level loses its position due to an ATP fault. The line ahead is straight and there is no opposite turnout. After passing through two consecutive transponders, The on-board ATP should be able to obtain the position and running direction of the train. Its constraint relation expression is:

$$\begin{cases} Num\_Ba\_FB + Num\_Ba\_VB \\ + Num\_Ba\_IB + Num\_Ba\_LDR \\ \quad + Num\_Ba\_WB \geq 2 \\ Area = ALL\_Line \\ TestcaseNum = Every\_Target \\ Station\_Type = None \end{cases} \quad (1)$$

A test section of a subway line 10 is randomly selected, each feature quantity of this section is analyzed, and it is formalized into machine language. Its characteristic expression is obtained as follows:

Num_Ba_FB=2; Num_Ba_VB=0; Num_Ba_IB=1;

Num_Ba_LDR=1 ; Num_Ba_WB=0; Num_Si_Station=0

Num_Si_Section=1; Num_Si_Depot=0;

Num_Po_Station=0; Num_Po_Section=0

Num_Po_Depot=0; Num_Ax=2; Num_Ap=1;

Num_Tc=0; Num_Tr=1; Num_Zc=0; Name_ZC_Loca=1;

Name_CI_Locol=1; Num_SW=0; Station_Type=None;

Area=Section; Name_Line_Local=1

The analysis shows that there are more than two transponders in the test section, which meet the conditions; the execution area is the whole line, that is, the station, the section and the vehicle depot are all executed. This test section is an section, so the conditions are met; each qualified Each area is executed once, and this test section needs to be executed if the conditions are met; there is no requirement for the station type, and the matching is successful.

It can be seen that it is not difficult to assign each test case to test sections that meet the conditions. However, due to the constraint of the number of test case executions, each test case may need to be executed in multiple test sections, then , how to correctly and reasonably match all test cases to all test sections that meet the conditions is the difficulty and the key point. Combined with the matching method described above, a matching algorithm is designed, and the algorithm flowchart is shown in Figure 5.

The number of test case executions is a key variable, which determines the number of test sections matched by the test case. It covers all three cases, which are executed only once for the whole line, once in each concentrated area, and once in all areas that meet the conditions. And the test section is traversed, and finally all the corresponding execution sections can be found for each test case.

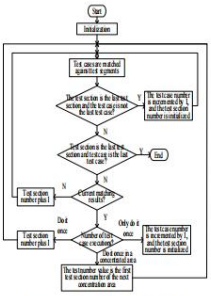

Figure 5: Flowchart of matching algorithm

The number of test case executions is a key variable, which determines the number of test sections matched by the test case. It covers all three cases, which are executed only once for the whole line, once in each concentrated area, and once in all areas that meet the conditions. And the test section is traversed, and finally all the corresponding execution sections can be found for each test case.

2.5 Generate CBTC System Test Sequences

Through the above steps, all the test cases have been allocated to the corresponding execution positions, and the final work is to connect them into several executable test sequences according to different train operation levels. The running level of the train is divided into interlock level, point level and CBTC level. Sorting by train operation class can improve the operability of the generated test sequences. Figure 6 shows the generation process of a test case. Multiple test cases can be executed in one section, and they are concatenated into a test sequence through the test case connection algorithm.

In order to make the compiled test sequence more efficient and executable, the constraints of the test cases and the process of the test train running on the line are analyzed, and the test cases are divided into: interlock level test cases, point level test cases, CBTC level test cases, mode Convert test cases.

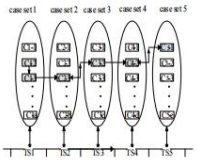

Figure 6: Generation of a test sequence

3.SOFTWARE

Traverse the CBTC system engineering acceptance test cases, search for mode conversion test cases, point-level test cases, interlock-level test cases, and CBTC-level test cases in turn, and connect them in series, and finally generate several executable test sequences.

The structure of the CBTC system engineering acceptance test sequence generation software is shown in Figure7. It is designed to store the execution constraints of the test cases and the characteristic quantities of the test sections in the data storage layer, establish and call the database through the SQL Server software, realize the functions of database query and test sequence generation in the application layer, and display and load various needs in the presentation layer. data and the final export results. In a word, the function realized by the test sequence generation software is mainly to generate the test sequence by using the test case data and the test section data.

The interface of the test sequence generation software is shown in Figure 8. 305 CBTC system engineering acceptance test cases written according to a subway line 10 are input into this tool, and the final generated test sequence is 65, which can be executed after manual testing and verification.

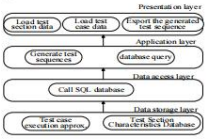

Figure 7: Structure diagram of test sequence auxiliary generation tool

4.CONCLUSION

There are many deficiencies in the use of test cases for the CBTC system engineering acceptance test. With reference to the relevant line data and test standards and requirements of a subway line 10, an engineering acceptance test case library covering 100% of the latest CBTC system interconnection requirements has been compiled. This paper studies the method of automatic generation of CBTC system engineering acceptance test sequence. This method is actually applied to the CBTC system simulation test platform for testing, and the feasibility is verified. The method of automatic

generation of test sequences based on formalization is universal, and the database can be changed according to different lines to generate test sequences of different test lines. The research of this test sequence generation method is beneficial to the development and realization of urban rail transit interconnection.

Figure 8: Test sequence assistant generation tool interface

REFERENCES

[1] Cui Junfeng. A brief discussion on the development of future rail transit train control system technology [J]. Railway Communication Signal Engineering Technology, 2020, 17(3):4.

[2] Gao Chunhai. Communication Based Train Control (CBTC) System [M]. Beijing:China Railway Press, 2018: 36-42

[3] Gario A, Andrews A, Hagerman S. Fail-safe testing of safety-critical systems: a case study and efficiency analysis[J]. Software Quality Journal, 2018,26(1):3-48.

[4] Han Xiao. Research on model-based safety testing method of high-speed railway train operation control system [D]. Beijing Jiaotong University, 2020. DOI:10.26944/d.cnki.gbfju.2020.000307.

[5] Liu Ling. "Research and Prospect of Intelligent Control Technology of Train Group Based on Virtual Coupling." Railway Communication Signal Engineering Technology 17.2(2020):9.

[6] Jiang Jianhua, Cui Ke. Development direction of urban rail transit train operation control system [J]. Urban Rail Transit Research, 2020, 23(11):4..

[7] Song Shuang. Research on automatic generation method of CBTC regional controller test sequence based on model [D]. Lanzhou: Lanzhou Jiaotong University, 2018.

ISBN 978-1-510-65509-6

SPIE
ISBN:978-1-5106-5509-6
P.O. Box 10, Bellingham, Washington 98227-0010 USA
SPIE.org

9.基于 GPRS 的微电网中蓄电池远程监测系统设计

工业仪表与自动化装置

GONGYE YIBIAO YU ZIDONGHUA ZHUANGZHI

（双月刊,1971 年创刊）

2021 年第 3 期（总 279 期） 2021 年 06 月 15 日出版

中国学术期刊综合评价数据库来源期刊
中国核心期刊（遴选）数据库收录
中国科技论文统计源期刊
（中国科技核心期刊）
RCCSE 中国核心学术期刊

主管单位：陕西鼓风机（集团）有限公司

主办单位：陕西鼓风机（集团）有限公司

协办单位：全国工业过程测量控制和自动化标准化技术委员会第三分技术委员会

编辑出版：《工业仪表与自动化装置》编辑部

主编：印建安

执行主编：王 航

责任编辑：秦 蕾

地址：西安市高新区沣惠南路 8 号

邮政编码：710075

电话：（029）81871277

E-mail：gyybbjb@126.com

http://yb-zdh.shaangu-group.com

广告部电话：13910037485

印刷单位：中闻集团西安印务有限公司

国内总发行处：中国邮政集团公司陕西省报刊发行局

订购处：全国各地邮局 发行代号：52—49

国外总发行处：中国国际图书贸易集团有限公司（北京 399 信箱）

国外代号：BM529

ISSN 1000-0682

CN61-1121/TH

广告经营许可证：6100004000062

全年订价：108.00 元，每期定价：18.00 元

本刊若有印刷、装订质量问题，请寄中闻集团西安印务有限公司技术科调换。邮编 710018

目 次

[期刊基本参数] CN61-1121/TH * 1971 * b * A4 * 148 * zh * P * 18.00 * 31 * 2021-06

基于 GPRS 的微电网中蓄电池远程监测系统设计

郭志成，郭　宁，李晓青

（兰州工业学院 电气工程学院，甘肃 兰州 730070）

摘要：为了满足微电网中储能蓄电池健康状态监测需求，该文基于 GPRS 技术设计一种远程监测系统。设计主要以检测蓄电池内阻为主，该系统以处理器 dsPIC30F6012 为核心，控制 DDS 芯片 AD9833 产生正弦波信号，经过恒流源驱动作用到蓄电池回路，再通过差分放大、带通滤波、有效值转换等电路采集蓄电池和参考电阻两端得到的交流电压信号，进而计算出蓄电池内阻。处理器获得相关数据后与设定限值比较，当数据异常时通过 GPRS 通信远程上传至上位数据中心服务器，提醒工作人员注意并进行相应处理，以提高微电网中储能装置运行的稳定性、可靠性。该系统设计简单、易于实现，具有一定的工程应用参考价值。

关键词：蓄电池内阻；AD9833；GPRS；监测系统

中图分类号：TM76　　**文献标识码**：A　　**文章编号**：1000 - 0682(2021)03 - 0035 - 04

Design of remote monitoring system for storage battery in microgrid based on GPRS

GUO Zhicheng，GUO Ning，LI Xiaoqing

(*Department of Electrical Engineering，Lanzhou Institute of Technology，Gansu Lanzhou 730070，China*)

Abstract：In order to meet the needs of energy storage battery health monitoring in the microgrid，a remote monitoring system is designed based on GPRS technology. The design mainly focuses on detecting the internal resistance of the battery. The system uses the processor dsPIC30F6012 as the core to control the DDS chip AD9833 to generate a sine wave signal，which is driven by a constant current source to the battery loop，and then through differential amplification，band - pass filtering，effective value conversion，etc. The circuit collects the AC voltage signal obtained at both ends of the battery and the reference resistor，and then calculates the internal resistance of the battery. The processor obtains the relevant data and compares it with the set limit value. When the data is abnormal，it is uploaded to the upper data center server via GPRS communication to remind the staff to pay attention and carry out corresponding processing to improve the stability of the energy storage device in the microgrid. The system design is simple，easy to implement，and has certain engineering application reference value.

Keywords：internal resistance of battery；AD9833；GPRS；monitoring system

0　引言

化石能源的过度开发和消耗，导致全球性的能源短缺和环境污染[1]，加速提高水能、风能、太阳能等绿色能源的分布式发电比重对改善能源结构及环境污染具有非常重要的意义。但是，分布式发电功率波动性、间歇性会对电网造成冲击或不利影响[2]，而微电网中的储能系统具有削峰填谷、抑制波动、能量缓冲的作用，将分布式电源以微电网的形式接入配电网，可有效解决此类问题[3]。蓄电池常用作微电网中的储能，其健康状况受实际充放电情况、环境温度等因素影响，且工作环境偏远导致蓄电池难以有效维护。蓄电池监测系统是解决上述问题的有效方法，针对上述情况，采用 GPRS 技术设计了蓄电池远程在线监测系统，及早发现问题并更换蓄电池，从而减少不必要的损失。

收稿日期：2020 - 09 - 21

基金项目：甘肃省高等学校创新能力提升项目(2019B - 181)

作者简介：郭志成(1978)，男，甘肃酒泉人，硕士研究生，讲师，主要研究方向为电能质量监测与控制。

1 系统概述

监测系统如图 1 所示由蓄电池状态数据采集终端、GPRS 通信、数据中心服务器三部分组成。

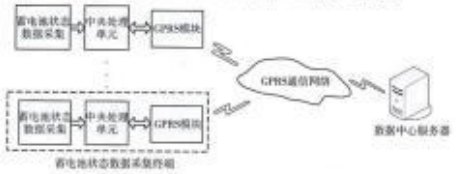

图 1 蓄电池状态监测系统结构

状态数据采集终端借助传感元件、采样处理电路等获取蓄电池的健康状态数据，通过对数据分析判断蓄电池健康状态，若有异常将数据发送给 GPRS 模块，数据中心服务器通过 GPRS 网络接受 GPRS 模块发出的数据，并将其中报警信息及时传给相关人员，便于对蓄电池进行维护更换，保证电池使用过程中的安全，实现蓄电池的实时远程监测。

2 系统硬件设计

蓄电池充电电压、电流 、温度是体现蓄电池当前状态的数据，可以使用相关传感元件方便测出，使用电流霍尔元件采集充电电流；对蓄电池两端的电压先经过电阻分压，再送入处理器片内 A/D 转换器，进行充电电压采集；使用温度传感器 DS18B20 紧贴蓄电池采集温度。蓄电池内阻值的变化是其健康状态的主要判断依据[4]，对其准确测量是一件复杂而困难的事情[5]，具有非常重要的意义，一般内阻值相对较小为毫欧级，且测量时无法与工作回路脱离，增加了测量的难度。该文主要对蓄电池内阻检测的硬件设计进行说明，具体内容如下。

2.1 蓄电池内阻检测原理

目前，可以用密度法、开路电压法、直流放电法、交流注入法等方法测量蓄电池内阻。其中密度法测量精度较差、适用范围窄，只适用非封闭式铅酸蓄电池内阻测量；开路电压法需要蓄电池与工作回路脱离，且再在浮充状态下，有可能得到错误的测量结果；直流放电法需要将一个很大的直流电流强制灌入蓄电池，并测量电池两端瞬时电压，根据欧姆定理算出内阻，但大电流对电池有一定损伤，需要蓄电池脱离工作回路做静态测试，无法实现远程在线动态监测；交流注入法是在蓄电池回路中注入一定频率的交流电流，采集蓄电池两端产生交流电压，并通过锁相放大方法抑制噪声干扰，测得蓄电池内阻，但是，锁相放大器使用复杂，交流信号的相位会受到蓄电池本身电容的影响，测量结果误差较大[6]。该文采用差分放大、带通滤波、有效值芯片获取相关检测信号，计算蓄电池内阻，简化电路设计，具体原理如图 2 所示。系统以处理器 dsPIC30F6012 为控制处理核心，首先控制信号发生器产生 1 kHz 的交流信号，作为耦合驱动电路的输入，产生交流恒流源注入蓄电池；信号采集采用信号输入回路与测量回路分开的四线法测量法来减小测量误差；蓄电池两端、参考电阻上采集的电压信号通过差分放大、带通滤波进行处理，提取出 1 kHz 的有用信号，最后通过有效值转换芯片得到蓄电池两端交流电压的有效值 U_s、参考电压有效值 U_{ref}，通过式(1)可计算出蓄电池的内阻 r。

$$r = \frac{U_s}{U_{ref}} R_r \tag{1}$$

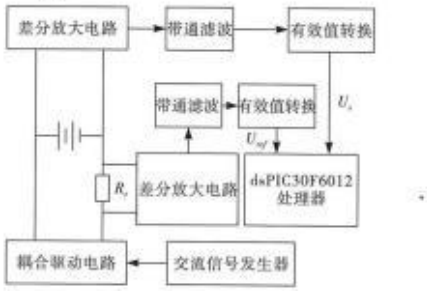

图 2 蓄电池内阻测量原理

2.2 交流信号发生器及驱动

采用 DDS 芯片 AD9833 产生内阻测量所需要的正弦信号，DDS 技术的原理是在 ROM 中存储单元地址、样点数与正弦波的时间轴、幅值相对应的一个周期正弦波采样点，将这些采样点按顺序读出再由 D/A 转换器输出，即可得到数字量化的正弦波，再经过滤波器平滑处理及周期的重复这一过程，最终得到连续的正弦信号。AD9833 内部完全集成 DDS 技术，且所需外围器件少，使电路设计简化，图 3 所示为正弦波发生电路原理图。AD9833 具有 3 线 SPI 串行通信接口，处理器 dsPIC30F6012 通过 FSYNC，SCLK，SDATA 管脚对 AD9833 进行控制，其中，FSYNC 为使能引脚，在进行串行通信时需置为低电平，SCLK 为串行时钟输入，SDATA 为串行数据输入端，数据是在串行时钟 SCLK 的作用下由 SDATA 端输入 AD9833 的，第 10 脚 VOUT 输出正弦信号接和 U7 组成的二阶有源低通滤波电路，滤除附

加在较低频率信号上的高频数字伪信号对波形进行平滑处理，最后由电压跟随器 U8 输出接后级电路。处理器 dsPIC30F6012 通过其 RC1 脚控制三极管 Q1 的通断，进而控制有源晶振的电源，当 RC1 = 1 时，Q1 关闭，切断有源晶振电源起到降耗的目的。

由 AD9833 产生的正弦交流电压信号还需经过 V/I 转换，产生交流恒流源向蓄电池注入交流电流，图 4 所示为基于 HowLand 的恒流源驱动电路，AD9833 正弦波发生电路的输出电压信号 V_0 作为恒流源电路的输入，I_{out} 为输出电流，根据虚短、虚断的分析方法可以得到公式 2 所示的输入电压与输出电流之间的关系[7]。

$$I_{out} = \frac{V_O}{R_{24}} \tag{2}$$

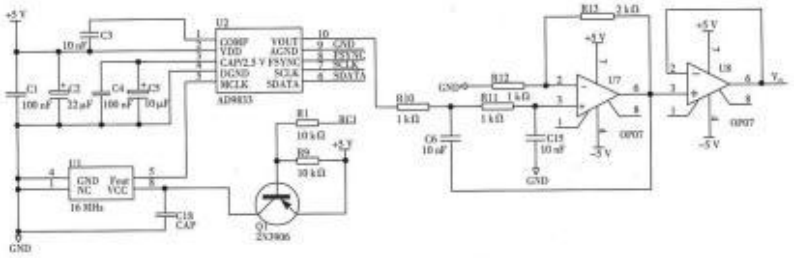

图 3　正弦波发生电路

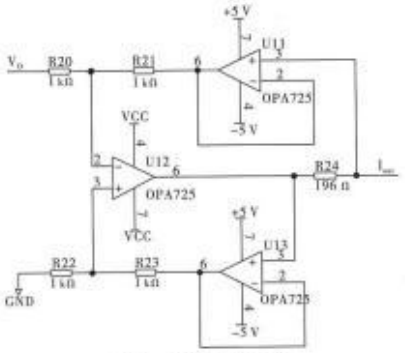

图 4　恒流源驱动电路

2.3　放大滤波电路

恒流源输出的电流在蓄电池内阻及参考电阻上产生的交流压降很小，易受共模干扰影响，先要选用共模抑制比高的精密差分放大电路对微弱信号进行放大，再通过中心频率为 1 kHz 的带通滤波器提取有用信号，剔除干扰。该文采用 AD620 设计差分放大电路，具体电路如图 5 所示采用两级放大，前级 U9 用 AD620 将信号放大 1000 倍，其放大倍数取决于电阻 R16 的阻值，C16，C17 的作用为避免蓄电池直流电对检测的影响，并与电阻 R14，R15 构成高通滤波电路；后级 U10A 由 TL082 构成反相比例放大电路对信号放大 10 倍，总的放大倍数为单级放大倍数乘积；末级 U10B 由 TL082 构成带通滤波器只使 1 kHz左右的信号通过。

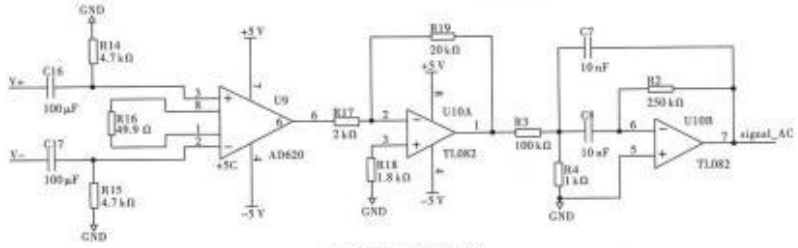

图 5　放大滤波电路

2.4　有效值转换

该文采用高精度、高宽带的有效值转换芯片 AD637，它可以精确得到与交流波形有效值对应等效的直流电压，其转换电路如图 6 所示。

Signal_AC 为带通滤波器的输出作为 AD637 交流信号输入，电阻 R5，R6 和电容 C9，C10 及 AD637 内部共同组成 Sallen - Key 滤波电路[8]，滤除输出端直流信号中的交流成分，RMS_DC 为最终输出与交流有

效值等效的直流信号，将其送入处理器 dsPIC30F6012 的片内 A/D 转换器即可获得交流信号有效值。

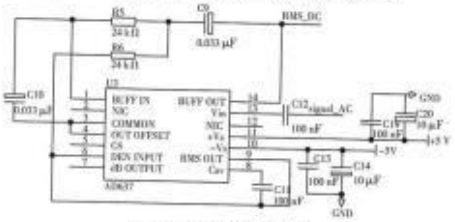

图 6　有效值转换电路

2.5　GPRS 通信

GPRS 通信网络技术成熟，几乎不受地域限制覆盖范围广，远程传输数据实时在线，可将采集的蓄电池状态数据借助它上传至上位数据中心服务器。该文采用 SIMCom 公司生产的 SIM900A 模块实现 GPRS 通信，它采用低功耗设计，内部集成了 TCP/IP 协议，简化了开发人员繁重的底层通信协议工作，缩短了开发时间。SIM900A 模块通过串口与处理器 dsPIC30F6012 进行命令和数据的传递，其中 SIM900A 模块的数据发送端 TXD、数据接收端 RXD 分别与 dsPIC30F6012 的 RXD，TXD 相连，通过发送 AT 指令实现对 SIM900A 的操作。

3　系统软件设计

采用 GPRS 网络作为数据传输媒介，对采集的分布式发电用蓄电池健康状态数据进行远距离传输，软件设计主流程图如图 7 所示。

该系统上电后先对处理器 dsPIC30F6012 进行初始化设置，主要包括外设端口分配及工作状态设定、中断寄存器设置、串行通信方式及波特率设置、SPI 设置，紧接着通过发送 AT 指令与 GPRS 网络建立连接，通过 SPI 接口向 AD9833 发送指令输出 1 kHz 的正弦信号，经过驱动电路作用在蓄电池上，由放大滤波及有效值芯片处理后送入处理器片内 A/D 转换器，dsPIC30F6012 读出转换结果后采用中值滤波去除干扰，并计算相应结果，最终与设定的限值进行比较，数据异常通过 GPRS 向上位机发送数据，引起工作人员注意。

4　结语

该文设计了微电网中使用的蓄电池监测系统，利用广泛使用 GPRS 无线通信技术，将采集的蓄电池健康状态数据远程传输至上位数据中心服务器，使蓄电池状态得到及时有效的监控，提高了新能源分布式发电系统运行的安全性、可靠性，具有非常重要的意义。该文设计的电路简单，易于实现，具有实际的工程应用参考价值。

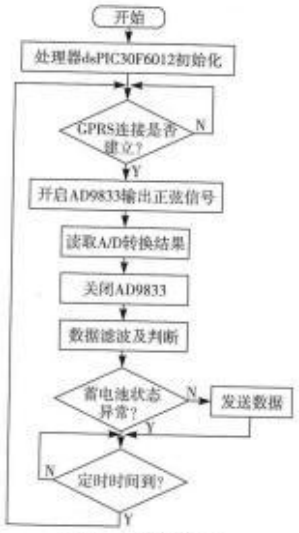

图 7　主程序流程图

参考文献：

[1] 边玉国，李双科. 蜂窝式水力发电探究[J]. 水利规划与设计，2017(09)：1－3＋10.

[2] 杨新法，苏剑，吕志鹏，等. 微电网技术综述[J]. 中国电机工程学报，2014，34(01)：57－70.

[3] 刘文洲，李宁，西灯考，等. 智能微电网研究综述[J]. 长春工程学院学报，2016，17(04)：29－32＋35.

[4] 顾华，曹基南，沈晓峰，等. 变电站蓄电池内阻测量方法优化及应用设计[J]. 电工技术，2019(11)：67－69.

[5] 谢永成，李光升，魏宁，等. 基于 LabView 的蓄电池内阻测量设计[J]. 电源技术，2020，44(01)：113－115.

[6] 曾庆勇. 微弱信号检测(第 2 版)[M]. 杭州：浙江大学出版社，2004：53－74.

[7] 田社平，于歆杰. 关于 HowLand 电流泵电路的分析与讨论[J]. 电气电子教学学报，2016，38(01)：43－45.

[8] 黄锐，曾国强，罗群，等. 一种用于金属安检门微弱信号处理电路的设计[J]. 测控技术，2014，33(04)：149－152.

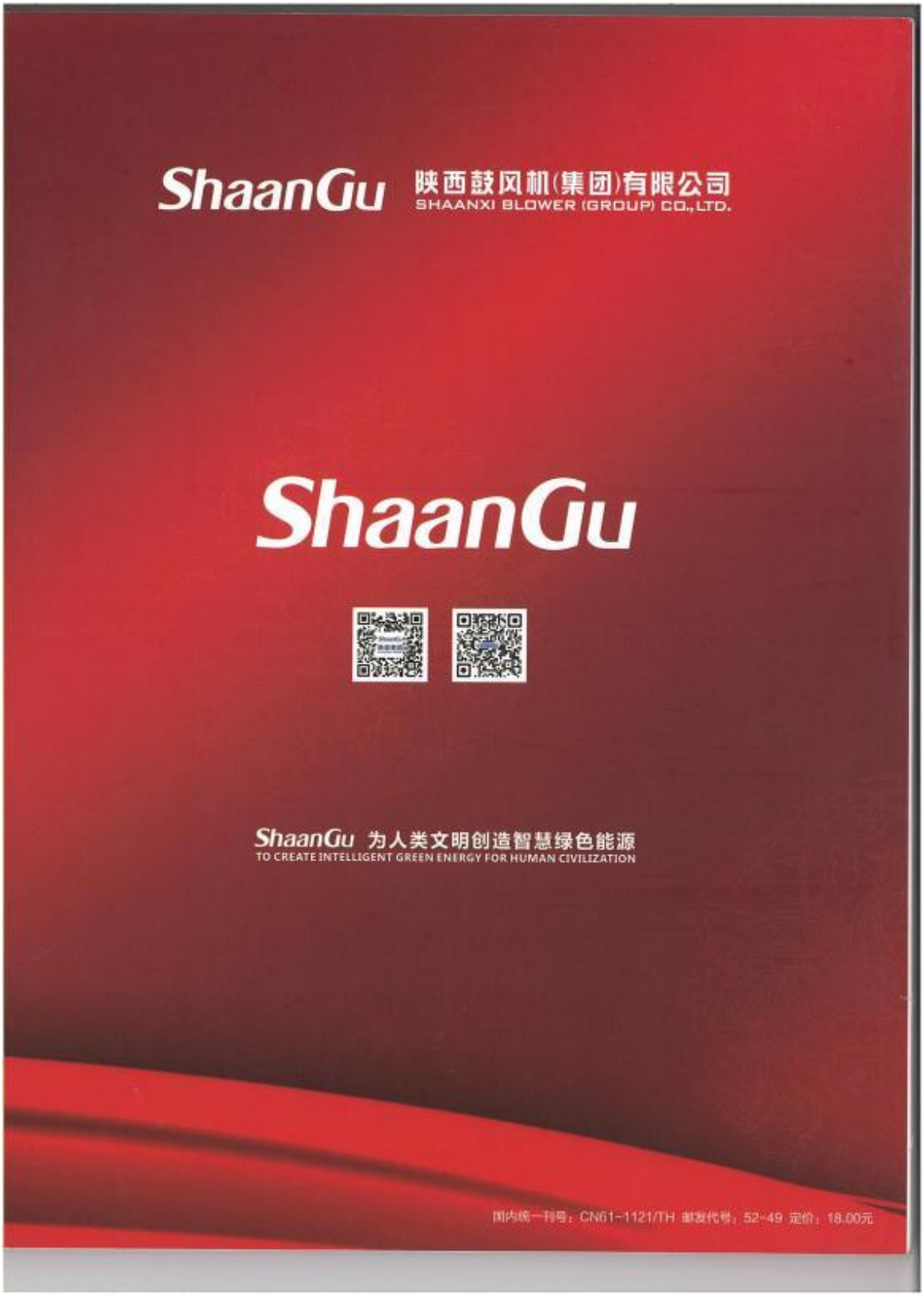
ShaanGu
陕西鼓风机(集团)有限公司
SHAANXI BLOWER (GROUP) CO.,LTD.
ShaanGu
ShaanGu 为人类文明创造智慧绿色能源
TO CREATE INTELLIGENT GREEN ENERGY FOR HUMAN CIVILIZATION
国内统一刊号：CN61-1121/TH 邮发代号：52-49 定价：18.00元

10.基于双 DSP 结构的电能质量监测和治理

兰州工业学院学报

第 28 卷　第 1 期(总第 121 期)　　2021 年 2 月

目　　次

期刊基本参数:CN62-1209/Z * 1993 * b * A4 * 138 * zh * P * ¥ 10.00 * 1000 * 26 * 2021-02

JOURNAL OF LANZHOU INSTITUTE OF TECHNOLOGY

Vol.28 **No.**1(**Sum No.**121) **Feb.**,2021

CONTENTS

第28卷 第1期
2021年2月

兰州工业学院学报
Journal of Lanzhou Institute of Technology

Vol.28 No.1
Feb.2021

文章编号:1009-2269(2021)01-0081-05

基于双 DSP 结构的电能质量监测和治理

朱东山,郭 宁,党 媛

(兰州工业学院 电气工程学院,甘肃 兰州 730050)

摘要:为提高电能质量,对电能质量实时监测系统和治理方法进行深入分析,设计了基于双 DSP 结构的电能质量实时监测系统的硬件电路和软件.采用快速傅里叶算法进行了电能质量分析,通过三相瞬时无功 d-q 检测方法实现了对谐波的治理并进行了仿真试验.仿真结果表明:所用方法能够有效滤除谐波,大幅提高了电能质量.

关键词:电能质量;数据采集;快速傅里叶;三相瞬时无功

中图分类号:TM711 文献标志码:A

随着非线性负载的增加,谐波、无功等电能质量问题日趋严重,对电网的安全、经济运行和生产部门安全生产造成了许多负面影响,因此对电网电能进行监测和治理是很有必要的.目前,许多研究仅仅对电能质量进行了检测和分析,并未提出治理方案.本文深入分析了电能质量监测系统和电能治理方案,同时对电能治理方案进行仿真,验证了该方案的可行性.

1 电能质量检测系统硬件设计

1.1 系统结构

为了满足实时性和精确性,本文采用双 DSP 结构完成数据采样、参数计算、通信以及人机交换.为了满足实时性要求和精确计算,设计采用 DSP28335 作为核心处理器.系统结构如图 1 所示.

1.2 调理电路设计

通过调理电路将大电压、大电流转化为 DSP28335 能承受的 0~3 V 的单极性采样电压.本文采用的交流电压传感器型号为 TV19G.由于电压传感器的输出为双极性信号,通过仪表放大器 INA128U,将输入 DSP28335 的采样电压调理为单极性.大电流信号调理方法与大电压信号调理方法类似,在此不做重复说明.电压调理电路如图 2 所示[1].

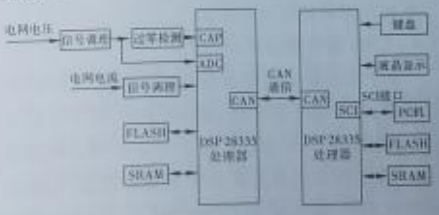

图 1 系统结构

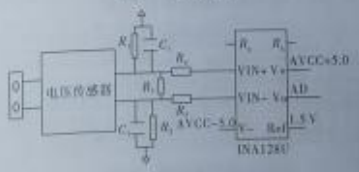

图 2 电压调理电路

1.3 锁相环设计

通过锁相倍频器实现每个交流周期采样的点数相同,这样可以避免由于电压频率波动造成电能质量参数分析误差.传统的硬件锁相倍频电路容易受干扰而造成工作不稳定而且成本高,本文采用软件方法实现锁相倍频,设计要求每个周期采样 256

收稿日期:2020-09-18
基金项目:甘肃省高等学校创新能力提升项目(2020A-142);兰州工业学院青年科技创新项目(19K-007)
作者简介:朱东山(1984-),男,甘肃武威人,工程师.

个点，通过过零检测电路，以及 DSP28335 的 eCAP 模块对基波电压信号上升沿进行捕捉，捕捉到上升沿时开启定时采样；当捕捉到下一次上升沿时，对采样点数进行分析，采样点数大于 256 则减小定时器 TDDR 和 PRD 的值，小于 256 则使 TDDR 和 PRD 值增大.

假设上一个基波周期内定时器中断次数为 N，PRD 和 TDDR 为系统初始化设定的周期寄存器值，TIM 为计数器停止时的值.则 TDDR 不变的情况下需要改变的 PRD 的值为

$$\Delta PRD=\left(\frac{N}{256}-1\right)*(PRD+1)+\frac{PRD-TIM}{256(TDDR+1)}.$$

一般取 TDDR 为 0，则有

$$\Delta PRD=\left(\frac{N}{256}-1\right)*(PRD+1)+\frac{PRD-TIM}{256}.$$

这种方法只需要 1 个基波周期就可以锁定频率，因此实时性好.电网基频变化范围一般在 48～52 Hz，因此可以确定相应的 PDR 范围，如果 PDR 不在此范围则确定故障发生.

1.4 CAN 通信电路设计

2 个处理器之间的通信传统方法采用的是串口通信，串口通信速度慢，通信距离短，抗干扰能力差，在此采用 CAN 通信实现 2 个 DSP 单元间的通信.CAN 总线具有通信速率快、传输距离远、可靠性高等优点[2].系统采用 CTM1050T 作为 CAN 收发器模块，图 3 为 CAN 通信硬件电路.

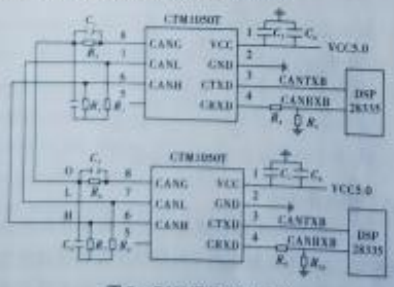

图 3 CAN 通信硬件电路

2 电能质量检测系统软件设计

2.1 中断程序设计

中断程序是整个软件的核心部分，电能质量相关参数的分析主要在中断函数中完成.定时器中断启动后，定时时间到即触发中断，在中断函数中读取 DSP28335 采样模块结果寄存器中的采样值，并记录采样点数，达到 256 个采样点时将中断关闭，并对采样数据是否同步进行判断[3].如果同步则对 1 个周期的采样数据进行分析计算，分析计算完成后中断再次开启.中断子程序流程如图 4 所示.

图 4 定时中断程序流程

2.2 CAN 通信程序设计

采用查询和中断方式，利用 TMS320F28335 的 eCAN 模块实现 CAN 通信.通过对通信模块的初始化，发送方 DSP 将要发送的数据写入 eCAN 模块寄存器对应的发送缓冲区；接收方 DSP 查询 CAN-RMP 寄存器的状态，判断是否收到有效数据，收到有效数据就会触发并中断读出接收到的数据[4].需要注意的是，发收双方邮箱 ID 号以及波特率必须一致.图 5 为 CAN 通信程序流程.

图 5 CAN 通信程序流程

2.3 上位机通信程序设计

本设计利用 VB6.0 完成上位机监控软件的设计，实现的功能主要有串口通信、电能质量参数的显示、电压电流波形显示、历史数据查询等.通过 MSComm 控件可以方便地实现串口通信，当接收缓冲区内的字节个数达到设定值后读取数据，通过 Timer 控件和 PictureBox 控件完成实时波形的绘

制 Data 控件与 Access 数据库结合，通过编写接口驱动程序实现数据的存储及历史数据的访问[5]。图 6 为上位机程序流程。

图 6　上位机程序流程

3　电能质量参数计算

采用傅里叶变换将 $u(t)$ 分解为基波和各次谐波之和，根据正弦函数和余弦函数的正交性有

$$a_{ku}=\frac{2}{T}\int_0^T u(t)\cos k\omega t\mathrm{d}t, \tag{1}$$

$$b_{ku}=\frac{2}{T}\int_0^T u(t)\sin k\omega t\mathrm{d}t, \tag{2}$$

式中：k 为各次谐波的次数($k=1,2,3,\cdots$)。

离散化后得

$$a_{ku}=\frac{2}{T}\sum_{n=0}^{N-1}u(n)\cos\frac{2\pi}{N}kn, \tag{3}$$

$$b_{ku}=\frac{2}{T}\sum_{n=0}^{N-1}u(n)\sin\frac{2\pi}{N}kn. \tag{4}$$

第 k 次电压谐波有效值为

$$U_{ku}=\sqrt{a_{ku}^2+b_{ku}^2}. \tag{5}$$

非正弦周期信号的有效值可以表示为

$$U=\sqrt{\frac{1}{N}\sum_{n=1}^{N}u^2(n)}, \tag{6}$$

$$I=\sqrt{\frac{1}{N}\sum_{n=1}^{N}i^2(n)}. \tag{7}$$

有功功率定义为

$$P=\frac{1}{T}\int_0^T u(t)i(t)\mathrm{d}t. \tag{8}$$

离散化后得

$$P=\frac{1}{N}\sum_{n=1}^{N}u(n)i(n). \tag{9}$$

为了减小误差，无功功率的计算采用时域数字移向法。定义无功为滞后 90° 的电压与电流的乘积[6]，则有

$$Q=\frac{1}{T}\int_0^T u(t)i\left(t+\frac{T}{4}\right)\mathrm{d}t. \tag{10}$$

离散化后得

$$Q=\frac{1}{N}\sum_{n=1}^{N}u(n)i\left(n+\frac{N}{4}\right). \tag{11}$$

视在功率为

$$S=UI. \tag{12}$$

畸变功率为

$$D=\sqrt{S^2-Q^2-P^2}. \tag{13}$$

4　电能质量治理

用有源滤波器补偿无功和抑制谐波已成为近年来研究的热点，控制和检测方法是设计有源滤波器的关键技术。基于三相瞬时无功理论的 d-q、p-q 法是目前应用比较广泛的谐波检测方法[7]。p-q 法实时性好，但文献[8]的试验表明，p-q 法在电压有畸变的情况下检测出来的畸变电流有较大的误差。为了提高检测精度，本文用 d-q 法来进行谐波检测。d-q 法的原理是将电流 i_a、i_b、i_c 经 C_{32} 变换到两相正交坐标系 dq 中，然后从变换后的电流 i_d 和 i_q 中去除与补偿电流相关的成分，再经过 C_{32} 逆变回到 abc 坐标系中，得到期望的指令电流值[9-10]。谐波电流检测原理如图 7 所示。

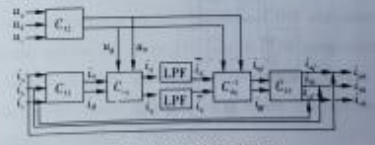

图 7　谐波电流检测原理

有功电流 i_d 和无功电流 i_q 可表示为

$$\begin{bmatrix}i_d\\i_q\end{bmatrix}=C_{dq}C_{32}\begin{bmatrix}i_a\\i_b\\i_c\end{bmatrix},$$

其中，

$$C_{32}=\sqrt{\frac{2}{3}}\begin{bmatrix}1&-\frac{1}{2}&-\frac{1}{2}\\0&\frac{\sqrt{3}}{2}&\frac{\sqrt{3}}{2}\end{bmatrix},$$

$$C_{4s}=\begin{bmatrix}\cos\theta & \sin\theta\\ -\sin\theta & \cos\theta\end{bmatrix}=\frac{1}{\sqrt{u_\alpha^2+u_\beta^2}}\begin{bmatrix}u_\alpha & u_\beta\\ -u_\beta & u_\alpha\end{bmatrix}.$$

将 i_d、i_q 滤波后分解出直流分量，经过 C_{4s}^{-1} 变换和 C_{23} 变换得出基波电流的值，即

$$\begin{bmatrix}i_{af}\\ i_{bf}\\ i_{cf}\end{bmatrix}=C_{23}C_{4s}^{-1}\begin{bmatrix}i_d\\ i_q\end{bmatrix}.$$

将基波电流与三相负载电流 i_a、i_b、i_c 相减，即可得出负载电流的谐波分量 i_{ah}、i_{bh}、i_{ch}.

用 Matlab 中 Simulink 工具搭建仿真模型，Matlab 提供有 d-q 变换模块，为检测出谐波和无功分量提供了方便.仿真模型电源电压取峰值 2 040 V、频率 50 Hz 的交流电，L_a、L_b、L_c 取 0.43 mH，U_d 取 4 200 V.本文采用滞环控制的方法产生 PWM 信号，来控制三相桥 IGBT 的导通和关断.该方法把指令电流和逆变器输出的补偿电流的差值通过滞环比较方式限制在一定的环宽内，根据这一规则来控制 IGBT 的关断和导通，开关频率取 3.5 kHz.这种方法实现起来简单，电流响应速度快.图 8 为仿真电路，治理前后的电流波形如图 9~10 所示.

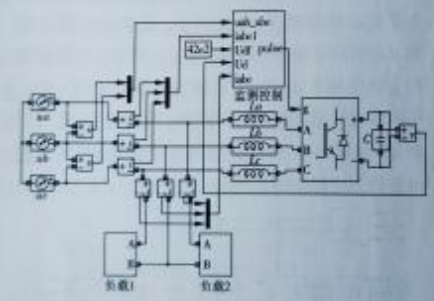

图 8 仿真电路

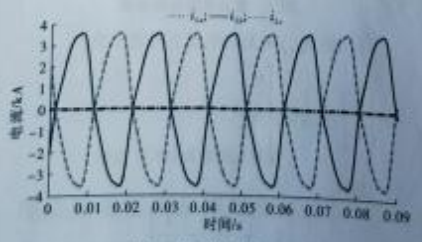

图 9 治理前电流波形

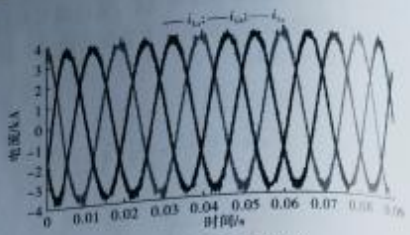

图 10 治理后电流波形

由图 9~10 可以看出，治理前电流波形畸变严重，经治理后三相电流基本正弦化，治理效果良好.

5 结语

本文深入分析并设计了电能质量监测系统的硬件电路和软件结构，采用双 DSP 结构增加了系统的实时性和精确性.提出了基于瞬时无功 d-q 检测的方法，并进行了仿真试验，表明运用此方法进行电能质量治理效果显著.

参考文献：

[1] 刘陵顺.TMS320F28335DSP 原理及开发编程[M].北京：北京航空航天大学出版社，2011.

[2] 饶运涛.现场总线 CAN 原理与应用技术[M].北京：北京航空航天大学出版社，2003.

[3] 孙志强，田铭兴.基于 DSP28335 的电能质量监测系统设计[J].水电能源科学，2013(6)：233-235.

[4] 高阳，李永红，岳凤英，等.基于 DSP 和 FPGA 的 CAN 总线监视系统设计[J].电子器件，2016(1)：164-167.

[5] 范逸之.利用 Visual Basic 实现串并行通信技术[M].北京：清华大学出版社，2001.

[6] 张伏生，耿中行，葛耀中，等.电力系统谐波分析的高精度 FFT 算法[J].中国电机工程学报，1999，19(3)：63-66.

[7] 李晓青，王小会，李慧玲.基于 NSGA-Ⅱ的并网型风光互补发电系统协调控制[J].测控技术，2017(12)：86-89，92.

[8] 王雪丹，张立娟.有源电力滤波器 2 种电流检测方法的仿真研究[J].煤矿机械，2009，30(7)：40-42.

[9] 王兆安，杨君，刘进军.谐波抑制和无功功率补偿[M].北京：机械工业出版社，1998.

Power Quality Monitoring and Management Based on Dual DSP Structure

ZHU Dong-shan, GUO Ning, DANG Yuan
(School of Electrical Engineering, Lanzhou Institute of Technology, Lanzhou 730050, China)

Abstract: In order to improve power quality, real-time monitoring system of power quality and management methods were studied deeply in this paper. The hardware and software of it are designed based on double DSP structure. Power quality is analyzed by using the fast Fourier algorithm, on the basis of detecting and analyzing power quality rapidly and accurately. The harmonic managements of Power grid are realized through the method of Three-phase instantaneous reactive power d-q detection, the simulation experiment is done. The method used can effectively filter out harmonics and greatly improve the power quality.

Key words: power quality; data collection; fast Fourier; three-phase instantaneous reactive

(责任编辑:杨春玲)

(上接第75页)

Development of Spline Shaft Three-tiers C/S Structure Information Database Based on COM

HE Chao
(Zhongan Aviation Equipment Limited Corp., Tianjin 300300, China)

Abstract: Combining with the characteristics of COM (Component Object Model) component, on UG platform the design method by using COM component technology to develop the three-tiers database system is introduced. The parameters information database of spline shaft is taken as the research object, with the use of the three-tiers C/S structure, content focuses on the developing general steps of database system based on COM component technology in UG, which includes the establishment of database and the UG menu, the use of COM components and the client application program. Finally the development content of spline shaft parameters database system is realized, which provides a valuable reference for the secondary development of CAD system on the UG platform.

Key words: COM; UG; spline shaft; three-tiers C/S; database; secondary development

(责任编辑:杨春玲)

本刊被以下检索系统收录
○中国学术期刊(光盘版)数据库
○中国学术期刊综合评价数据库
○CEPS 中文电子期刊全文数据库
○万方数据系统科技期刊群数据库
○中文科技期刊数据库

兰州工业学院学报
LANZHOU GONGYE XUEYUAN XUEBAO
(双月刊 1993 年创刊)
第 28 卷 第 1 期 2021 年 2 月 25 日

JOURNAL OF LANZHOU
INSTITUTE OF TECHNOLOGY
(Bimonthly Started in 1993)
Vol.28 No.1 Feb., 2021

主管单位 甘肃省教育厅
主办单位 兰州工业学院
编辑出版 《兰州工业学院学报》编辑部
地 址 甘肃省兰州市七里河区龚家坪东路 1 号
电 话 (0931)2862519
传 真 (0931)2862662
排版印刷 兰州中科印务有限责任公司
(兰州市天水中路 8 号
电话:8272947)
国内发行 兰州市邮政局
邮发代号 54-136
国外发行 中国出版对外贸易总公司
北京 782 信箱
国外发行代号 DK62009
E-mail: lgzxb0931@126.com(理科)
lxgyxyxb@163.com(文科)

Authorized by Educational Bureau of Gansu Province
Sponsored by Lanzhou Institute of Technology
Edited and Published by Editorial Department of Journal of Lanzhou Institute of Technology
Address: No.1 Gongjiaping East Road, Qilihe District, Lanzhou 730050, Gansu, China
Tel:(0931)2862519
Fax:(0931)2862662
Composed and Printed by Lanzhou Zhongke Printing Co., Ltd.
Distributed abroad by China National Publishing Industry Trading Corporation
(782 P.B., Beijing)
http://journal.lzit.edu.cn

刊号:ISSN 1009-2269 / CN 62-1209/Z
国内定价:10.00 元
ISSN 1009-2269

11、Research on Intelligent Operation and Maintenance Scheme of

Railway Signal System Based on Big Data

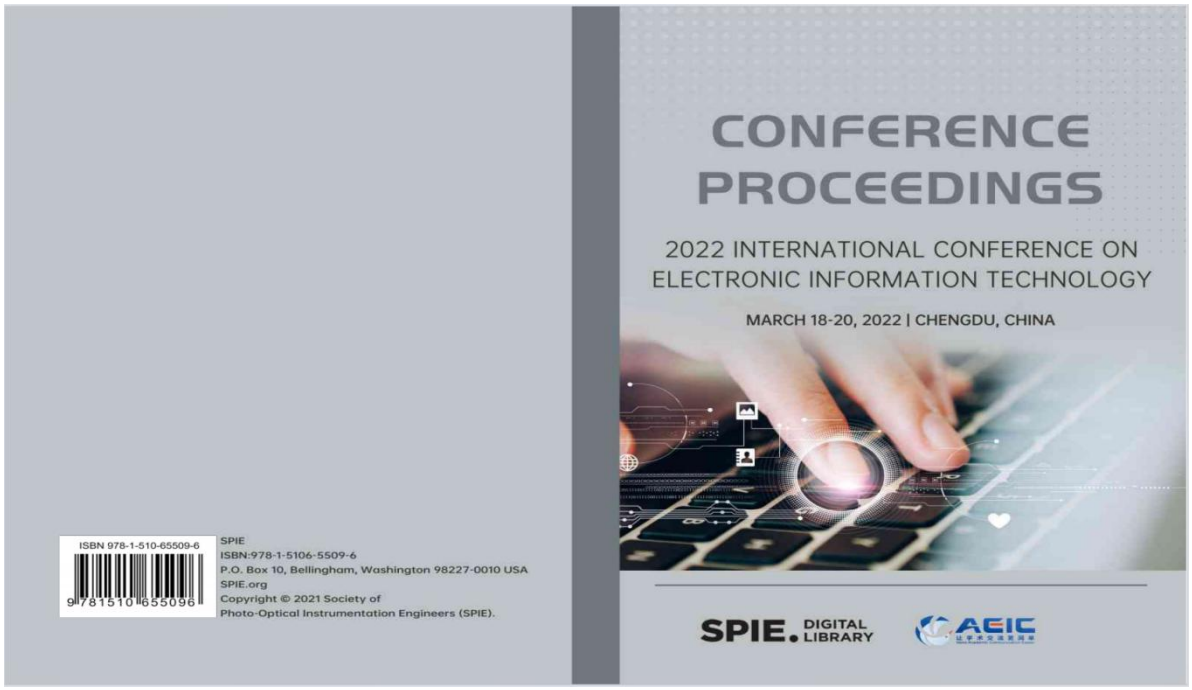

1. Research on Intelligent Operation and Maintenance Scheme of Railway Signal System Based on Big Data

Zhu, Dongshan (1); Shi, Dongdong (1)

Source: *Proceedings of SPIE - The International Society for Optical Engineering*, v 12254, 2022, *International Conference on Electronic Information Technology, EIT 2022*; **ISSN:** 0277786X, **E-ISSN:** 1996756X; **ISBN-13:** 9781510655096; **DOI:** 10.1117/12.2640054; **Article number:** 12254 1U; **Conference:** 2022 International Conference on Electronic Information Technology, EIT 2022, March 18, 2022 - March 20, 2022; **Sponsor:** Academic Exchange Information Center; **Publisher:** SPIE

Author affiliation: (1) Lanzhou Institute of Technology, School of Electrical Engineering, Gansu, Lanzhou, China

Abstract: With the continuous expansion of the scale of my country's railway electrical system and the increasingly complex equipment functions, the requirements for ensuring the safe, stable and long-term operation of the electrical system are becoming more and more urgent. The operation and maintenance system is mainly through manual maintenance, which is inefficient. With the continuous development and application of technologies such as information technology and intelligent terminals in my country, intelligent monitoring technology has been gradually applied to the maintenance of signal systems. In order to facilitate the electric service personnel to grasp the operating equipment status in real time, optimize the equipment maintenance process and improve the maintenance efficiency. This paper comprehensively considers the daily maintenance, operation, emergency response operation process and related precautions of the signal system, and combines key technologies such as data access, data fusion, data visualization, fault prediction and health management to realize the analysis and design of intelligent operation and maintenance application functions. Provide reference for the improvement of railway signal operation and maintenance level and the transformation of electric service operation and maintenance mode. © 2022 SPIE. (11 refs)

Main heading: Big data
Controlled terms: Data fusion - Data visualization - Information management - Maintenance - Railroads - Signal systems
Uncontrolled terms: Complex equipment - Electric services - Electrical systems - Intelligent - Intelligent maintenance - Intelligent operations - Maintenance schemes - Operation schemes - Operations and maintenance - Railway signal
Classification Code: 723.2 Data Processing and Image Processing - 723.5 Computer Applications - 913.5 Maintenance
Funding Details: Number: 2021a-157, Acronym: -, Sponsor: Gansu Education Department;
Funding text: Innovation Fund Project of Gansu Provincial Department of education, project name: Application Research of integrated intelligent management system for urban waste power generation and transportation (Project No.: 2021a-157).
Database: Compendex
Data Provider: Engineering Village

Abstract

Detailed

Compendex Refs

Research on Intelligent Operation and Maintenance Scheme of Railway Signal System Based on Big Data

Accession number: 20222612285223

Authors: Zhu, Dongshan [1]; Shi, Dongdong [1]

Author affiliation: [1] Lanzhou Institute of Technology, School of Electrical Engineering, Gansu, Lanzhou, China

Source title: Proceedings of SPIE - The International Society for Optical Engineering

Abbreviated source title: Proc SPIE Int Soc Opt Eng

Volume: 12254

Part number: 1 of 1

Issue title: International Conference on Electronic Information Technology, EIT 2022

Issue date: 2022

Publication Year: 2022

Article number: 122541U

Language: English

ISSN: 0277786X

E-ISSN: 1996756X

CODEN: PSISDG

ISBN-13: 9781510655096

Document type: Conference article (CA)

Conference name: 2022 International Conference on Electronic Information Technology, EIT 2022

Conference date: March 18, 2022 - March 20, 2022

Conference location: Chengdu, China

Conference code: 180151

Sponsor: Academic Exchange Information Center

Publisher: SPIE

Abstract:
data-language='eng' data-ev-field='abstract'>With the continuous expansion of the scale of my country's railway electrical system and the increasingly complex equipment functions, the requirements for ensuring the safe, stable and long-term operation of the electrical system are becoming more and more urgent. The operation and maintenance system is mainly through manual maintenance, which is inefficient. With the continuous development and application of technologies such as information technology and intelligent terminals in my country, intelligent monitoring technology has been gradually applied to the maintenance of signal systems. In order to facilitate the electric service personnel to grasp the operating equipment status in real time, optimize the equipment maintenance process and improve the maintenance efficiency. This paper comprehensively considers the daily maintenance, operation, emergency response operation process and related precautions of the signal system, and combines key technologies such as data access, data fusion, data visualization, fault prediction and health management to realize the analysis and design of intelligent operation and maintenance application functions. Provide reference for the improvement of railway signal operation and maintenance level and the transformation of electric service operation and maintenance mode.

Number of references: 11

Main heading: Big data

Controlled terms: Data fusion - Data visualization - Information management - Maintenance - Railroads - Signal systems

Uncontrolled terms: Complex equipment - Electric services - Electrical systems - Intelligent - Intelligent maintenance - Intelligent operations - Maintenance schemes - Operation schemes - Operations and maintenance - Railway signal

Classification code: 723.2 Data Processing and Image Processing - 723.5 Computer Applications - 913.5 Maintenance

DOI: 10.1117/12.2640054

Funding Details:

Number	Acronym	Sponsor
2021a-157	-	Gansu Education Department

Funding text:
Innovation Fund Project of Gansu Provincial Department of education, project name: Application Research of integrated intelligent management system for urban waste power generation and transportation (Project No.: 2021a-157).

Database: Compendex

‹ Back to results

Get it!

PROCEEDINGS OF SPIE

SPIEDigitalLibrary.org/conference-proceedings-of-spie

Research on intelligent operation and maintenance scheme of railway signal system based on big data

Dongshan Zhu, Dongdong Shi

Dongshan Zhu, Dongdong Shi, "Research on intelligent operation and maintenance scheme of railway signal system based on big data," Proc. SPIE 12254, International Conference on Electronic Information Technology (EIT 2022), 122541U (23 May 2022); doi: 10.1117/12.2640054

SPIE.

Event: International Conference on Electronic Information Technology (EIT 2022), 2022, Chengdu, China

Research on Intelligent Operation and Maintenance Scheme of Railway Signal System Based on Big Data

Dongshan Zhu[1], Dongdong Shi[1]
[1]School of Electrical Engineering, Lanzhou Institute of Technology, Lanzhou Gansu, China
f_author zhuds@lzit.edu.cn, s_author 963898691@qq.com

Abstract

With the continuous expansion of the scale of my country's railway electrical system and the increasingly complex equipment functions, the requirements for ensuring the safe, stable and long-term operation of the electrical system are becoming more and more urgent. The operation and maintenance system is mainly through manual maintenance, which is inefficient. With the continuous development and application of technologies such as information technology and intelligent terminals in my country, intelligent monitoring technology has been gradually applied to the maintenance of signal systems. In order to facilitate the electric service personnel to grasp the operating equipment status in real time, optimize the equipment maintenance process and improve the maintenance efficiency. This paper comprehensively considers the daily maintenance, operation, emergency response operation process and related precautions of the signal system, and combines key technologies such as data access, data fusion, data visualization, fault prediction and health management to realize the analysis and design of intelligent operation and maintenance application functions. Provide reference for the improvement of railway signal operation and maintenance level and the transformation of electric service operation and maintenance mode.

Keywords: Railway signal, Intelligent, operation and maintenance, Big data.

1. Introduction

With the high-speed construction and development of my country's railways, the construction and operation of a large number of lines has led to a sharp increase in the number of railway-related professional equipment, while the signal system has a complex structure, various types of equipment and wide distribution, requiring a large number of operation and maintenance personnel to ensure the normal and stable operation of the system. Due to the increasing difficulty of operation and maintenance management, the problems of intelligence, integration and informatization of signal system operation and maintenance need to be solved urgently (Shi, 2020). The construction of signal intelligent operation and maintenance system based on big data has become the main development trend of signal maintenance system. In order to predict and avoid the adverse effects caused by equipment failures, improve the work efficiency of signal maintenance personnel, and ensure the safe and stable operation of railway transportation, the intelligent monitoring technology centered on comprehensive intelligent acquisition and information management is applied to the signal operation and maintenance system. At present, the signal equipment is mainly divided into on-board equipment and trackside equipment according to the layout location, and its monitoring methods are divided into two types: train monitoring and trackside centralized monitoring (Hu, 2019).

Train monitoring is to capture and obtain the dynamic data of the on-board equipment during the train operation, and connect the obtained data with the base station through the train-ground communication technology to ensure the safe operation of the train; the monitoring of the trackside equipment is mainly by collecting power at the station. The analog quantity and switch quantity information of basic signal equipment such as turnouts, track circuits, etc., and for equipment with monitoring functions such as interlocks, power screens, and smart filaments, the relevant status information can be obtained through the interface, and the alarm will be timely when there is a fault. Although the intelligent monitoring technology has been applied to a certain extent in the signal operation and maintenance system, there are still some problems to be solved. Literature (Guo, 2012) studies the visual model of computer interlocking system based on the method of graph theory model, and uses time series and fuzzy reasoning methods to intelligently diagnose the complex faults of the system; Literature (Xue, 2020) analyzes the scene of the Sichuan-Tibet railway line Based on the environment and survey data, the functions and technical conditions of the signal intelligent operation and maintenance system are studied in combination with user needs; Reference (Li, 2020) starts from the system level of

International Conference on Electronic Information Technology (EIT 2022)
edited by Zhongyu Li, Hilal Imane, Proc. of SPIE Vol. 12254, 122541U
© 2022 SPIE · 0277-786X · doi: 10.1117/12.2640054

signal operation and maintenance, defines the associated signal system and builds a layered architecture model, and proposes A dynamic quantitative assessment and risk early warning scheme is implemented, and the operation status assessment, risk early warning and fault diagnosis of the signal system are realized.

First, the large amount of unstructured data such as sensor monitoring data, image information, and operation logs generated in the daily operation of railways is not conducive to data analysis and system decision-making; secondly, the types of signal system operation and maintenance data are diverse and continuously accumulated, and traditional relational databases have become very difficult. It is difficult to process these multi-source and heterogeneous massive data. In order to maximize the value of operation and maintenance big data, the obtained data is standardized and normalized, so that it can be used for intelligent operation and maintenance data analysis to provide data support for system decision-making (Yang, 2015). This paper introduces the structure of the railway signal system, analyzes the source of the operation and maintenance big data, proposes the problems existing in the data processing process at this stage, designs the railway signal intelligent operation and maintenance system architecture, and studies the key technologies and system functions.

2. Railway Signal System Structure

The railway signal system is mainly composed of train control system, interlock system, dispatch system, signal centralized monitoring system and communication equipment. According to the location of equipment layout, it is mainly divided into: dispatch center, station equipment, trackside section equipment, on-board equipment, depot And maintenance center, its system structure is shown in Figure 1. At present, the signal maintenance support system is to complete the functions of external power grid monitoring, cable-to-ground insulation test, power-to-ground leakage current test, switch monitoring, track circuit monitoring, fuse alarm monitoring, temperature and humidity collection and other functions at the station; System and dispatching system interface, obtain the status information of these devices, and issue an alarm in time when there is a fault; the monitoring host performs fault diagnosis on the collected signal device parameters, provides maintenance suggestions, and guides users to maintain the equipment.

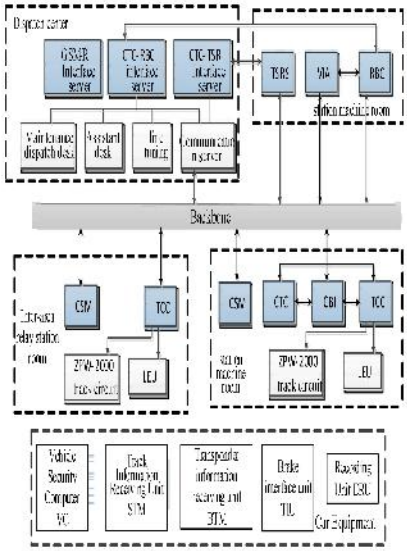

Figure 1 Schematic diagram of the signal system structure.

The current monitoring system still has the following deficiencies:

(1) The monitoring system only obtains line current and voltage information through sensors and other equipment, and collects communication data information through the interface between devices, but cannot perform intelligent analysis and processing on the monitored data information, and cannot accurately determine whether the equipment is in a normal or faulty state. . At this stage, it mainly depends on the maintenance personnel to analyze and judge the equipment status according to their own professional knowledge and experience.

(2) The large amount of data obtained cannot be comprehensively processed among the monitored equipment, the monitoring base station and the monitoring system. The data obtained by the monitoring train and the data obtained by the monitoring station can only be analyzed and processed separately, and the train-ground data cannot be shared in real time. Failure to comprehensively consider the relationship between personnel operation, equipment status, and operating environment, and failure to intelligently analyze the entire system from an overall perspective.

(3) There are many sources of monitoring data with different structures, such as system information collection data, dispatcher and driver operation instructions, maintenance personnel recording logs, etc. For these multi-source heterogeneous data obtained, there are inconsistencies in terminology, format, content, etc. Due to non-standard problems, the maintenance system cannot directly use multi-source heterogeneous data for intelligent analysis and decision support.

3. Research On Intelligent Operation and Maintenance Scheme of Railway Signal System

3.1 Monitoring System Structure

The intelligent operation and maintenance system mainly includes data sources, data collection and storage, data analysis and application, and data display (Fang, 2021). The system structure diagram is shown in Figure 2.

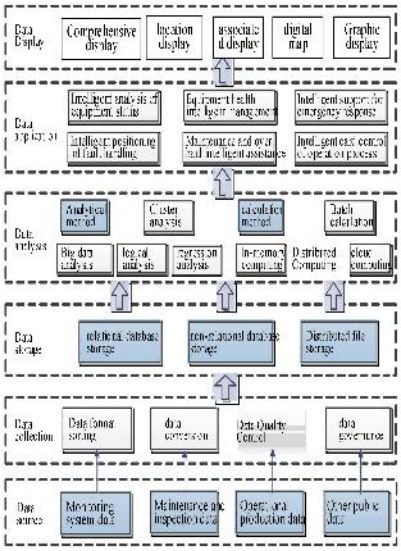

Figure 2: Structure diagram of intelligent monitoring system.

(1) The data sources mainly include monitoring system data, maintenance and overhaul data, operation and production data and other public data. The monitoring system data includes analog and switching information of basic signal equipment such as power equipment, turnouts, and track circuits. For equipment with monitoring functions such as interlocks, power screens, and smart filaments, the relevant status information can be obtained through the interface; maintenance and repair The data mainly include maintenance logs, equipment history, daily inspection records and other

data; the operation and production data mainly include driving plans, operation timetables, and dispatcher command records.

(2) Data collection refers to the merging and integration of various data, such as formatted data such as speed, distance, acceleration, equipment status, driving status, and line status, as well as unformatted data such as video, image, sound, maintenance records, and system logs. The method of extracting, transforming and merging the acquired data attributes is standardized, and is realized by matching information such as time and place to avoid data confusion or ambiguity.

(3) Data storage is to classify and store the normalized data according to the characteristics of date, location, relational and non-relational. With the continuous accumulation of operation and production data, a large amount of storage space is required. The data can be cleaned regularly through periodic cleaning, and data cleaning can be performed for one month, three months, half a year, or one year according to the needs.

(4) Data analysis and calculation are the core of data processing. Relevant data or key data can be extracted according to requirements, and the extracted data can be preprocessed to avoid large calculation errors caused by data noise. Through logical analysis, regression analysis and cloud computing It is necessary to analyze and calculate the data by other methods. Finally, it is necessary to measure the accuracy and quality of the calculation results, so that it can more accurately reflect the value of big data.

(5) Data application is based on data analysis and calculation results, and realizes functions such as fault location, fault diagnosis and disposal, emergency response command and process, daily maintenance key objectives, fault prediction, equipment health and full life cycle management.

(6) Data display is to display the results of data analysis and calculation on the platform through data visualization technology and human-computer interaction technology (Luo, 2021), which can more intuitively present intelligent monitoring to users through graphics, network topology maps, equipment models, etc. As a result, various display needs of electric service personnel are met.

3.2 Intelligent Operation and Maintenance Cloud Computing Platform

Cloud computing is a collection of low-consumption and high-efficiency virtual resource services that connect a large number of necessary hardware in a certain form through the Internet for the purpose of application, and flexibly adjust as the demand changes. While reducing infrastructure investment, it can reduce equipment maintenance and increase computing power. Storage capacity will not be restricted. Storage in the cloud ensures data security. Data will not be lost due to damage to a certain hard disk. Broadband and ubiquitous connectivity allow users to access data regardless of location.

The smart electricity operation and maintenance cloud collects the monitoring and detection data of each system in the electricity intelligent perception network. By integrating and storing these data, real-time and non-real-time data clusters can be classified and processed separately; real-time query, search, and more Dimensional analysis; at the same time, combined with the operating status information of each related equipment, use intelligent algorithms to quickly and accurately locate faults. Completely solve the problems of mutual isolation and difficult interconnection between systems.

The Railway Bureau Cloud is the data storage center of the entire Railway Bureau, which includes all regional nodes within the scope of the Railway Bureau. It consists of a large number of storage devices. The station edge cloud under the railway bureau cloud consists of storage devices of fixed regional nodes. The secondary cloud storage solution of the railway bureau cloud and the station edge cloud enables the railway bureau to maintain and manage the storage space within the bureau in a unified manner, and is more flexible in system expansion.

3.3 Intelligent Operation and Maintenance Big Data Analysis

Big data is a massive, high-growth and diversified information asset that requires new processing modes to have stronger decision-making, insight discovery and process optimization capabilities. The real value of big data technology lies in the integration and processing of massive and meaningful data. That is to say, only by fine-processing and deep mining of data can the value of big data be reflected. In the railway intelligent operation and maintenance system, the precision processing and deep mining capabilities of data are realized by artificial intelligence algorithms. The artificial intelligence algorithms rely on the massive data accumulated by the railway operation and maintenance system for a long time.

Big data and cloud computing are interdependent. Big data must adopt a distributed architecture, using cloud computing distributed processing, distributed database and cloud storage, and virtualization technology to process massive data. When using manual data analysis, in the face of huge data, it is difficult to analyze the real ins and outs of the event, which may lead to wrong inferences; but using big data technology, the truth of the event can be quickly analyzed.

With the continuous improvement of the safety requirements of railway traffic, the intelligent operation and maintenance of railways faces greater challenges. Therefore, there is an urgent need for the application of big data. Make full use of the data obtained by the intelligent perception system to provide key basis for the core business application of railway intelligent operation and maintenance. Use the status data of the long-term or short-term operation of each system to carry out joint analysis and in-depth mining. Predict possible failures of equipment. Find factors that may affect driving safety in the process of driving in advance, and prevent and rectify in a targeted manner. It can effectively reduce the probability of failure. It can also reduce the stress of data analysis of maintenance personnel. The intelligent operation and maintenance system conducts trend analysis on big data such as text, video images, and voice generated by related services, providing strong data support for the sustainable development of the railway operation and maintenance system.

3.4 Intelligent Analysis and Assisted Decision-Making

Through the use of cloud computing and big data technology to deeply mine and analyze the massive data generated by each perception subsystem, it can inspire the innovative thinking of big data users, so as to realize auxiliary decision-making. Cloud computing and big data technology can propose a variety of solutions to a problem, and select the best solution according to the actual situation. Utilize the unique global perspective of big data. Predict the rules of operation and maintenance. Visualize the process and results of the analysis. At the same time, the details can be traced throughout the whole process; Probability; realize unified collection and format standardization of data from each system. Through the use of cloud computing and big data technology, the production operation command, centralized monitoring and security warning, equipment life cycle management, and cross-professional and cross-industry linkage are realized intelligently.

4. Key Technologies of Big Data Intelligent Operation and Maintenance System

At present, the main technologies used in big data include data collection and integration, data analysis and mining (such as Map Reduce technology launched by Google, development of distributed file system GFS, Big Table distributed parallel database technology), data visualization and human-computer interaction Technology (such as tag cloud, history streaming technology, etc.). The following will introduce the data access, data fusion and fault prediction health management technologies used in the signal system:

(1) Data access technology: Railway signal professional data can be divided into static data and dynamic data according to characteristics. Static data includes stable data such as equipment names and attributes, and dynamic data includes maintenance and inspection records, alarm information, operation commands, scheduling commands, and equipment action records, train running records and other real-time updated and growing data; according to the type can be divided into real-time data, file data, picture and video data, message records and other data. In the current data access technology, the resource-oriented REST standard is used to realize the data interface by using HTTP verbs, status codes, headers, etc. The RESTFUL-style interface separates the front and back ends, which can reduce the data transmitted through the network, and use JSON as data exchange at the same time. Format, which can avoid security problems such as data injection, and is suitable for accessing static data. Kafka is a high-throughput publish-subscribe messaging system with high throughput, low coupling, and strong scalability, which can be used to transmit dynamic data (Deng, 2005).

(2) Data fusion technology: The data obtained by the signal intelligent operation and maintenance system is diverse, and these data with different structures are fused to standardize the data specification. First, the conversion from database to RDF needs to be formally defined (LUO, 2021). The conversion from local data to overall data requires strict reasoning and logical verification, which is an important step to ensure data merging, semantic consistency, and complete conversion; The closure algorithm of the RDF(S) ontology expresses the knowledge in the RDF(S) ontology graph by inferring and calculating each node of the RDF(S) ontology, and can consider the date, time, location and other information in the data to complete the data matching; Finally, the similarity between the RDF(S) ontology and the data after fusion is compared to verify the accuracy of the fusion data.

(3) Failure prediction and health management: Equipment failure prediction and health management (PHM) technology can determine equipment performance based on data, monitor and diagnose equipment failures, and predict the occurrence of failures in advance (Liu, 2021). According to the predictions, electrical maintenance personnel can take maintenance measures or fault-tolerant measures in advance to ensure operations. PHM mines key parameters through platform big data, realizes fault identification and diagnosis through data comparison and analysis, and proposes maintenance strategies according to fault handling procedures and equipment maintenance procedures. PHM also has equipment health status assessment and life tracking functions. It can realize comprehensive diagnosis, prediction and health management at different levels and levels from boards, modules to components to equipment to systems.

At present, there are more and more complicated and complicated sources of monitoring data records for railway signal equipment, which will cause problems such as insufficient data accuracy and incomplete data sets caused by data transmission problems. Therefore, we use the data fusion model to improve its accuracy. The flow chart of its algorithm is shown in Figure 3.

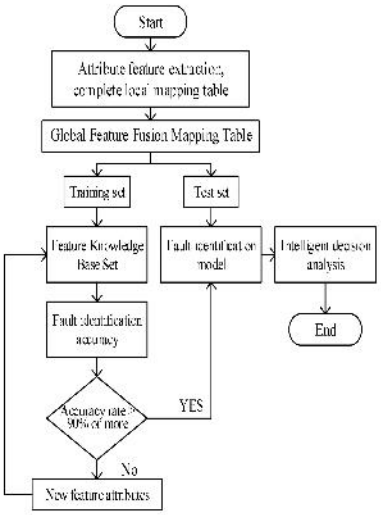

Figure 3: The algorithm flow chart is shown in the figure.

5. Conclusion

The big data platform intelligent system collects the monitoring indicators of each component and node of the big data platform, displayed in the form of a chart. The overall diagram of the intelligent operation scheme of its big data railway signal system is shown in Figure 4. Therefore, in this paper, the data in the experimental process is cleaned in advance, each device data corresponds to each relevant attribute, the non-key influencing attributes are removed, the main attribute is retained, the redundant data characteristic description is normalized, the device data record library is constructed, and the data of each device is analyzed. The feature sets the boundary of the knowledge base, improves the redundant feature description between equipment states, and fuses it into a new equipment data feature mapping table. The data feature fusion is preliminarily completed, the data quality is improved, and the data fusion efficiency is improved. Its overall design is as follows

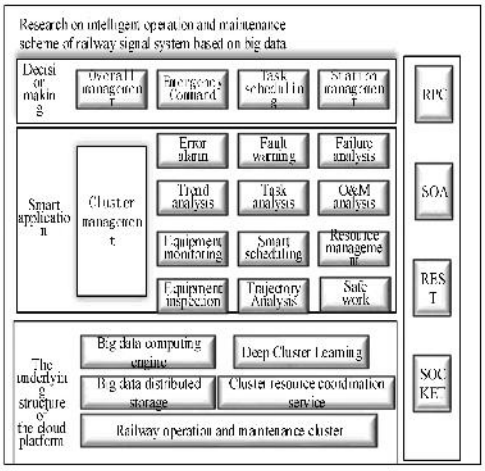

Figure 4: Overall diagram of the smart operation scheme.

Intelligent operation and maintenance system has become the main direction of railway operation and maintenance development, driven by big data of signal system, standardizing multi-source heterogeneous data through data processing technology, comprehensively using data access technology, data fusion technology, data intelligent analysis, fault Diagnosis and equipment health status assessment technology realizes integrated supervision of signal equipment and comprehensive management and control of fault prediction. With the continuous development of science and technology in our country, the integration and intelligence of the signal monitoring system are realized, data analysis and intelligent diagnosis are provided for electric personnel, and a friendly human-machine interface is built through data visualization technology, which promotes the equipment from planned repair to state repair. It can improve the efficiency of fault handling, reduce the maintenance cost of the signal system, and provide technical support for the realization of intelligent operation of the railway system.

FUND PROJECT

Innovation Fund Project of Gansu Provincial Department of education, project name: Application Research of integrated intelligent management system for urban waste power generation and transportation (Project No.: 2021a-157).

REFERENCES

[1] Deng Y, Ruckhaus E, Subrahmanian V.S. A Graph Foundation for Integrating RDF Ontologies [C]. Proceedings of the Twentieth National Conference on Artificial Intelligence (AAAI-2005), Pittsburgh, Pennsylvania: USA, 2005: 1442-1450.

[2] Fang Guanghua. Research on Intelligent Operation and Maintenance System of Urban Rail Signals[J].Electric Transmission of Locomotive,2021(02):92-99.

[3] Guo Jin, Zhang Yadong, GUO, et al. Analysis and Thinking of China's High-speed Railway Signal System [J]. Journal of Beijing Jiaotong University, 2012, 36(5):5.

[4] Hu Xiaomin. Application of intelligent monitoring technology of railway signal system in my country[J].People's Communications,2019(06):79.

[5] Li Gang, Lu Peiling. Research on intelligent operation and maintenance technology of high-speed railway signal based on data drive[J]. Railway Transportation and Economy, 2021, 43(10): 1-67.

[6] Lin Peng, Tian Yu, Yuan Zhiming, Zhang Qi, Dong Hairong, Song Haifeng, Yang Chunhua. Research on Hierarchical Architecture Model of High-speed Railway Signal System Operation and Maintenance [J/OL]. Journal of Automation: 1-10[2022-01-22].
[7] Luo Hao, Zhao Ying, Guan Zebin. Application function development of communication intelligent operation and maintenance in railway electric affairs big data platform [J]. RailwayComputerApplication,2021,30(03):27-31.
[8] Shi Cong. Intelligent operation and maintenance system for urban rail transit communication signal specialty [J]. Urban Rail Transit Research, 2020, 23(8): 172-176.
[9] Xu Yue, Zhu Ming, Cai Liang, Chen Yong, Zou Shaowen. Research on Technical Conditions and Schemes of Signal Operation and Maintenance System of Sichuan-Tibet Railway [J]. Railway Communication Signal Engineering Technology, 2020,119(11):35-39.
[10] Yang Lianbao. Research on big data standardization and operation and maintenance decision support of high-speed railway signal system [D]. Beijing Jiaotong University, 2015.
[11] Zhou Su, Wang Wen. Big Data Visualization [M]. Beijing: Tsinghua University Press, 2016: 42-44.

12、Study on Corn Ear Drying System Based on Fuzzy Control

Proceedings

2022 IEEE 5th International Conference on Electronics Technology

(ICET 2022)

May 13-16, 2022

Chengdu, China

Table of Contents

2022 IEEE 5th International Conference on Electronics Technology (ICET)

Part-2

2022 IEEE 5th International Conference on Electronics Technology (ICET)

Study on Corn Ear Drying System Based on Fuzzy Control

Dong Shan Zhu
Lanzhou Institute of Technology
School of Electrical Engineering
Lanzhou, China
zhuds@lzit.edu.cn

Dong Dong Shi
Lanzhou Institute of Technology
School of Electrical Engineering
Lanzhou, China
963898691@qq.com

Yuan Dang
Lanzhou Institute of Technology
School of Electrical Engineering
Lanzhou, China
352231344@qq.com

***Abstract*—In order to solve the problems of long drying time and unstable drying performance of corn ear by manual operation, a temperature and humidity control method based on fuzzy control is proposed in this paper. According to the analysis of corn ear drying process, the measured temperature and humidity are selected as fuzzy input variables, and the fuzzy rules are formulated. The fuzzy set of control variables is obtained by fuzzy reasoning, and the accurate control value of ventilation door opening is calculated by the maximum membership average method. The application results show that the control method has good dynamic response, anti-interference ability and robustness. On the premise of ensuring the quality of corn seeds, the drying time is shortened from 72 hours to 60 hours, which improves the work efficiency of the production line and reduces the labor intensity of operators.**

Keywords*—Drying barn, corn ear, temperature and humidity, fuzzy control

I. INTRODUCTION

The moisture content of corn ears is about 35% at harvest time. The traditional way of corn ear drying is natural drying. When the moisture content drops to a safe storage moisture (about 13%), it will go through threshing, screening, in the warehouse and storage, and enter the stage for sale. The natural drying process is affected by the weather and may last for a long time, during which a lot of labor (turning the sun) are needed. If you do not work in time, it may cause mildew and freezing damage, reduce the quality and germination rate of corn seeds, and bring losses to enterprises and farmers [1].

The corn ear drying process is one of the processes in the corn seed mechanical processing production line. Corn ear drying technology adopts a scientific process. Under the premise of not damaging the quality of corn seeds, the temperature and humidity of the drying process are controlled, and the moisture content of corn ears can be quickly reduced in a relatively short time, so that it can meet the requirements of safe storage standards [2-5]. The focus of the drying process is to ensure the quality of corn seeds. This technology has completely changed the traditional method of natural drying of corn ears for a long time, liberating labor and reducing unnecessary losses during the drying process.

The drying method is to send the hot air generated by the heat source into the drying bin as the drying medium, and the hot air will take away the moisture from the corn ears. The specific drying requirements are as follows: the newly harvested corn ears have high water content and strong metabolism, and they must be dried at low temperature first. Under the condition that the temperature is 5~10°C higher than normal temperature, after continuous drying for 2~3 hours, then gradually increase the temperature to 43°C and perform high-temperature drying [6-9]. It can be seen that the temperature and humidity control of hot air is the key to the corn ear drying process. This article intends to use fuzzy control technology to adjust the temperature and humidity of the corn ear drying process.

II. CORN EAR DRYING PROCESS

The technological process of the corn seed mechanical processing production line is: ear feeding → mechanical peeling → ear selection → drying → threshing → pre-cleaning → temporary storage (steel silo) → cleaning → classification → specific gravity selection → coating → packaging → storage.

The corn ear drying process is mainly composed of ear transportation system (ear feeding part, feeding belt conveyor, distributing system, discharging belt conveyor, collecting belt conveyor), heating system (boiler, heat exchanger, ventilator, hot air conveying system), corn ear drying warehouse group and control system (computer monitoring system, drying warehouse group PLC control system) and other parts.

A. Drying Bin and Sensor Layout

The corn ear drying bin group is composed of multiple drying bins alternately and back to back. The cross-sectional view of the drying bin is shown in "Fig. 1".

The temperature and humidity sensors of drying bin A_i and B_i are respectively arranged on the wall of the bin on one side of the discharge door, with a range of 0~50°C and 0~100%RH, and an accuracy of ±0.5°C and ±3%RH. A temperature sensor and a wind pressure sensor are installed in the upper air duct. The range is -20~100°C and 0~1MPa, and the accuracy is ±1°C and ±0.01 MPa.

Fund Project: Gansu University Innovation Fund project, project name: Application Research of integrated intelligent management system for urban waste power generation and transportation (Project No.: 2021a-157).
Project name: Research and practice project on the training mode of innovative and integrated talents under the background of new engineering Item No. LGYCXJG-22-08.

978-1-6654-8507-4/22/$31.00 ©2022 IEEE

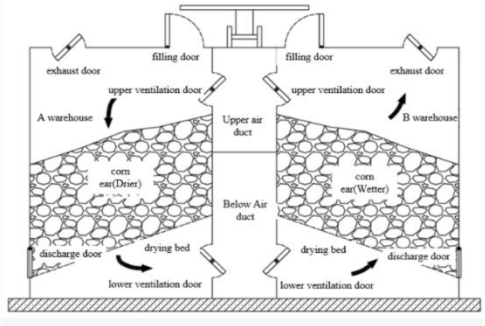

Fig. 1. Schematic diagram of drying bin section (lower ventilation doors, filling doors, exhaust doors and discharge doors).

B. Corn Ear Drying Processt

It is assumed that the corn ears in the drying warehouse A_i have been dried for a period of time, and the moisture content is low, which is also called the dry warehouse; the corn ears in the drying warehouse B_i are freshly harvested, and the moisture content is high, which is also called the wet warehouse.

The normal drying process is as follows: the filling door, exhaust door and discharge door in the drying warehouse A_i are closed, the opening of the upper and lower ventilation doors is adjusted by the PLC control system; the filling door, the upper ventilation door and the discharge door in the drying warehouse B_i are all closed, and the opening of the lower ventilation door and the exhaust valve are also controlled by the PLC control system. The direction of hot air flow is shown by the arrow in "Fig. 1".

When the corn ears in the drying bin A_i have been dried, the control system is required to close the upper and lower ventilation doors. At this time, the drying warehouse B_i is transformed from a wet warehouse to a dry warehouse, and through selection operations, it cooperates with other drying warehouses on the A_i side to continue the drying operation. After the warehouse is changed, the flow of hot air needs to be reversed.

III. Fuzzy Control of Temperature and Humidity in Drying Warehouse

A. Language Variables of the Fuzzy Controller

Take the drying warehouse A_i as an example to discuss. The input variables of the fuzzy controller are the signals T_A and R_A collected and processed by the temperature and humidity sensor, the transmitter and the PLC, and the output variables are the upper and lower ventilation door opening control signals. In this way, the temperature and humidity control system of the drying chamber is a fuzzy controller with dual input and single output. The schematic diagram of the temperature and humidity control system of the drying chamber is shown in "Fig. 2".

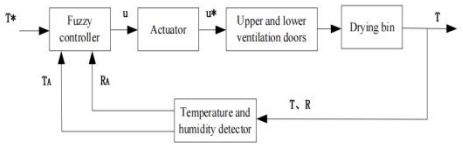

Fig. 2. Schematic diagram of temperature and humidity control system for drying bin

In "Fig. 2", T* is the desired temperature of the drying bin, and is the actual temperature of the drying bin. The control quantity obtained by fuzzy rules, fuzzy reasoning and defuzzification is sent to the vent door stepper motor drive system to adjust the opening degree of the upper and lower vent doors.

B. The Membership Function of Language Variables

The physical domain of the input variable T_A (x) is [0, 50], which represents the temperature range of 0~50°C. Divide the temperature into 6 fuzzy sets: TD (0~10°C), TJ (0~20°C), TS (10~30°C), TM (20~40°C), TB (30~50°C) and TG (40~50°C). The triangular membership function is selected to realize the fuzzification of temperature, and the expression is

$$\mu_{temperature}=\begin{cases}\mu_{TD}(x)=(10-x)/10 & 0\le x\le 10\\ \mu_{TJ}(x)=\begin{cases}x/10 & 0\le x\le 10\\ (20-x)/10 & 10\le x\le 20\end{cases}\\ \mu_{TS}(x)=\begin{cases}(x-10)/10 & 10\le x\le 20\\ (30-x)/10 & 20< x\le 30\end{cases}\\ \mu_{TM}(x)=\begin{cases}(x-20)/10 & 20< x\le 30\\ (40-x)/10 & 30< x\le 40\end{cases}\\ \mu_{TB}(x)=\begin{cases}(x-30)/10 & 30\le x\le 40\\ (50-x)/10 & 40\le x\le 50\end{cases}\\ \mu_{TG}(x)=(x-40)/20 & 40< x\le 100\end{cases} \quad (1)$$

The membership function of the temperature fuzzy set is shown in "Fig. 3".

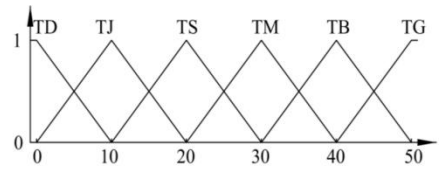

Fig. 3. Triangular membership function of input variable TA

The physical theory domain of the input variable RA(y) is [0, 100], which represents the humidity range of 0~100%RH. The humidity is divided into 6 fuzzy sets: RD (0~20%RH), RJ (0~40%RH), RS (20~60%RH), RM (40~80%RH), RB (60~100%RH) and RG (80~100%RH). The triangular

membership function is selected to realize the fuzzification of humidity, and its expression is

$$\mu_{\text{humidity}}=\begin{cases}\mu_{RD}(y)=(20-y)/10 & 0\le y\le 20\\ \mu_{RJ}(y)=\begin{cases}y/20 & 0\le y\le 15\\ (40-y)/10 & 20\le y\le 40\end{cases}\\ \mu_{RS}(y)=\begin{cases}(y-20)/20 & 20\le y\le 40\\ (60-y)/20 & 40<y\le 60\end{cases}\\ \mu_{RM}(y)=\begin{cases}(y-40)/20 & 40<y\le 60\\ (80-y)/20 & 40<y\le 60\end{cases}\\ \mu_{\text{RB}}(y)=\begin{cases}(y-60)/20 & 60\le y\le 80\\ (100-y)/20 & 80\le y\le 100\end{cases}\\ \mu_{RG}(y)=(y-80)/20 & 80<y\le 100\end{cases} \tag{2}$$

The membership function of the humidity fuzzy set is shown in "Fig. 4".

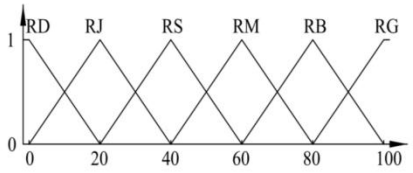

Fig. 4. Triangular membership function of input variable RA

The physical domain of the output variable $u(z)$ is [0, 90], 0° represents the vent door is closed, and 90° represents the vent door is fully open. Divide the control amount into 7 fuzzy sets: KB (open 0°~close), KS (open 15°), KD (open 30°), KF (open 45°~half open), KG (open 60°), KH (open 75°) and KK (open 90°~full open). The triangular membership function is selected to realize the fuzzification of the control quantity, and its expression is

$$\mu_{\text{Control amount}}=\begin{cases}\mu_{KB}(z)=(15-z)/10 & 0\le z\le 15\\ \mu_{kS}(z)=\begin{cases}z/15 & 0\le z\le 15\\ (30-z)/15 & 15\le z\le 30\end{cases}\\ \mu_{KD}(z)=\begin{cases}(z-15)/15 & 15\le z\le 30\\ (45-z)/15 & 30<z\le 45\end{cases}\\ \mu_{KF}(z)=\begin{cases}(z-30)/15 & 30<z\le 45\\ (60-z)/15 & 45<z\le 60\end{cases}\\ \mu_{KG}(z)=\begin{cases}(z-45)/15 & 45<z\le 60\\ (75-z)/15 & 60\le z\le 75\end{cases}\\ \mu_{\text{KH}}(z)=\begin{cases}(z-60)/15 & 60\le z\le 75\\ (90-z)/15 & 60\le z\le 75\end{cases}\\ \mu_{KK}(z)=(z-75)/15 & 75<z\le 90\end{cases} \tag{3}$$

The membership function of the control variable fuzzy set is shown in "Fig. 5".

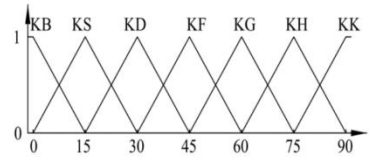

Fig. 5. Triangular membership function of output variable u

C. *Fuzzy Control Rule Table*

Design fuzzy rules based on the operating experience of industry technicians, and the fuzzy rules formulated are

Rule 1: When the temperature is low and the humidity is high, the ventilation door is opened 90°;

Rule 2: When the temperature is low and the humidity is moderate, the ventilation door is opened 60°;

Rule 3: When the temperature is moderate and the humidity is high, the ventilation door should be opened 75°;

Rule 4: When the temperature and humidity are both moderate, open the ventilation door at 45°;

Rule 5: The temperature is moderate and the humidity is low, and the ventilation door is opened 30°;

Rule 6: When the temperature is high and the humidity is moderate, open the ventilation door 15°;

Rule 7: When the temperature is high and the humidity is low, open the ventilation door at 0°.

According to this fuzzy rule design standard, a fuzzy rule table is established, as shown in Table I.

TABLE I. FUZZY RULE TABLE FOR TEMPERATURE AND HUMIDITY CONTROL OF DRYING CHAMBER

Vent door z		Temperature x					
		TD	TJ	TS	TM	TB	TG
Humidity y	RD	KF	KD	KD	KS	KB	KB
	RJ	KF	KF	KD	KD	KS	KB
	RS	KG	KF	KF	KD	KD	KS
	RM	KH	KG	KF	KF	KD	KD
	RB	KK	KH	KG	KF	KF	KD
	RG	KK	KK	KH	KG	KF	KF

D. *Fuzzy Reasoning*

(1) Rule matching

Assuming that current temperature and humidity data of the drying bin measured by the sensor is x_0 =35°C, y_0 =55%RH, and the corresponding membership degrees are $\mu_{TM}=0.5$, $\mu_{TB}=0.5$, $\mu_{RS}=0.25$, $\mu_{RM}=0.75$. Comparing Table I, we can get 4 matching fuzzy rules, as shown in Table II.

TABLE II. FUZZY INFERENCE RESULT

Vent door z		Temperature x					
		TD	TJ	TS	TM(0.5)	TB(0.5)	TG
Humidity y	RD	0	0	0	0	0	0
	RJ	0	0	0	0	0	0
	RS (0.25)	0	0	0	$\mu_{KD}(z)$	$\mu_{KD}(z)$	0
	RM (0.75)	0	0	0	$\mu_{KF}(z)$	$\mu_{KD}(z)$	0
	RB	0	0	0	0	0	0
	RG	0	0	0	0	0	0

(2) Rule trigger

It can be seen from Table II that there are 4 triggered rules namely,

Rule21: IF x is TM and y is RS then z is KD;

Rule22: IF x is TM and y is RM then z is KF;

Rule27: IF x is TB and y is RS then z is KD;

Rule28: IF x is TB and y is RM then z is KD.

(3) Rule premise reasoning

In the same rule, the conclusion of the rule is obtained through the relationship of "and" between the premises, then the credibility of the total premise of each rule is

Rule21: min（0.5,0.25）=0.25;

Rule22: min（0.5,0.75）=0.5;

Rule27: min（0.5,0.25）=0.25;

Rule28: min（0.5,0.75）=0.5;

TABLE III. THE TOTAL CREDIBILITY OUTPUT OF EACH RULE IS SHOWN

Rule premise		Temperature x					
		TD	TJ	TS	TM	TB	TG
Humidity y	RD	0	0	0	0	0	0
	RJ	0	0	0	0	0	0
	RS	0	0	0	min(0.25, $\mu_{KD}(z)$)	min(0.25, $\mu_{KD}(z)$)	0
	RM	0	0	0	min(0.5, $\mu_{KF}(z)$)	min(0.5, $\mu_{KD}(z)$)	0
	RB	0	0	0	0	0	0
	RG	0	0	0	0	0	0

(4) Total output of fuzzy control system

The total output of the fuzzy control system is the union of the credibility reasoning results of each rule, namely

$$\mu_{out} = \max\begin{Bmatrix} \min(0.25, \mu_{KD}(z)), \min(0.25, \mu_{KD}(z)), \\ \min(0.5, \mu_{KF}(z)), \min(0.5, \mu_{KD}(z)) \end{Bmatrix}$$

E. Defuzzification Operation $\mu_{KD}(z)$

The fuzzy inference process of the ventilating door of the drying warehouse is realized by programming in MATLAB, and the maximum membership degree of the ventilating door of the drying warehouse can be obtained as μ=0.5 , Substituting equation (3) to obtain the values of $\mu_{KD}(z)$ and $\mu_{KF}(z)$

$$\begin{cases} \mu_{KD}(z) = (45 - z)/15 = 0.5 \\ \mu_{KF}(z) = (z - 30)/15 = 0.5 \end{cases}$$

The solution is: Z_1=Z_2=37.5

Using the maximum membership average method, the accurate output can be obtained as

$$z^* = \frac{z_1 + z_2}{2} = 37.5$$

That is, when the temperature in the drying chamber is 35°C and the humidity is 55%RH, the opening of the upper and lower ventilation doors is 37.5°.

IV. CONTROL SYSTEM DESIGN

In the control system of the corn seed machining production line, the hardware adopts Siemens S7-1200 series PLC, and the software adopts modular programming method. The subprogram modules and their functions related to the temperature and humidity control of the drying bin are shown in Table IV.

TABLE IV. SUBROUTINE MODULES AND FUNCTIONS

Program block	Name	Description
OB1	Cycle Execution	FC4 (Analog filter) FC5 (Scale transformation) FC6 (Inverse scaling) FC7 (Analog processing) FC8 (Manual control of drying bin) FC9 (Automatic control of drying bin)
OB35	CYC_INT5	
OB100	Complete Restart	
DB1	Operating data	
DB2	Digital quantity	
DB3	Analog	

Before the fuzzy control system of temperature and humidity in the drying chamber is put into use, the drying process is controlled manually, and the average drying time per chamber is 72 hours. After the control system was put into use, the drying process was changed to automatic control. According to multiple batch tests on site, the drying time was shortened to about 60 hours.

The drying time is closely related to the process parameters such as the hot air temperature, air pressure and flow rate of the upper air duct. If the hot air temperature and air pressure fluctuate greatly, the drying process time will be affected. In fact, during normal production, the hot air system is closed-loop controlled by the frequency converter, which can basically ensure the stability of the hot air temperature and air pressure.

V. CONCLUSION

(1) The temperature and humidity fuzzy control system of the drying chamber designed in this paper has good dynamic response, anti-disturbance ability and robustness. It provides a technical guarantee for the further optimization of the system for the segmented drying.

(2) The control method designed in this paper effectively shortens the drying time (from 72h to 60h), improves the work efficiency of the production line, and reduces the labor intensity of the operators while ensuring the quality of corn seeds.

(3) Due to the long drying process of corn ears and many uncertain factors, and the fuzzy control system is an open-loop control system, the control performance needs to be further improved.

FUND PROJECT

Gansu University Innovation Fund project, project name: Application Research of integrated intelligent management system for urban waste power generation and transportation (Project No.: 2021a-157).

PROJECT NAME

Research and practice project on the training mode of innovative and integrated talents under the background of new engineering. Item No. LGYCXJG-22-08.

REFERENCES

[1] Zhang Jie. Research and application of drying system based on multivariable fuzzy control [D]. Shanghai Jiaotong University.

[2] Chen Hongjun, Gao Guoli. Research on grain drying control system based on fuzzy control [J]. Times Agricultural Machinery, 2016(11):2.

[3] Dai Fei, Zhang Fengwei, Han Zhengsheng, et al. Design and experimental research on mechanical drying device for corn ears [J]. 2022(3).

[4] Wang Guojie, Mu Gang, Huo Jin, et al. Design and experiment of ice-low temperature heat pump drying control system for Penaeus vannamei based on fuzzy control [J]. Food and Machinery, 2021, 37(7):8

[5] Chen L, Wang G W, Zhao W Y, "The design of monitoring system for corn ear drying based on Kingview," Journal of Chinese Agricultural Mechanization, vol.36, pp.160-164,2015.

[6] Wei B, Yang D H, Li B C, Wang H D, "Intelligent assembled steel structure corn ear drying production line," China Seed Industry, 2020, pp. 67-70.

[7] Chen H J, Gao G L, "Research on Grain Drying Control System Based on Fuzzy Control," Times Agricultural Machinery, vol.43, pp. 62-63, 2016.

[8] Sun Chuanzhu, Wang Xiangyou, Wei Zhongcai. Experimental research on corn ear drying under different temperature conditions [J]. 2022(4).

[9] Liu H Y, Zhang M W, "Design of control system of corn threshing device based on embedded," Journal of Agricultural Mechanization Research, vol.41, pp.206-210,2019.

2022 IEEE 5th International Conference on Electronics Technology (ICET 2022)

Conference XPLORE COMPLIANT Version
IEEE Catalog Number: CFP22P18-ART
ISBN: 978-1-6654-8508-1

USB Version
IEEE Catalog Number: CFP22P18-USB
ISBN: 978-1-6654-8507-4

Additional copies of this publication are available from

Curran Associates, Inc.
57 Morehouse Lane
Red Hook, NY 12571 USA
+1 845 758 0400
+1 845 758 2633 (FAX)
email: curran@proceedings.com

13、电气自动化设备中 PLC 控制系统的应用

电气自动化设备中 PLC 控制系统的应用

朱东山，党　媛

（兰州工业学院，甘肃　兰州　730050）

摘要：我国的电气工程及自动化技术发展迅速，逐渐走到了世界的前列，其在一些发电厂、变电站等领域都有涉及，电气工程技术和自动化技术的发展水平直接影响着我国的社会生产力，特别在建设工业化社会的关键阶段。对于电气工程及其自动化项目来说，对它的自动化控制和管理一定要越来越科学化、规范化、严格化，才能够保证电气工程及其自动化，在日常的工作方面的正常的维护与保养问题，进一步促进电气自动化的发展。

关键词：PLC 技术；电气自动化设备；控制系统

PLC 是一种数字运算操作的电子系统，主要在医学制造工业、化工工业、冶金工业等领域有广泛的应用。同时 PLC 还应用在一些编程软件领域，它主要是通过继电器来进行逻辑控制处理的。我国电气自动化设备中 PLC 控制系统的应用已经有几十年的历史，但是相较于全世界最顶尖的电气强国而言还存在一定的差距，因此，要对此进行继续探索和改革。要与当今时代飞速发展的互联网、大数据、人工智能等技术紧密结合，不断将更先进的技术应用到电气自动控制中，本文以 PLC 技术为切入点，对 PLC 技术在电气自动控制中的应用进行研究具有重要作用。

1　PLC 技术的概述

1.1　PLC 技术的应用原理

PLC 主要应用于工业领域，是专门为了工业环境下的应用而设计的，也是当代工业控制的核心。而且 PLC 的应用面较广，功能较为强大，使用起来也较为方便，所以大多都被用在很多的工业领域。通过 PLC 技术系统对使用者所用的程序内部进行扫描，然后在此基础上依据扫描出现的结果采用信号控制的方法进行传输信息，把它传输到与之相应的执行机构中，然后通过 CPU 对整个进行的过程的作用，最后使起 CPU 发挥循环的效应，在这样循环的过程中，可以减少不必要的时间，既节约了时间又保证了整个系统的正常运行。如果 PLC 技术在电气系统中被合理应用，在运行的过程中就会对其内部的线路进行相对应的连接，连接的过程就是要确保电气控制系统的顺利运行。由 PLC 技术处理后留下的数据，大部分都是采用逻辑代数的方式进行存储，这是为了保证在实际的系统控制过程中发生突然状况时，系统自己能够通过增加数据或者删除与运行过程中无关数据的形式对发生的状况做出相应的处理，这样的设置能够有效满足控制系统的高要求。

1.2　PLC 技术的特点

PLC 是一种以实现在工业环境的应用中进行良好操作为目的而设计的利用数字来进行运算操作的电子系统。PLC 主要采用的是一类可编程的存储器在内部存储程序方面进行有序的控制。而且 PLC 在定时技术等方面有着很重要的存储作用。PLC 随着技术的发展，现在大多采用微型计算机技术来对工业控制装置进行逻辑控制。PLC 在三维处理算法方面的多种操作将这些处理技术像流水线一样串联在一起，从而保证了整个过程的结构清晰，提高代码的简洁性和重用性。作为 PLC 技术运用中的工作人员，系统运行前，首先要进行的工作就是选择正确合理的梯形图和逻辑图，还有与之相关的编程语言等，这样尽管自己的计算机技术不够熟练，也能够按照相关的工作步骤进行操作，然后系统进行高速运行，这是为了方便操作的人员进行现场调控和使用。另外，在系统的修改或者处理的过程中，操作人员若想借用开关对此进行系统进行更好的掌管，PLC 技术正好可以帮助实现这个操作。PLC 技术通过与上位机一起组成一个较为繁杂的系统，然后设定自动化控制模式进行控制。它的优点在于该系统的稳定性特别的强，它不受工作环境的影响，不论是在多么恶劣还是正常的工作环境条件下，它都能够进行正常的工作运行。自动化的出现，代表了一种高新技术的体现，它在人们生活中有着很高的地位，自动化对准确度要求非常高的对自动化的设计生产都有着高标准要求。电气工程如果只靠人工去实现技术的突破往往有难度，而且还要耗费大量的时间。

PLC 技术的不断应用可以促进电气行业自动化发展的进程逐步使准确率提高，不断促进电气行业的发展。

2 电气自动化设备中 PLC 控制系统的应用

2.1 在程序控制和闭环控制中的要点

PLC 技术能够有效地完善系统控制，并且能够使自动化控制系统运行地更加顺利。这项技术还能提升发电厂的经济效益，有效提高了电厂的工作效率。因此，为了使 PLC 技术在电气工程及其自动化控制的程序上更高效率地使用，相关的工作人员一定要设计出科学合理的应用方案。PLC 技术的运用能够满足各大厂家企业的需求，因为它的使用可以有效地控制各项电气设备。在闭环控制中，该技术使得整个系统更加安全，有效地避免控制运行过程中大的故障出现。对于 PLC 技术来说，其对自动化的应用处在信息技术的环境中，PLC 技术和自动化的技术联系紧密，互辅互助。电力自动化技术主要就是将其信息的处理技术以及电子智能技术和网络通信技术三者技术相结合起来的一项综合性的技术，电力自动化技术在不断地应用和发展过程中逐渐趋于完善。在电力工程中使用电力自动化技术可以使其充分的应用在电力系统的远程监控管理内容中，从而有效地提升工程的自动化管理水平。电力自动化技术对于我国的电力发展水平也有着至关重要的作用，它能够在一定程度上促进我国电力发展水平的提高，从而使得我国的电力资源得以充分的利用充分利用，电力资源也是我国目前在电力发展过程中的一个重要方向，所以电力自动化技术与我国电力发展的方向相结合，更加提升了电力工程中电力自动化技术的重要性。

2.2 在开关控制过程中的应用要点

在 PLC 技术出现前，各个大型厂家在电气工程自动化控制过程中采用的操作方式一般都很繁琐，而且还不能保证整个运行过程的安全性，一旦遇到恶劣的环境，该系统就不能正常运行，大大地降低了工作的效率。但是 PLC 技术的出现拯救了整个过程中遇到的各方面的困难。PLC 技术采用的是计算机技术，将继电器和通信技术进行融合，以确保能够控制电气工程中的各项设备，这可以大大地提高了电气工程中各项工作的效率。

2.3 提高技术人员的整体水平

相关技术人员应当有实践经验，动手能力必须达标；同时还要拥有高强度的心理素质，在遇到困难时不会因为处境恶劣而感到恐慌，仍然能够镇定自若地解决问题。但是如今许多企业招聘的技术人员往往只能解决某些特定的问题，或是比较常见的问题，这样当发生突发情况时，可能因为技术人员的自身能力无法达到而对整个电器工程造成一定的影响，甚至会加大整个工程的资金预算。PLC 课程是工业化的一门课程，相较其他课程来说实践性较强。传统教学模式是采用课堂教学方式，学生属于被动接受的状态，对于培养学生的编程能力和调适能力有很大的阻碍，所以最大限度地利用实验室来进行教学，一方面不仅可以提高学生对 PLC 课程中编程的调适能力，而且还可以让学生对于这门课程有更深刻了解。同时进行实验室利用实验室来进行教学会增加这门课程中老师与学生的互动性提高 PLC 课程里师生之间配合的默契度。在 PLC 实验装置上所进行的操作，由于都是模拟的实验操作，所以学生也并不能够将 PLC 设备与其他的输入输出设备相结合，根本无法让学生从心底里面真正地理解，长此以往学生的实际动手能力就会下降，对于实验装置的操作能力也会下降。任何工业化项目都不是凭借一个人的力量就可以完成的，大多都需要十几个人甚至上百人的合作才能够完成。

2.4 关于 PLC 技术应用的建议

根据当前的科学技术的发展趋势可以看出，在以后科学家们肯定还会研究出更多更加新型高效的电气工程设备。因此，在其他高级新型设备出现前，要掌控好 PLC 技术，根据现在的运行环境，完善现有的设备，让 PLC 技术在运用过程中发挥极致的作用，以此来推动我国目前电气工程的发展，使得电气工程的应用更加智能化自动化。现阶段，PLC 技术的合理应用是电气工程及其自动化控制中的发展关键，也可能是未来发展的前景。因此，研究人员可以根据当前 PLC 技术在电气工程及其自动化控制中的应用现状进行分析，通过完善计算机组网可以减少 PLC 技术在电气控制系统中的不足之处。对于电气工程及其自动化项目进行优化的过程是一个整体性的过程，同时对于其项目的优化，也是一个整体性系统方面进行优化的过程，这都关系到电气自动化方面的规划建设，以及工程项目日常工作性能方面的维护，这 3 个方面对于其电气工程及其自动化项目进行优化是非常重要的，电气工程及其自动化的工作者以及技术人员一定要具有专业的技术能力以及专业的技能知识，从而在对于其电气工程及其自动化进行工作时，有相应的知识积累以及经验的积累，可以及时准确地来收集一些关于电气工程及其自动化的数据信息，从而在进行必要的检测，同时在工作的过程中还可以掌握其有关的一些实践内容将其自己去了学到的理论知识与实践内容相结合起来进一步的提升自己的能力，要想完成通讯电气工程质量方面的检测任务就一定要对于通信接通方面的整体比例要有明确的认知和明确的了解，从而进一步的掌握电气自动化方面整体的一个体系布局量，对于电气自动化系统在运行的过程中所产生的一些问题来进行相应的研究和了解。从而制定出有关的对策，进一

步的完善电气自动化系统。

2.5 PLC 技术的发展趋势

随着信息时代的飞速发展，当前时代发展的主要趋势就是数字信息化技术的发展，要想使 PLC 技术能够适应这个飞速发展的社会，研究人员就要结合当前社会的发展特点，对 PLC 技术应用过程中出现的各种的状况进行不断完善，争取让 PLC 技术适用于社会发展的各个领域中，然后促进各个行业的发展。PLC 技术的应用受所处环境温度和湿度的影响，它的适用温度大概在 0℃ ~50℃之间，湿度≤ 85℃。因此，只有合理控制好所处的环境 PLC 技术才能发挥最大的作用，低于这个最适温度和湿度只能使 PLC 技术发挥微弱的作用，超过了最适温度和湿度，就会会使 PLC 技术发挥相反的作用。相关的技术人员可以研究出一个自动化控制的系统去调节周围的运行环境，当环境不适时，这个系统就会自动调节使得周围的环境达到最适的运行环境。改变系统的干扰能力。由于我国的电力行业极速发展，所以人类对该系统运营的安全性要求也越来越高。此外，PLC 技术应用的过程是一个非常复杂的过程，所以需要技术人员在该技术运用过程中仔细观察，研究出是什么干扰该系统的运行，然后进行改进，不断发现不断改进不断完善，渐渐地让 PLC 技术运用的防干扰能力越来越强。

3 结束语

综上所述，PLC 技术以其独特的优势在电气工程和自动化发展进程中取得了越来越广泛的应用，对 PLC 技术展开深入地研究符合当下时代发展的特点。与电气工程与自动化控制相关工作的过程中工作人员在把 PLC 技术融合与电气工程前，务必要制定一套完整安全合理的技术运用方案，还要重视在该新型技术的使用的过程中，工作人员必须保持态度严谨，确保在工作过程中及时发现该技术在使用过程中出现的问题，并且做好及时的应对措施。

作者简介：朱东山（1984-），男，籍贯：甘肃武威，学历：本科，研究方向：智能控制、工业自动化。

基金项目：兰州工业学院青年科技创新项目，无人机自主无线充电平台的研究与实现（19K-007）。

参考文献：

[1] 刘宁 . 关于 PLC 技术应用于电气自动控制中的分析与研究 [J]. 信息周刊 ,2019(42):60.

[2] 沈晓姣 . 关于 PLC 技术应用于电气自动控制中的分析与研究 [J]. 区域治理 ,2018(52):186.

[3] 高山 . 关于 PLC 技术应用于电气自动控制中的分析与研究 [J]. 内燃机与配件 ,2018(5):197-198.

（上接第 177 页）

们试图通过政策和法规等方面的互相协调，更好地建设网络制度，让信息传输和计算机网络的使用更加便捷。必须创建一种新型的经济管理模式，才能够让计算机网络更好地为人们生活和工作创造价值，这也是本文研究的初衷。

3.4 未来发展趋势

信息化的建设，在未来可以更好地让信息技术支撑品牌管理和保护人们数据的安全。品牌方应该积极采取各种计算机的应用方式，让自己的品牌深入群众的生活，并且更好地维护群众生活的安全。而安全信息的管理在这个过程中至关重要，能够保证品牌建设的效果。与此同时，也可以侧面加速信息传输的质量和效率，让人们之间的沟通更加便捷更加高效。

4 结束语

网络信息资源在信息社会中占据重要的地位，引导着人们的生活内容和信息传输的效率，在很多方面伴随着人们的生活和工作。如果在这个过程中，没有让计算机网络和信息传播有更可靠的保证，就会让人们的生活和工作受到严重的干扰，甚至会泄露个人隐私发生意想不到的突发事件，所以必须引起全社会的共同关注。在这个过程中，积极应用正确的制度和技术，才能够管控这一不确定因素，让人们的生活越来越好，同时能够让计算机在现今社会中得到更好的发展。

作者简介：陶星星（1981-），男，籍贯：湖南永州，学历：硕士研究生，职称：高级工程师，研究方向：电子计算机。

参考文献：

[1] 龙振华 . 大数据时代计算机网络信息安全及防护策略 [J]. 中国管理信息化 ,2019(2206):161-162.

[2] 蔡彬彬 , 孙忠辉 . 计算机网络信息安全问题及防护策略研究 [J]. 长春理工大学学报（自然科学版),2019(4023):128-132,137.

[3] 唐庆谊 . 大数据时代背景下人工智能在计算机网络技术中的应用研究 [J]. 数字技术与应用 ,2019(3710):72-73.

[4] 周亿城 , 陈靖 , 唐满华 , 等 . 大数据背景下计算机网络信息安全风险和解决对策研究 [J]. 科技创新与应用 ,2020(35):83-84.

14、无线可充电传感器网络安全充电任务

产业与科技论坛 2021 年第 20 卷第 5 期

无线可充电传感器网络安全充电任务调度问题探讨

□朱东山

【内容摘要】随着现代化信息技术的飞速发展，使得无线充电技术得到了广泛的关注和应用。经过一段时间的发展，无线可充电传感器网络在医疗领域、智能电网等多个行业中都有着重要的应用。因此，要重点关注其充电任务的调度问题，使得无线可充电传感器网络安全充电效用最大化。本文首先对无线可充电传感器网络进行介绍，然后说明了最大化有效充电能量问题，在此基础上提出了小规模传感器网络缩短充电时间的集中式算法以及大规模传感器网络缩短充电时间的分布式算法，从而保证传感器网络整体有效充电能量最大化的同时减少充电的时间。

【关键词】无线可充电传感器网络；安全充电；任务调度

【基金项目】本文为兰州工业学院青年科技创新项目“无人机自主无线充电平台的研究与实现”（编号：19K－007）研究成果。

【作者简介】朱东山（1984.4～），男，甘肃武威人，兰州工业学院工程师；研究方向：自动化、人工智能、无线充电

为了进一步解决无线可充电传感器网络安全充电效用的最大化问题，需要重点关注充电器充电方案的设计以及调度传感器节点的设计，从而保证无线可充电传感器网络工作性能的最优。现阶段，大部分的研究都是对于静态充电器场景安排相应的充电方案，对于可移动充电器场景进行路径的选取以及充电任务的调度方案，但是这样就会忽略了静态充电器场景下充电任务调度方案实现的可行性。因此，为了在安全充电的情况下，完成无线可充电传感器网络充电效用的最优化以及充电时间的最短，应针对静态充电器下的安全充电任务调度问题，提出较好的调度方案。

一、无线可充电传感器网络概述

无线可充电传感器网络主要指通过无线充电技术给传感器节点完成充电的传感器网络，其中，网络中的传感器节点包含天线等设备，可以实现对充电器发射电磁辐射能量的接收功能。此外，因为电磁波随着环境的变化不会发生太大的改变，所以极大地减少了由于电线老化等现象而造成的一系列安全隐患，增加了无线可充电传感器网络的安全性能。

另外，利用非接触式的充电方法，能够便利的给植入人体内的小型化设备完成充电操作，比如人工心脏起搏器等。现阶段，由于受到投资成本、电能转化效率等因素的影响，无线可充电传感器网络还没有得到较为广泛的应用，但是随着信息化技术的不断发展，无线可充电传感器网络已经有效地应用在医疗、教育、智能电网等领域当中，并且在将来会得到了广泛的发展。

无线可充电传感器网络的主要特点包括：一是能够持续化的工作，传感器节点的能量可以不断地进行补充，所以能够持续的进行工作；二是维护成本较低，无线可充电传感器网络不需要定期更换电池，其节点的能量能够持续地进行补充，所以维护成本较低；三是能量可控，能够通过调整充电方案来完善无线可充电传感器网络的能量分布问题；四是对环境的危害较小，无线可充电传感器网络能够持续的、重复的工作使用，不需要电池的供给，因此较为环保。

二、最大化有效充电能量

最大化有效充电能量问题即 ROCK－R 问题，利用区域离散化技术解决这一问题的非线性问题，把约束线性化，再提出一个可行解正则化方法，缩小求解的空间，从而将 ROCK－R 问题变为线性规划问题。

（一）区域离散化。利用误差控制的区域离散化方式，通过分段常量函数近似非线性充电函数模型，以便把二维区域分为几个离散化、电磁辐射是常数的小区域。一是利用分段常量函数近似非现象充电函数模型，根据和充电器间距离进行分割，并且保证误差在可控的范围中。把充电器当作圆心，线段为半径画圆形，其圆环上的电磁辐射用一个常数表示。二是平面将会被划分为若干个的子区域，因为各个充电器在子区域的电磁辐射值为常数，由于电磁辐射具有可加性质，所以各个子区域的电磁辐射值是全部充电器在区域内电磁辐射的和，其结果也是一个常数。因此，安全充电的限制就是全部子区域的电磁辐射小于已有的安全阈值。

（二）可行解正则化。随着时间的不断变化，充电器充电功率的调节因子也在发生改变，因此我们要建立一个动态的模型，并且解决在一定时间内最优控制的问题。所以，在这一过程中，我们可以利用哈密顿－雅可比－贝尔曼偏微分方程（HJB 方程）。此方程为连续系统中动态规划的基本方程，主要说明了连续时间系统的最佳控制问题。对于解决在全部状态空间下的最优控制问题而言，需要用到哈密顿－雅可比－贝尔曼偏微分方程。一是要确定控制函数，使得性能指标最小化。对于全部控制区域来说，只要符合 HJB 方程，就能够保证系统的性能指标达到最小。二是直接求解 HJB 方

程较为困难，因此，针对本文研究的内容，应用可行解正则化方法，把所有的可行解变为正则化的问题，从而完成有效的充电能量。针对 ROCK－R 问题，要保证其任意的可行解和正则化形式等价，从而使得有效充电能量完全一样。

（三）线性规划问题。由于 ROCK－R 问题中的目标函数为非线性，给模型的求解带来了一定困难，所以我们可以引入一个参数量，把有效充电能量问题变化为线性规划的问题。那么就可以通过求解线性规划方程来确定目标方程的最优解，保证目标函数的最优化。

三、小规模传感器网络缩短充电时间的集中式算法

（一）问题的分析。针对 ROCK－R 问题，通过可行解正则化方法能够保证充电时间间隔的充电功率可行解的抽象化表达方式，从而得到二次约束线性优化模型。在安全充电任务调度问题中，要保证有效充电能量最大，同时使得充电时间最短。由于充电的时间是不知道的，对于传感器网络的有效充电能量具有 2 类情况：若充电时间大于充电结束时间，无线可充电传感器网络会一直接收充电器传输的电能，此时有效充电总能量为这一段时间内的总值；若充电时间小于等于充电结束时间，那么无线可充电传感器网络只能在一定的时间范围内接收充电器传输的电能。

（二）基于线性规划的二分搜索算法。为了降低求解过程的复杂性，保证收敛时间，提高求解精度，因此，可以使用基于线性规划的二分搜索算法（LP－GTA）。此算法根据有效充电能量对于充电时间的单调性，对充电时间进行直接遍历，然后再求解线性规划问题，进而确定最优解。

根据有效充电能量对充电时间的单调递增这一性质，当无线可充电传感器网络充电结束之后，或者获取到了全部充电能量，其有效的充电能量将会达到最大值，而且将一直保持不变，此时，在解空间结构中对有效充电能量最大值的拐点进行求解，那么相应的充电时间就是所要求解的最短充电时间。除此之外，此算法不仅能够在线性时间中获得最大有效充电能量，而且也可以获得其最短充电时间对应的最优充电方案，而且基于线性规划的二分搜索算法的求解时间仅和求解精度以及线性规划问题模型有一定的联系。

总而言之，对 ROCK－R 问题的求解就是对有效充电能量最大值的拐点进行求解，此算法极大地降低了时间的复杂程度，使得充电时间得到减少，同时很好地解决了无线可充电传感器网络安全充电任务调度问题。

四、大规模传感器网络缩短充电时间的分布式算法

（一）网络划分。在利用分布式算法的过程中，需要重点解决的问题就是无线可充电传感器网络中充电器的充电范围是相互覆盖的，但是安全充电调度任务要求全部网络当中的任意一个点的电磁辐射值要比设定的安全阈值小，那么被覆盖的无线可充电传感器网络的辐射约束就不能通过区域数据计算相应的电磁辐射值，这就意味着分布式计算方式不能在一定程度上确保电磁辐射的安全。

所以，为了利用分布式算法来缩短大规模无线可充电传感器网络的充电时间，可以把相互关联的网络区域进行网络划分，分为多个子区间，使得区域之间是相互独立的，没有相互覆盖的充电范围。此外，还要保证传感器网络划分的网格区域能够把充电器的辐射范围全部覆盖。此时，传感器获取到的数据只能在每一个子区域内传播，减少了网络传输的延时，进而有效地进行分布式处理。

（二）关于 ROCK 问题的分布式算法。利用分布式算法，能够保证最大有效充电能量达到最优化，在最大程度上缩减充电的时间。对于无线可充电传感器网络的 ROCK 问题，利用分布式算法需要保证同时求得最大有效充电能量以及最短充电时间的近似边界值。针对每一个子区域内应用小规模传感器网络缩短充电时间的集中式算法，所有子区域的最大有效充电能量的和是全局有效充电能量值，那么对应的最短充电时间的最大值就是全局的充电时间。此外，由于各个子区域之间是相互独立存在的，因此可以将最大有效充电能量的和看作为近似边界值，但是此时的最短充电时间不能采用此种形式。针对此问题，为了求出算法的最优近似边界，可以利用区域放缩的方式，针对一个子区域，不是计算出最大有效充电能量，而是求得其合适的目标有效充电能量，然后对相应的有效充电能量及其时间进行解耦。除此之外，利用电磁辐射放缩的方式，保证局部的电磁辐射约束角度和全局方案的电磁辐射约束角度相同。利用这两种方式不仅能够求得最大有效充电能量的近似边界值，而且能够固定最短充电时间的近似边界值。

五、结语

本文通过对无线可充电传感器网络安全充电任务调度问题的探讨，使我们了解到了，为了进一步解决无线可充电传感器网络安全充电效用的最大化问题，需要重点关注充电器充电方案的设计以及调度传感器节点的设计，从而保证无线可充电传感器网络工作性能的最优。因此，利用小规模传感器网络缩短充电时间的集中式算法以及大规模传感器网络缩短充电时间的分布式算法，不仅能够有效地解决无线可充电传感器网络的 ROCK 问题，而且能够保证最大有效充电能量达到最优化，在最大程度上缩减充电的时间。

【参考文献】

[1] 柯志军. 无线传感器网络分簇路由算法研究 [D]. 华中师范大学，2016

[2] 东华理工大学. 一种网络安全的检测装置：CN202020022415.X [P]. 2020－05－29

[3] 刘蕴钢，朱江，徐雁冰，等. 无线可充电传感器网络充电算法研究 [J]. 传感器与微系统，2020，39（2）：14～17

[4] 郑翔，孙震，许彤彤. 无线可充电传感器网络充电调度算法研究 [J]. 廊坊师范学院学报（自然科学版），2020，20（1）：35～39

[5] 吴宝瑜，万鹏，王高峰，等. 无线可充电传感器网络能耗分级充电策略 [J]. 传感技术学报，2019，32（8）：1253～1260

[6] 韦荣槐，李舒，张艳玲，等. 电力物联网建设环境下可充电无线传感器网络能效与路由优化策略 [J]. 电测与仪表，2019，56（22）：31～36